

**Dissertation zur Erlangung des Doktorgrades
der Fakultät für Chemie und Pharmazie
der Ludwig-Maximilians-Universität München**

**Biochemical and cell biological
characterisation of the SUMO E1
activating enzyme Aos1/Uba2**

Katarzyna Chmielarska

aus

Kielce, Polen

2005

Erklärung

Diese Dissertation wurde im Sinne von § 13 Abs. 3 bzw. 4 der Promotionsordnung vom 29. Januar 1998 von Prof. Dr. Frauke Melchior and Prof. Dr. Patrick Cramer betreut.

Ehrenwörtliche Versicherung

Diese Dissertation wurde selbständig, ohne unerlaubte Hilfe erarbeitet.

München, 6.10.2005

Katarzyna Chmielarska

Dissertation eingereicht am 6.10.2005

1. Gutachter: Prof. Dr. Patrick Cramer
2. Gutachter: Prof. Dr. Alexander Pfeifer

Mündliche Prüfung am 20.12.2005

TABLE OF CONTENTS

LIST OF ABBREVIATIONS	1
1 SUMMARY	4
2 INTRODUCTION	4
2.1 Overview	4
2.2 Molecular mechanism of Sumoylation	9
2.2.1 Enzymes mediating the SUMO pathway	9
2.2.2 SUMO-Activating Enzyme (E1)	10
2.2.3 SUMO-Conjugating Enzyme (E2)	13
2.2.4 E3 ligases	14
2.2.5 SUMO processing and deconjugation	18
2.3 Function of SUMO modifications	19
2.3.1 Molecular consequences of sumoylation	20
2.3.2 Pathways in which SUMO was found	21
3 MATERIALS AND METHODS	24
3.1 Materials	24
3.1.1 Chemicals and materials	24
3.1.2 Reagents and reaction kits	25
3.1.3 Buffers and solutions	26
3.1.4 Cell culture	28
3.1.5 Antibodies	29
3.1.6 Recombinant proteins	31
3.1.7 Plasmids	31
3.1.8 Important oligonucleotides	32
3.1.9 Bacterial strains	33

3.2 Molecular biology methods	34
3.2.1 Plasmid DNA purification (miniprep)	34
3.2.2 Plasmid DNA (midi, maxiprep)	34
3.2.3 Preparation of chemically competent cells	34
3.2.4 Estimation of DNA concentration	35
3.2.5 Digestion of plasmid DNA with restriction endonucleases	35
3.2.6 DNA purification	36
3.2.7 Ligation of DNA insert into vector DNA	36
3.2.8 Transformation into DH5 α	36
3.2.9 Polymerase Chain Reaction (PCR)	37
3.2.10 Mutagenesis	37
3.2.11 Sequencing	40
3.2.12 Organ extracts	40
3.2.13 RNA isolation	40
3.2.14 RT-PCR	41
3.3 Cell biology methods	41
3.3.1 Cell lines	41
3.3.2. Transient transfection	42
3.3.3 Fluorescence microscopy	43
3.3.4 Reporter luciferase assay	43
3.4 Biochemistry methods	44
3.4.1 SDS-PAGE	44
3.4.2 Coomassie staining	44
3.4.3 Silver staining	44
3.4.4 Immunoblotting	45
3.4.5 Expression and purification of recombinant proteins	46
3.4.6 Measurement of protein concentration	48
3.4.7 <i>In vitro</i> SUMOylation	48
3.4.8 Fluorescence Resonance Energy Transfer (FRET)	48
3.4.9 Generation and purification of rabbit or goat polyclonal antibodies	50
3.4.10 Immunoprecipitation	50

3.4.11 His-SUMO pull down	52
3.4.12 Mass Spectrometry	52

4 RESULTS

4.1 PART 1: <u>Characterisation of an Uba2 splice variant</u>	54
4.1.1 Identification of Uba2 splice variant	54
4.1.2 Generation and characterisation of Uba2 polyclonal antibody in goat	56
4.1.3 <i>In vivo</i> and <i>in vitro</i> analysis of Uba2 splice variant	59
4.1.4 Finding new binding partners for Uba2 full length and Uba2 splice variant	64
4.2 PART 2: <u>Identification of a novel SUMO target</u>	66
4.2.1 Affinity purification and characterisation of Aos1 polyclonal antibody	66
4.2.2 α Aos1 antibodies decorate the nucleus and Golgi structures	70
4.2.3 A small fraction of Aos1 and Uba2 are present in insoluble pellet fractions	70
4.2.4 Aos1/Uba2 is present in Golgi fraction	73
4.2.5 Identification of a new binding partner (ELKS) for Aos1	73
4.2.6 Published functions of ELKS	76
4.2.7 Generation of recombinant ELKS	78
4.2.8 Generation and characterisation of ELKS polyclonal antibodies	81
4.2.9 Conformation of ELKS-Aos1 interaction	83
4.2.10 Subcellular localisation of ELKS	85
4.2.11 Recombinant of ELKS and Aos1 do not bind	88
4.2.12 Rab6 is not the binding factor between ELKS and Aos1	88
4.2.13 ELKS does not interact directly with SUMO <i>in vitro</i>	90
4.2.14 Identification of binding partner candidates for Aos1 and ELKS	91
4.2.15 ELKS interacts with RanBP2 in interphase cell extract	93
4.2.16 ELKS does not interact directly with BP2 Δ FG <i>in vitro</i>	94

4.2.17 ELKS does not inhibit sumoylation	95
4.2.18 ELKS is SUMO modified on 3 distinct lysine residues	98
4.2.19 ELKS sumoylation decreases its NFκB stimulating activity	106
5 APPENDIX	110
6 DISCUSSION	112
6.1 Characterisation of variant Uba2	112
6.2 Identification of a novel SUMO target	113
5.2.1 Identification of a new Aos1 binding partner	113
5.2.2 ELKS is a protein implicated in NFκB signaling and vesicle transport	114
6.3 Identification of additional ELKS and Aos1 binding partners suggest possible functions in vesicle transport and NFκB signaling	117
6.4 ELKS is a new SUMO substrate	118
6.5 SUMO does not change ELKS localisation and Rab6 interaction	119
6.6 ELKS negatively regulates the NFκB signaling pathway	120
6.7 RanBP2-an E3 ligase for ELKS?	122
7 REFERENCES	124
8 ACKNOWLEDGMENTS	139
9 PUBLICATIONS	140
10 CURRICULUM VITAE	141

ABBREVIATIONS

aa	amino acid
Ac	acetat
AP	aprotinin
ATP	adenosine-5'-triphosphate
bp	base pair
BSA	bovine serum albumin
cDNA	complementary DNA
Cys	cysteine
Da	dalton
dNTP	2'-Didesoxynucleosid-5'-triphosphate
ddH₂O	double-distilled water
DEPC	diethyl pyrocarbonate
DMEM	Dulbecco's modified Eagle's medium
DMSO	dimethyl sulfoxide
DTT	dithiothreitol
<i>E. coli</i>	<i>Escherichia coli</i>
ECL	enhanced chemoluminescence
EDTA	ethylenediaminetetraacetic
EGTA	ethyleneglycoltetra acetic acid
FBS	fetal bovine serum
FCS	fetal calf serum
FITC	fluorescein isothiocyanate
FPLC	fast protein liquid chromatography
g	centrifugation force
g	gramm
GFP	green fluorescent protein
GTP	guanosine-5'-triphosphate
h	hour(s)
HA	Hemagglutinin

HEPES	N-(2-Hydroxyethyl)piperazine-N'-(2-ethanesulfonic acid)
His	Histidine
HPLC	high-performance liquid chromatography
IF	immunofluorescence
IgG	immunoglobulin G
IP	immunoprecipitation
IPTG	isopropylthiogalactoside
kb	kilobase(s)
l	liter
L/P	leupeptin/pepstatin
LB	Luria-Bertani-Medium
m	mili
M	molar (mol/l)
min	minute(s)
mRNA	messenger ribonucleic acid
MW	molecular weight
μ	micro
n	nano
nc	nitrocellulose
NCS	newborn calf serum
NEM	N-ethylmaleimide
NFκB	nuclear factor kappa B
NPC	nuclear pore complex
OD	optical density units
ORF	open reading frame
p	pico
PAGE	polyacrylamide gel electrophoresis
pH	potential hydrogen
PBS	phosphate buffered saline
PCR	polymerase chain reaction

RT-PCR	reverse transcription-polymerase chain reaction
pfu	<i>Pyrococcus furiosus</i> (DNA polymerase)
PMSF	phenylmethanesulfonyl fluoride
RIPA	radio-immunoprecipitation assay
RNase	ribonuclease
rpm	revolutions per minute
RT	room temperature
RT-PCR	reverse transcription followed by PCR
<i>S. cerevisiae</i>	<i>Saccharomyces cerevisiae</i>
SDS	sodium dodecyl sulfate
s	second(s)
TB	transport buffer
TEMED	N, N, N',N'-Tetramethylethylenediamine
TNFα	Tumor necrosis factor alpha
Tris	Tris-(hydroxymethyl)-aminomethane
Triton X-100	t-octylphenoxy polyethoxyethanol
Tween 20	polyoxyethylenesorbitan monolaurate
ub	ubiquitin
UV	ultraviolet light
v/v	volume per volume
w/v	weight per volume
V	volt
Vol	volume
WB	Western Blot

1 SUMMARY

Small ubiquitin-related modifier (SUMO) is a protein that is attached to lysine residues in a variety of target proteins. Sumoylation of proteins can alter their intracellular localisation, stability, activity and interaction with other proteins. The pathway of sumoylation is analogous to that of ubiquitination. The reaction is ATP dependent and requires the E1-activating enzyme (Aos1/Uba2), the E2-conjugation enzyme (Ubc9) and for most target proteins SUMO E3 ligases.

The aim of this study was to characterise the SUMO E1 enzyme, a heterodimer consisting of the subunits Aos1 and Uba2. On one hand I characterised an Uba2 splice variant, which lacks one exon encoding 50 amino acids. Using RT-PCR I could determine the tissue specific distribution of the Uba2 splice variant. I furthermore showed that Uba2 variant protein is still able to form an active E1 enzyme complex with Aos1. I could demonstrate that variant Aos1/Uba2 complex is fully active in RanGAP1 sumoylation with SUMO1 or SUMO2. This finding was surprising in light of the missing amino acids, and will have implications for the understanding of E1 function.

A large part of my work was dedicated to the identification and characterization of a novel SUMO substrate called ELKS. According to literature, ELKS proteins have been linked to intracellular membrane traffic and NF κ B signaling pathways. I identified ELKS in membrane fractions as a binding partner for the Aos1 subunit of the SUMO E1 enzyme and confirmed *in vivo* interaction with ELKS antibodies that I generated. Because recombinant proteins did not interact directly, I searched for potential bridging factors. Neither SUMO nor Ubc9 or Rab6 (one ELKS partner) mediated interaction between ELKS and Aos1. Performing a large scale immunoprecipitation and analysis by mass spectrometry, I could find several candidates, including nucleoporin RanBP2, a SUMO E3 ligase. This suggested that ELKS may be a target for sumoylation. Indeed, I could show that ELKS was SUMO-modified *in vivo* and *in vitro*. Moreover, RanBP2 enhanced ELKS sumoylation. By mass spectrometry I identified two SUMO acceptor sites in ELKS. Mutation of these two residues had no effect on ELKS localisation, but strongly inhibited ELKS induced NF κ B activation. In conclusion, work described in this thesis implicates sumoylation as an important mechanism for ELKS function in NF κ B signaling.

2 INTRODUCTION

2.1 Overview

Posttranslational protein modifications

Posttranslational modification of proteins is a fundamental mechanism of modulating their function, activity or localisation after their synthesis has been completed. One class of modifications involves addition of a small chemical group to amino acids, e.g. through phosphorylation, acetylation, ADP ribosylation or methylation, while the second class involves attachment of larger macromolecules, such as polypeptides in the case of ubiquitylation, sumoylation or polysaccharides.

The ubiquitin system is the prototype for a newly recognized family of pathways that result in the covalent modification of target proteins. These systems use different ubiquitin-like proteins, different enzymes, and act on different substrates, but share a common chemistry (Osaka et al., 1998; Hochstrasser, 1998; Mizushima et al., 1998). Modification with ubiquitin was the first identified case where the modifier itself is a small polypeptide. Ubiquitin, a 76-residue protein (8 kDa), is attached through its C terminus to exposed amino groups on proteins in a reaction that involves three enzymes — a ubiquitin activating enzyme (E1), a ubiquitin conjugating enzyme (E2) and a ubiquitin ligase (E3) (Figure 1); (Pickart et al., 2004). ATP is required to form a thioester bond between the C-terminal carboxyl group of ubiquitin and the active site Cys of an E1. The E1 transfers ubiquitin to an E2, which is also linked to ubiquitin through a thiolester bond. E2s bind to specific E3 enzymes that bind directly to the protein substrates. E3s can themselves form a thioester bond with ubiquitin (HECT-domain E3s) before substrate attachment, or can function as a bridge between an activated E2 and its target (RING and U-box E3s). Ubiquitin is usually attached to the ϵ -amino group of a lysine on a target protein through an isopeptide bond (see Figure 1), although ubiquitylation can also occur at the free N-terminus of a protein. Ubiquitylation reactions are reversed by the action of deubiquitylating enzymes (DUBs) of which there are many types (Borodovsky et al., 2001; Amerik et al., 2004).

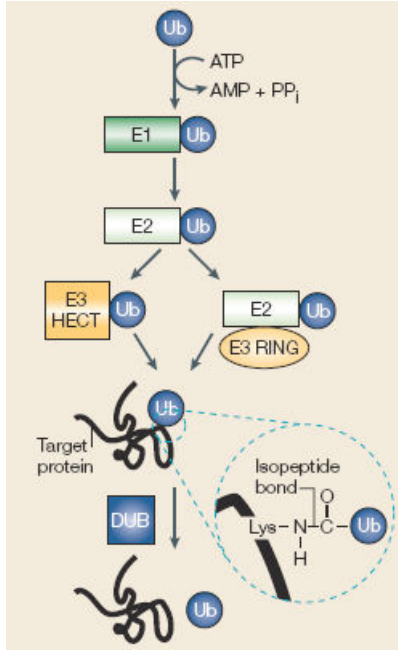


Figure 1. Ubiquitin conjugation. Ubiquitin is activated by the ubiquitin-activating enzyme (E1), and is subsequently transferred to a ubiquitin-conjugating enzyme (E2). In most cases, the E2 enzyme and the protein substrate both bind specifically to a particular ubiquitin-protein ligase (E3), and the activated ubiquitin moiety is then transferred to the protein substrate (From Hicke et al., 2005).

Originally, the major role of ubiquitin was identified with substrate protein degradation by the 26S proteasome (Coux et al., 1996), and characteristic of proteins sent to the proteasome were polyubiquitin chains attached to it. More recently, other functions of ubiquitin have been discovered that do not involve proteasome-dependent proteolysis. Some proteins are modified by a single ubiquitin (monoubiquitylation) or short ubiquitin chains. This modification, instead of sending proteins to their death through the proteasome, regulates processes as diverse as membrane transport, histone regulation, or budding of retroviruses from the plasma membrane (Hershko et al., 1998; Deng et al., 2000; Pickart, 2001; Hicke et al., 2001).

Over the last few years a number of proteins related to ubiquitin have been discovered, the so-called ubiquitin domain proteins (UDPs) and ubiquitin-like proteins (UBLs). Members of the first class, ubiquitin domain proteins do not act as modifiers but instead contain an ubiquitin like domain as part of their linear sequence (Jentsch et al., 2000; Hochstrasser et al., 2000). However, unlike proteins targeted by Lys-48 chains, the UDP does not get degraded. The second class, UBLs, act as posttranslational modifiers in a manner analogous to ubiquitin (Jentsch et al., 2000). This class includes Nedd8 (also

called Rub1), Apg8, Apg12, ISG15, and Small Ubiquitin-like MOdifier protein (SUMO). Each of these class proteins are structurally related (Figure 2). They have the potential to alter the conformation of the target, to convey a new surface to their substrate resulting in the ability to interact with a new partner, or to mask existing binding sites.

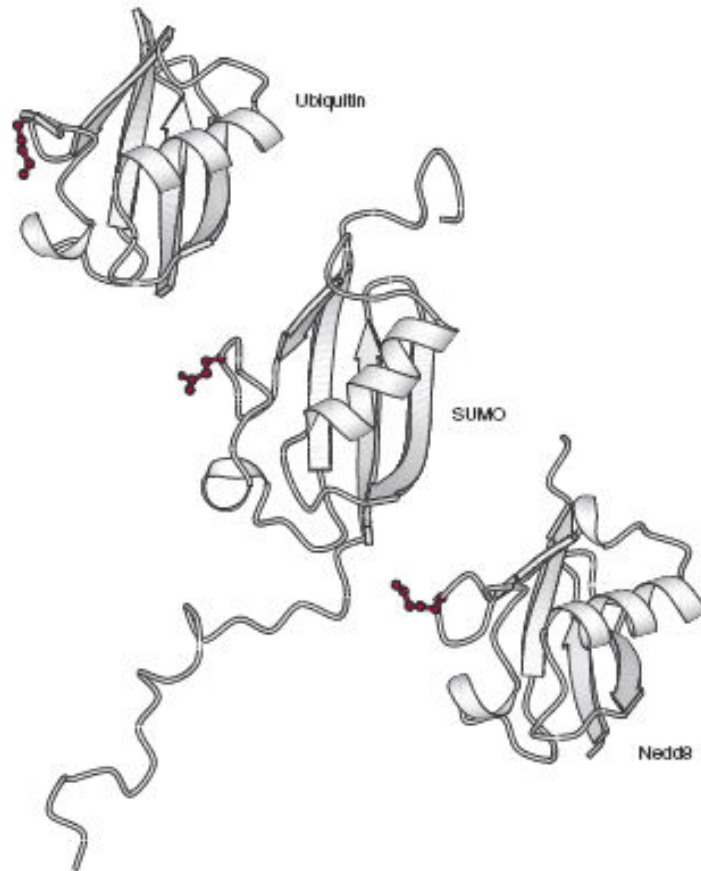


Figure 2. Members of the ubiquitin protein family: Ubiquitin; SUMO Nedd8. (From Walsh Ch., 2005)

The SUMO family

SUMO is probably the most prominent member of the ubiquitin like modifiers (Melchior 2000; Johnson 2004). SUMOs constitute a highly conserved protein family found in all eukaryotes and are required for viability of most eukaryotic cells, including budding yeast, nematodes, fruit flies, and vertebrate cells in culture (Hayashi et al., 2002; Epps et

al., 1998). In multi-cellular organisms, SUMO conjugation takes place in all tissues at all developmental stages. *Saccharomyces cerevisiae* contains only one SUMO homologue, while the mammalian SUMO family consists of four members: SUMO-1, -2, -3 and -4 (Figure 3). SUMO-2 and SUMO-3 are very similar at the amino acid level (87 % sequence identity), but they are only 47 % identical to SUMO-1 (Figure 3). SUMO-1 is a 101 amino acid polypeptide and although it only shows 18% homology to ubiquitin, the three-dimensional structures of both proteins are very similar (Bayer et al., 1998). NMR structure analysis (Bayer et al., 1998) revealed that SUMO-1 contains the characteristic $\beta\beta\alpha\beta\beta\alpha\beta$ ubiquitin fold common to ubiquitin-like proteins (Mayer et al., 1998). Both proteins contain a Gly-Gly-motif at the C-terminus, which is essential for conjugation to target proteins. A characteristic feature for SUMO-1 related proteins is a flexible N-terminal extension of 10-20 amino acids, which is absent in ubiquitin and some other ubiquitin-like proteins (Mahajan et al., 1997; Bayer et al., 1998).

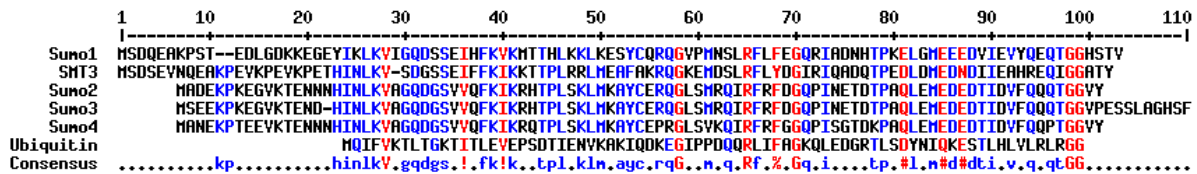


Figure 3. Sequence alignment of SUMO family members and ubiquitin. Sequence comparison of the human SUMO family members (SUMO-1, -2, -3 and -4) to the yeast SUMO homologue SMT3 and to human ubiquitin. Identities are shown in red, similarities in blue.

SUMO conjugation influences the function of its targets in many ways, for example by changing its subcellular localisation, altering their interactions with other macromolecules, regulating protein-protein interactions and/or stability, and finally it promoting assembly of several multi-protein complexes. However, in contrast to ubiquitin SUMO does not target substrates directly for proteasome-dependent proteolysis.

2.2 Molecular mechanism of Sumoylation

2.2.1 Enzymes mediating the SUMO pathway

The pathway of sumoylation is analogous to that of ubiquitination, but SUMO conjugation involves a different set of enzymes (Figure 4). Some of these enzymes such as the SUMO-activating enzyme (E1) and SUMO-conjugating enzyme (E2) show sequence similarity to their counterparts in the ubiquitin system, and are conserved from yeast to humans. Similar to the ubiquitin system, an inactive SUMO is converted to its active form by removal of its last four amino acids to leave two essential glycine residues at the C-terminus. This allows activation by formation of a thioester between the C-terminal glycine of SUMO and a cysteine from the SUMO-activating E1 enzyme (Aos1/Uba2) transfer to a conjugating E2 enzyme (Ubc9), and conjugation to the ϵ -amino group of specific lysine residues on target proteins (Johnson et al., 1997). In most cases, the last step requires SUMO-specific ligases (see figure 4); (Johnson et al., 2002).

Unlike ubiquitin, SUMO is usually targeted to a lysine within a consensus sequence (Φ KXE), where Φ is a hydrophobic amino acid, K the modified lysine, X any amino acid and E a glutamate.

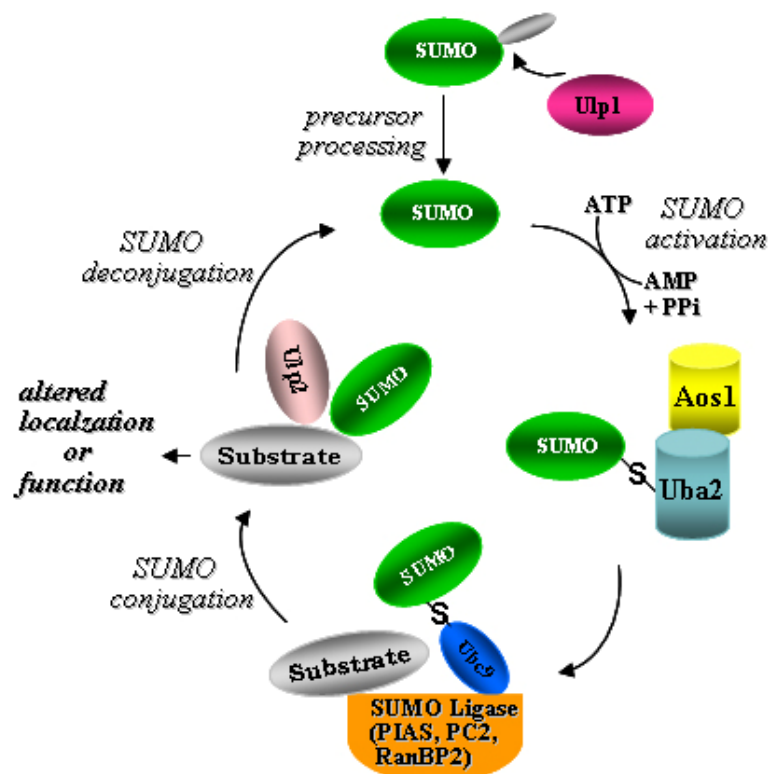


Figure 4. SUMO conjugation/deconjugation cycle. SUMO is synthesized as a precursor and processed by hydrolases to make a double glycine motif available for conjugation. The C-terminus of mature SUMO needs first to be activated by the SUMO activating enzyme (E1), a heterodimeric protein composed of Uba2 and Aos1. Activation is ATP-dependent, proceeds via a SUMO-adenylate intermediate, and results in SUMO being linked by a thioester to a cysteine residue in Uba2. Activated SUMO is then transferred, in a transesterification reaction, to a cysteine residue of Ubc9, a conjugating enzyme (E2) specific for SUMO. In conjunction with SUMO ligases (E3), Ubc9 conjugates SUMO to a variety of substrate proteins. The resulting isopeptide bond is stable and its disruption requires a desumoylating enzyme (From Dohmen et al., 2004).

2.2.2 SUMO-Activating Enzyme (E1)

Most organisms contain a single SUMO-activating enzyme. The *S. cerevisiae* ubiquitin E1 Uba1 is a 90 kDa monomer that contains a cysteine residue in its active site. Uba1 and its homologs from other organisms are very similar to each other (53% identity between *S. cerevisiae* Uba1p and human ubiquitin E1). Their most striking features are two copies of a ~150-residue domain (Figure 5, domain I) that contains a potential nucleotide-binding motif and is also found in several other proteins, such as *E. coli* thiF (Vander Horn et al., 1993) and chlN (Pitterle et al., 1989). The second copy of this domain in E1 is followed directly by a region containing the active site Cys residue (Cys600 in Uba1p) that forms the thioester with ubiquitin (domain III in Figure 5), (Hatfield et al., 1992). Interestingly, the SUMO E1 is a heterodimer composed of Aos1 (SAE1) and Uba2 (SAE2) proteins (Dohmen et al., 1995). Aos1 shares 29% sequence identity with the N-terminal region of the ubiquitin E1. Most of the sequence similarity is found in two separate regions at the N- and C-terminus of Aos1 (domains I and II in Figure 5), (Johnson et al., 1997). Uba2 is similar to the C-terminal region of Uba1, with two regions of greater similarity (domain I/domain III and domain IV in Figure 5). Uba2 contains a Cys residue (Cys173) corresponding to the E1 active site. E1s and Uba2 share another region of high sequence similarity (domain IV), the function of which is unknown. This suggests that Aos1 and Uba2 combine to carry out functions analogous to those performed by the single protein Uba1.

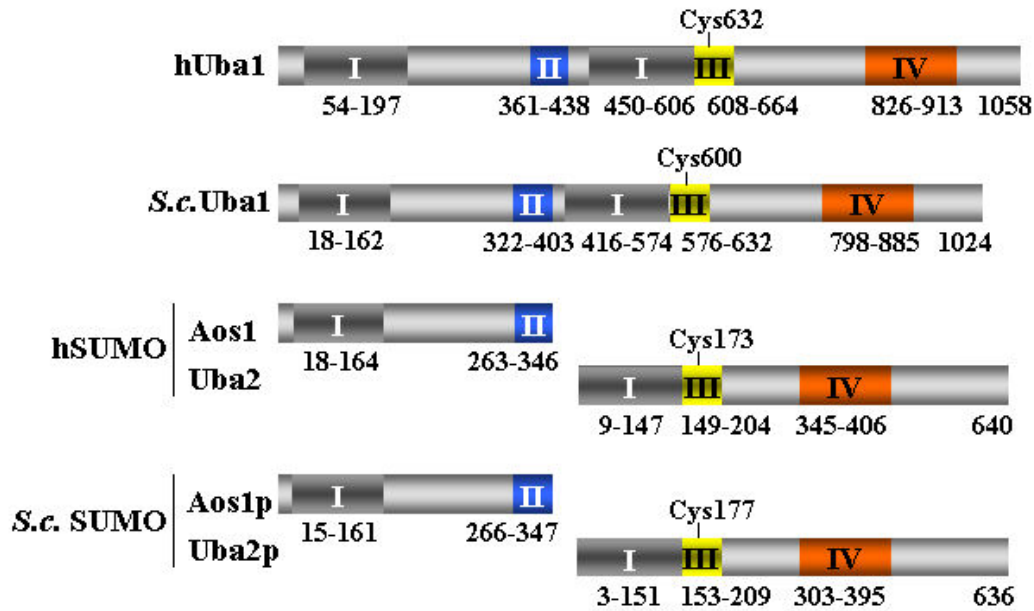


Figure 5. Schematic representation of homologous domains in human ubiquitin E1 enzyme, hUba1; *S. cerevisiae* (*S.c.*) ubiquitin E1, Uba1p; human SUMO-1 activating enzymes, Aos1 (SAE1) and Uba2 (SAE2); *S. cerevisiae* SUMO-activating enzymes, Aos1p and Uba2p. Domain I includes a potential nucleotide-binding motif and is found in a number of proteins, such as *E.coli* thiF and chlNB, not involved in activation of Ub-like proteins. In E1s, domain III contains the active site cysteine residue which forms a thioester with the C-terminus of Ub. SUMO Uba2 shares this domain including the conserved cysteine residue (Cys177). Domains II and IV are each found in several other proteins in addition to E1s, but nothing is known about their functions. Modified from Desterro et al., 1999.

Very recently structures of human heterodimeric Aos1/Uba2-Mg·ATP and Aos1/Uba2-SUMO1-Mg·ATP complexes were determined by Lois and Lima, 2005 (Figure 6 A&B). The structure revealed that Uba2 contains three important domains, the adenylation domain and two additional domains located on either side of the Uba2 adenylation active site (Figure 6). The first was referred to as the catalytic Cys domain (159–386) since it contained Cys173, responsible for E1-SUMO thioester bond formation. The second was termed the UbL or Ubiquitin-Like domain (442–549) due to its structural similarity to Ub and other Ubl modifiers (Lois and Lima, 2005).

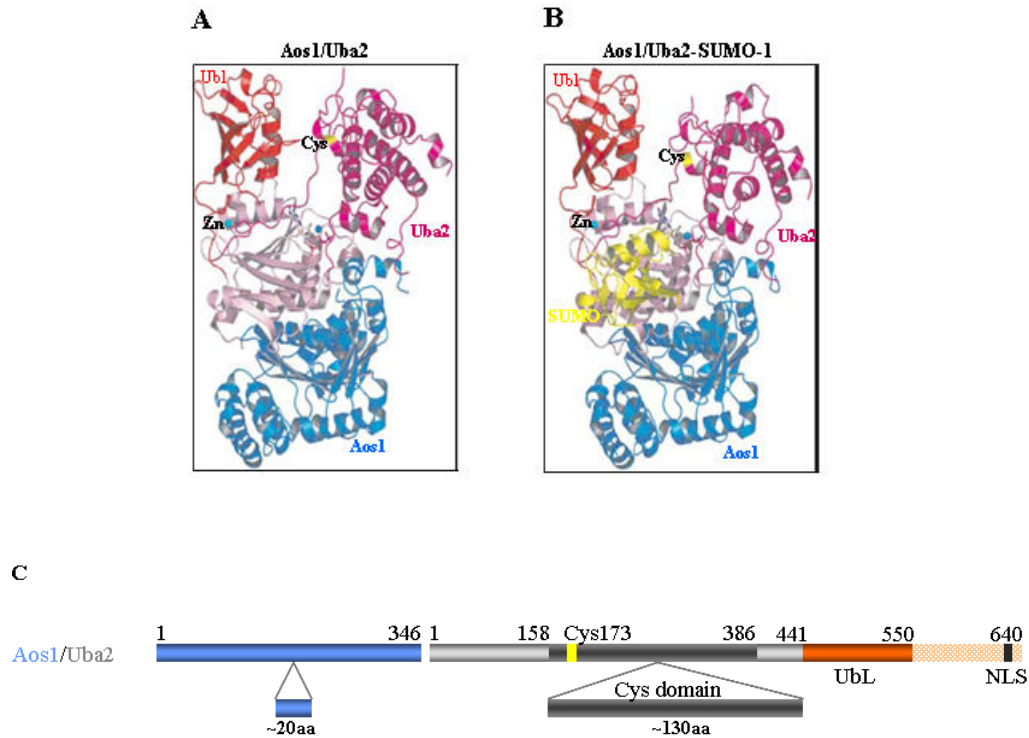


Figure 6. Structure of the SUMO activating enzyme. (A) Ribbon diagram of the Aosl/Uba2 heterodimer. Aosl is colored blue and Uba2 is colored shades of pink, magenta, and red. (B) Ribbon diagram of the Aosl/Uba2-SUMO-1 complex. SUMO is colored yellow. Catalytic Cys and UbL domains are labeled. The active site cysteine is labeled and colored yellow. (C) Schematic representation of Aosl/Uba2. Aosl is showed in blue (1-346 aa) and Uba2 in grey and orange (1-640 aa). From Lois and Lima 2005.

Like the E1 for Ub, the SUMO-activating enzyme (E1) catalyzes a three-part reaction. First, the C-terminal carboxyl group of SUMO attacks ATP, forming a SUMO C-terminal adenylate and releasing pyrophosphate. Next, the thiol group of the active site cysteine in the E1 attacks the SUMO adenylate, releasing AMP and forming a high-energy thioester bond between the E1 and the C terminus of SUMO. Finally, the activated SUMO is transferred to a cysteine in the E2 (Johnson et al., 1997).

Consistent with the functions as an E1 enzyme, most cellular Uba2 and Aosl is found as a heterodimer (Azuma et al., 2001). However, the two-subunit structure of the SUMO E1 suggests that they have additional function and might be regulated separately. Interestingly, levels of human Aosl were found to be regulated during the cell cycle. The level of Aosl protein increased as cells progressed through S phase, followed by a substantial decrease in G2 phase, whereas Uba2 levels remained unchanged during cell

cycle (Azuma et al., 2001). These data suggested that regulation of SUMO activating enzyme might be mediated via Aos1.

The expression pattern of SUMO E1 showed detectable levels of each mRNA in many different mammalian adult and embryo tissues, as well as from cultured cells, indicating that Aos1 and Uba2 are ubiquitously expressed (Azuma et al., 2001).

Both SUMO E1 subunits have been demonstrated to be localised in the cell nuclei with a diffuse localization of species ranging from yeast to mammals (Dohmen et al., 1995; Azuma et al., 2001). However, low level of E1 enzyme is also clearly present in the cytoplasm (Pichler et al., 2002).

In addition to Ubc9 and SUMO, only one other binding partner has been described for the SUMO E1 enzyme. This binding partner is the poly (A) polymerase Pap1, normally responsible for the addition of the adenylate tail to the 3' end of mRNA (del Olmo et al 1997). Uba2 depleted extract was tested in *in vitro* polyadenylation experiments and polyadenylation activity was significantly reduced. This experiment indicated that components of the polyadenylation machinery depend on SUMO modification however, Pap1 was not shown to be modified by SUMO.

2.2.3 SUMO-Conjugating Enzyme (E2)

Ubc9 is the only SUMO-conjugating enzyme in yeast and invertebrates and most likely in vertebrates as well (Hayashi et al., 2002). The presence of only one SUMO E2 contrasts with the Ub pathway where multiple E2s participate in ubiquitylating distinct sets of substrates. Like the genes for SUMO, Aos1 and Uba2, the gene encoding Ubc9 is essential in all organisms tested except *S. pombe* (al-Khodairy et al., 1995; Seufert et al., 1995; Tanaka et al., 1999).

In a transesterification reaction, activated SUMO is transferred from the Uba2 subunit of SUMO-activating enzyme to a single SUMO-conjugating enzyme (E2) known as Ubc9 (Figure 4). As a result, a SUMO-Ubc9 thioester intermediate is formed (Johnson et al., 1997 and Desterro et al., 1997).

Ubc9 is a predominantly nuclear protein (Seufert et al., 1995), but studies on Ubc9 in mammals have shown that at least a fraction of it is present in the cytoplasm and associated with cytoplasmic and nucleoplasmic filaments of the nuclear pore complex (NPC), (Pichler et al., 2002; Zhang et al., 2002). A patch surrounding the active site cysteine of Ubc9 binds directly to the Φ KXE consensus sequence in the substrate (Bernier-Villamor et al., 2002 and Tatham et al., 2003). A second region on Ubc9, separate from the active site, binds directly to SUMO and is involved in transfer of SUMO from E1 (Bencsath et al., 2002). Interestingly, not all of the activities of Ubc9 appear to involve enzymatic activity. For example, Ubc9 mediates nuclear targeting of homeobox protein Vsx-1 via binding to its nuclear localization signal (Kurtzman et al., 2001).

In many studies, mainly using the yeast two-hybrid technique, Ubc9 was found to be an interaction partner of a very large number of proteins, such as p53, Rad51, Rad52, c-Jun or the glucocorticoid receptor. Most of these have turned out to be targets for sumoylation (Gottlicher et al., 1996; Shen et al., 1996).

2.2.4 E3 ligases

Three distinct types of SUMO ligases (E3s) have been discovered recently (reviewed in Johnson 2004; Pichler and Melchior 2004): PIAS (Protein Inhibitor of Activated STAT family), originally discovered as inhibitors of STAT transcription factors (Shuai et al., 2002), RanBP2 (Ran Binding Protein), (Pichler et al., 2002) and PC2 (polycomb group protein), (Kagey et al., 2003). These proteins are identified as E3 enzymes because they promote transfer of SUMO from the E2 to the substrate (Hershko et al., 1998).

PIAS

The eukaryotic family of PIAS proteins is evolutionarily conserved from yeast to humans. In yeast *S. cerevisiae* only two members of this family (Siz1/Siz2) were found, while in higher eukaryotes this family is more diversified. The human family of PIAS

proteins consists of at least five members, PIAS1, PIAS3, the α and β splice variants of PIASx, and PIASy (Shuai et al., 2002).

All mammalian PIAS share a characteristic domain structure that is schematically shown in Figure 7. Within the N-terminus of PIAS a region of about 35 amino acids spans a so called SAP module (Figure 7) (Aravind et al., 2000). A common feature of SAP-containing proteins is their ability to bind to chromatin. Another characteristic feature of PIAS proteins is the presence of a cysteine/histidine-rich domain, known as Miz-zinc finger or SP-RING domain (Hochstrasser M. 2001, Jackson P. K 2001; Pichler and Melchior, 2004).

Work by several laboratories demonstrated that all mammalian PIAS proteins exert SUMO-ligase activity towards various mammalian SUMO-target proteins (eg. Sachdev et al., 2001; Sapetschnig et al., 2002). Importantly, PIAS proteins themselves are covalently modified by SUMO in a process that also requires the integrity of the SP-RING domain (Schmidt et al., 2002 and Kotaja et al., 2002).

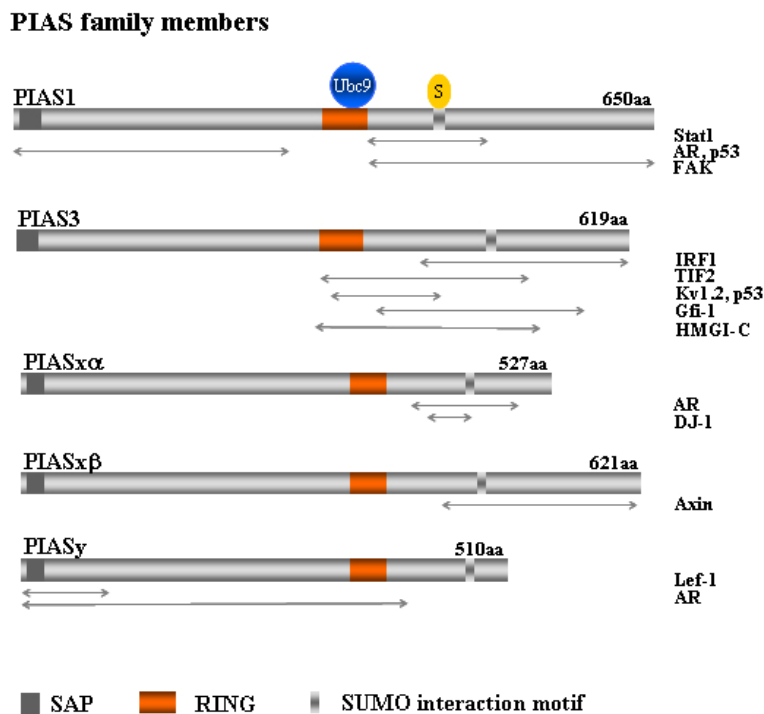


Figure 7. Human PIAS family members. PIAS contain an N-terminal SAP domain, a SP-RING believed to be the Ubc9 interaction site, and a SUMO binding motif. Arrowheads indicate mapped substrate interaction domains [PIAS1: Stat1 (Liao et al., 2000), AR (Tan et al., 2000), p53 (Kahyo et al., 2001), and FAK

(Kadare et al., 2003); PIAS3: IRF1 (Nakagawa et al., 2002), TIF2 (Jimenez-Lara et al., 2002), Kv1,2 (Kuryshv et al., 2000), p53 (Wible et al., 2002), Gfi -1 (Rodel et al., 2000), and HMG-C (Zentner et al., 2001); PIAS α : AR (Moilanen et al., 1999) and DJ-1 (Takahashi et al., 2001), PIAS β : Axin (Rui et al., 2002); and PIAS γ : LEF-1 (Sachdev et al., 2001) and AR (Gross et al., 2001)]. Modified from Pichler and Melchior 2004.

PIAS1 and PIAS3 are found in all cell types, whereas PIAS α and PIAS γ appear to be expressed primarily in testis (Chung et al., 1997; Gross et al., 2001). PIAS α , PIAS β , PIAS γ , PIAS1, and PIAS3 all enrich in intranuclear dots, which are, at least in part, PML nuclear bodies (Sachdev et al., 2001; Kotaja et al., 2002; Miyauchi et al., 2002). In addition, they localise to the nucleoplasm and at low levels in the cytoplasm.

Sumoylation of many substrates can be stimulated by several different PIAS proteins, upon overexpression both in cells and *in vitro*. More recently, mammalian PIAS proteins have been shown to induce sumoylation of the androgen receptor (Nishida et al., 2002), STAT1 (Ungureanu *et al.*, 2003), MDM2 (Miyauchi *et al.*, 2002), Smad4 (Lee *et al.*, 2003), p53 and c-Jun (Schmidt and Muller, 2002), thereby mostly suppressing the transactivating properties of these transcription factors.

RanBP2

A second type of SUMO E3 is the nucleoporin RanBP2/Nup358 (Pichler et al., 2002). RanBP2, a 358 kDa protein, is a core component of the cytoplasmic filaments of nuclear pore complexes (Wu et al., 1995; Yokoyama et al., 1995), where it interacts with sumoylated RanGAP. RanBP2 was itself one of the first SUMO targets to be identified (Saitoh et al., 1998). RanBP2 contains multiple domains including an N-terminal leucine rich domain, four binding domains for the small GTPase Ran, a zinc finger domain, two 50 amino acid internal repeats (IR1 and IR2), a cyclophilin like domain, and multiple FG repeats. Detailed characterisation revealed that the SUMO E3 activity resides in a ~30-kDa domain including the internal repeat (IR) domain (Figure 8). This domain shares no obvious primary or tertiary structural homology with any other known E3 ligase (Pichler et al., 2004; Tatham et al., 2005; Reverter et al., 2005).

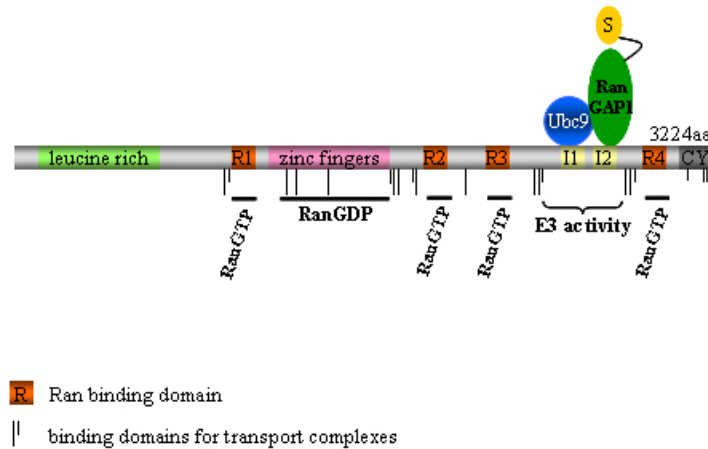
RanBP2

Figure 8. Architecture of RanBP2. Domain structure of RanBP2. Domains implicated in binding to components of the Ran pathway or SUMO1 conjugation machinery are indicated. For more details, see Yokoyama et al. (1995), Saitoh et al. (1998), Matunis et al. (1998), Yaseen et al., 1999 and Pichler and Melchior 2004).

In addition to having the capacity to act as an E3 in the sumoylation of several proteins, the IR domain forms a stable trimeric complex with SUMO-RanGAP1 and Ubc9, and thus it is responsible for the localisation of SUMO-RanGAP1 to the nuclear pore (Saitoh et al., 1997; Matunis et al., 1998). This domain in the presence of E1, E2, SUMO and ATP was sufficient to mediate *in vitro* sumoylation of Sp100 and HDAC4 (Pichler et al., 2002 and Kirsh et al., 2002), but *in vivo* targets are still unknown.

Pc2

A third reported E3 for SUMO is the polycomb group (PcG) protein Pc2 (Kagey et al., 2003). PcG proteins form large multimeric complexes, which are microscopically detectable as discrete foci, so-called PcG bodies within cell nuclei (Figure 9b). Pc2 contains an N-terminal chromatin organization modifier (chromo) domain and a C-terminal “C-box”, but are otherwise unrelated. Whereas the chromodomain is responsible for chromatin binding, the C-box is required for gene repression (Figure 9a). The human PcG protein PC2 recruits the transcriptional co-repressor CtBP as well as Ubc9 to PcG

bodies, and stimulates CtBP sumoylation *in vivo* and *in vitro* (Kagey et al., 2003). Similar to PIAS and RanBP2, PC2 itself is modified by sumoylation (Kagey et al., 2003).

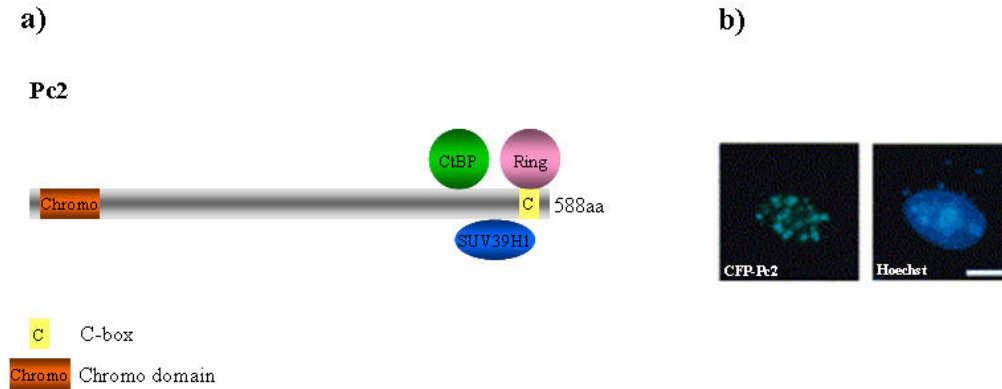


Figure 9. a) Schematic domain of Pc2. Pc2 contains an N-terminal chromodomain and a C-terminal “C-box”. Interaction sites for CtBP, RING1 and SUV39H1 are indicated (Pichler and Melchior 2004). b) Illustration of polycomb bodies inside the nucleus in COS-1 cells. Immunofluorescence picture taken from Kagey et al., 2003.

2.2.5 SUMO processing and deconjugation

SUMO cleaving enzymes play important roles at two critical steps in the SUMO cycle (Figure 4). They remove SUMO from proteins, making the modification reversible, and they also provide a source of free SUMO to be used for conjugation to other proteins. Free SUMO is generated both from newly synthesized SUMO, which must be cleaved to remove a short C-terminal peptide, and from desumoylation of existing conjugates. Two “ubiquitin-like modifier proteases”, Ulp1 and Ulp2, were found in *S. cerevisiae* (Figure 3). SUMO-cleaving enzymes contain a ~200 amino acid domain located at the C-terminus (the Ulp domain) that contains the SUMO cleaving activity (Mossesova et al., 2000). The Ulp domain does not share sequence similarity with the enzymes that cleave Ub. Instead, it is related to a number of viral proteases (Li et al., 1999). The different SUMO-cleaving enzymes have varying N-terminal domains, which are apparently regulatory and target the enzymes to different parts of the cell (Panse et al., 2003; Hang et

al., 2002). Ulp1 localises to the nuclear pore complex and is required to cleave both the SUMO precursor and SUMO conjugates from other proteins; whereas Ulp2 localises to the nucleus and does not cleave the precursor. Additionally Ulp2 appears to desumoylate a distinct set of conjugates (Li et al., 1999; Schwienhorst et al., 2000; Li et al., 2000).

To date seven Ulp1-related proteins with similar sequences have been identified in human cells, namely SENP1, 2, 3, 5, 6, 7 and 8 (Yeh et al., 2000). Of these, SENP1, SENP2 (also designed Axam, SuPr-1, SSP3, and SMT3IP2), and SENP6 have been shown to have SUMO processing or deconjugating activity *in vitro* (Gong et al., 2000; Hang et al, 2002; Kim et al., 2000). However, SENP8 has recently been shown to encode a de-neddylating activity and not a de-sumoylating activity (Gan-Erdene et al., 2003; Mendoza et al., 2003). SENP1 is nuclear and SENP3 is a nucleolar localised protein. In contrast SENP2 generated by differential splicing is found in cytoplasm, nuclear pore, and nuclear body.

2.3 Function of SUMO modifications

Many of the known targets of sumoylation are nuclear proteins with important roles in regulating transcription, chromatin structure, and DNA repair. Furthermore, the nuclear targets of many signaling pathways (such as TGF β , wnt, and cytokine signaling) are posttranslationally modified by SUMO. Examples of proteins known to be modified by SUMO are shown in Figure 10.

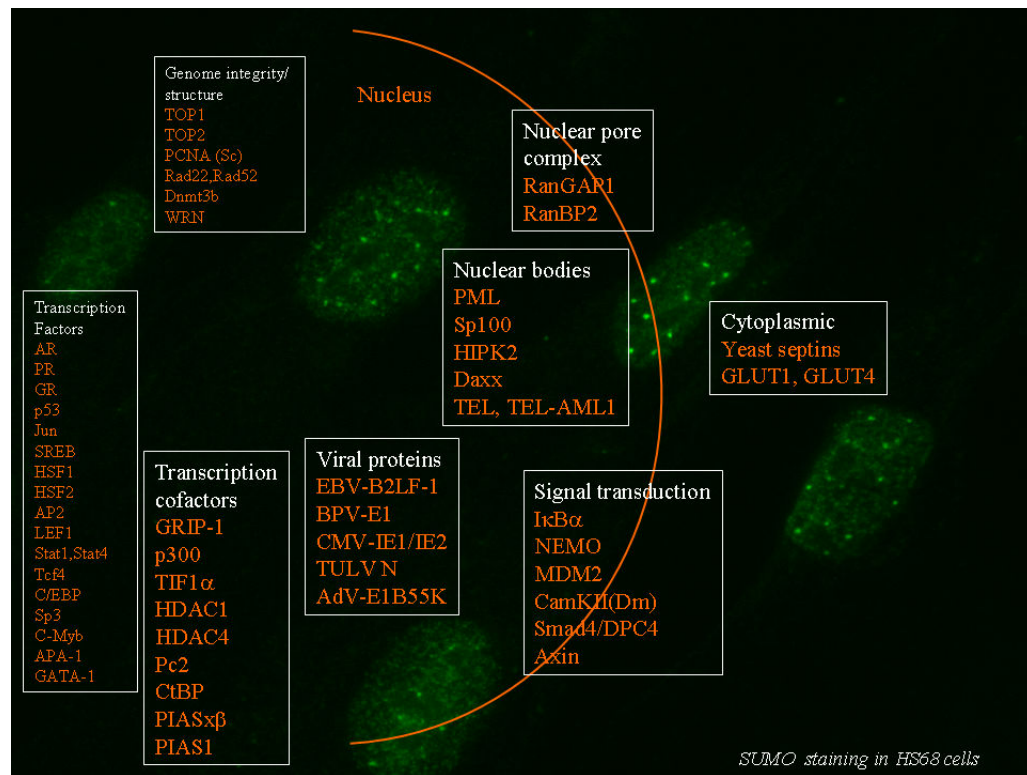


Figure 10. SUMO substrates grouped by function. Many SUMO modified proteins function in regulation of transcription, chromatin structure, maintenance of the genome, and signal transduction. (Modified from Seeler and Dejean 2003).

2.3.1 Molecular consequences of sumoylation

The effects of SUMO modification are diverse and appear to be substrate dependent. Molecular consequences of sumoylation include: a) inhibition of protein-protein interaction, b) promotion of protein-protein interaction and c) alteration of protein-DNA interaction. Phenotypically, this can result in changes of intracellular location, stability or activity. Examples are described below.

Inhibition of protein-protein interaction

Masking of a binding site upon sumoylation was shown recently for the association between CtBP (C-terminal binding protein of adenovirus E1A) and the PZD domain of nNOS protein. CtBP is a corepressor that is often associated with transcription repressors via a PxDSL motif (Boyd et al., 1993; Schaeper et al., 1995). It is usually nuclear, but

interaction with nNOS traps it in the cytoplasm (Lin X et al., 2003). Consistent with this, mutation of the SUMO acceptor site in CtBP resulted in its relocalisation from the nucleus to the cytoplasm. On a molecular level, SUMO attachment interferes with CtBP-nNOS interaction.

Promotion of protein-protein interaction

RanGAP1 was the first protein shown to be covalently modified by SUMO-1 (Matunis et al., 1996; Mahajan et al., 1997). Unmodified RanGAP1 is cytoplasmic, whereas SUMO-1 modification of RanGAP1 directs it to the nuclear pore complex (NPC). This is due to direct binding of sumoylated RanGAP1 to the nucleoporin RanBP2 (Mahajan et al., 1998; Matunis et al., 1998; Joseph et al., 2002). Recent studies revealed that this is not due to a conformation change, but rather sumoylation has been hypothesized to expose or create a new binding site on the C-terminal domain of RanGAP1 for RanBP2 (Matunis et al., 1998; Macauley et al., 2004).

Alteration of protein-DNA interaction

An interesting SUMO target is the thymine DNA glycosylase (TDG), a base excision repair enzyme that removes thymine or uracil from T·G or U·G mismatched base pairs (Hardeland et al., 2002; Baba D et al., 2005). Molecular mechanism of SUMO modification mediated modulation of enzymatic properties of TDG following that the enzyme became incapable of acting as a thymine-DNA glycosylase on a G·T substrate instead it showed enhanced uracil processing on a G·U substrate. A conformational change involving the N-terminal domain of TDG allows for non specific interactions with DNA that facilitate processing of substrates at the expense of enzymatic turnover. Sumoylation then reverses this structural change in the product bound TDG (Steinacher et al., 2005).

2.3.2 Pathways in which SUMO was found

Sumoylation contributes to a large number of cellular pathways, but is especially prominent in DNA repair, transcriptional regulation, signal transduction, and nucleocytoplasmic transport and many others. Some well-known examples will be described briefly.

DNA damage repair

PCNA (proliferating cell nuclear antigen) is exquisitely modulated by covalent post-translational modifications involving ubiquitin and the ubiquitin-related protein SUMO. After DNA damage activities of RAD6 and RAD18 result in the monoubiquitination of PCNA on K164, whereas activities of MMS2, UBC13, and RAD5 result in the formation of K63-linked polyubiquitin chains on K164 of PCNA. Ubiquitylation of PCNA appears not to target it for degradation but to activate it for participation in DNA repair processes mediated by the translation polymerase η and ζ (Stelter et al., 2003). Interestingly, K164 also serves as the acceptor lysine for SUMO attachment (Hoegge et al., 2002). As would be expected if SUMO is blocking ubiquitylation, genetic evidence indicates that SUMO conjugation inhibits damage-induced DNA repair and mutagenesis (Hoegge et al., 2002; Stelter et al., 2003).

SUMO as an ubiquitin antagonist

An antagonistic role for SUMO in ubiquitylation has first been reported in a study on I κ B α (Desterro et al., 1998). In unstimulated cells the NF κ B transcription factors are maintained in an inactive state by I κ B inhibitor proteins. In response to activation signals such as TNF α or PMA, I κ B α undergoes polyubiquitination at lysines 21 and 22 and is targeted for proteasome-mediated degradation, thereby releasing NF κ B family members. However, I κ B α is also modified by SUMO-1 on lysine 21, thus blocking ubiquitination and stabilizing the protein (Desterro et al., 1998).

An analogous system includes the inhibition of ubiquitin-dependent degradation of CREB (cAMP response element binding protein) by sumoylation after hypoxia (Comerford et al., 2003). Hypoxia results in a rapid phosphorylation-dependent degradation of CREB. This in turn triggers the induction of proinflammatory genes such as TNF α , leading to the activation of NF- κ B. However, prolonged treatment with

hypoxia conditions increases the amounts of sumoylated CREB and I κ B α . Additionally, overexpression of SUMO-1 stabilizes CREB in hypoxia. The same study demonstrated that SUMO-1 is transcriptionally induced in hypoxia. Based on these data, Comerford et al. proposed that SUMO-1 modification may represent a general anti-inflammatory signal that provides an “off switch” to the inflammatory response by stabilizing certain regulators and by nuclear targeting of others.

SUMO in transcription

SUMO modification of transcription factors can lead to transcriptional activation but is more often associated with transcriptional repression (Gill et al., 2004). An example of a mechanism by which an activator is turned into a repressor was observed for Elk-1. This transcriptional activator acts together with SRF (Serum Response Factor) in response to mitogenic stimulation. SUMO-modified Elk-1, however, recruits histone acetylase HDAC2 to promoters, which results in transcriptional repression (Yang et al., 2004). In contrast, removal of SUMO by mutation of the transcription factor Sp3 acceptor lysines or cotransfection with a SUMO protease dramatically increased transcriptional activity of Sp3 (Ross et al., 2002; Sapetschnig et al., 2002). This suggests that SUMO modification may contribute to the complex activity of Sp3, which has long been known to function as both an activator and a repressor of transcription dependent on context.

Another interesting example are diverse transcription factors with “synergy control motifs,” which were originally identified in the glucocorticoid receptor (GR) as peptide motifs that reduce GR-dependent transcription from promoters containing multiple GR binding elements (Iñiguez-Lluhi et al., 2000). The critical feature of synergy control motifs is a Φ KXE sequence, and these sites are sumoylated, suggesting that SUMO attachment reduces the positive synergistic effect of having multiple transcription factors bound to the same promoter (Iñiguez-Lluhi et al., 2000; Tian et al., 2002).

The work described in this thesis identified and characterised a novel SUMO substrate, called ELKS. ELKS has been linked to vesicle transport at the level of the Golgi complex (Monier et al., 2002). I could demonstrate that ELKS was modified with SUMO *in vivo* and *in vitro*, and suggest for the first time that this modification could be involved in vesicletransport.

3 MATERIALS AND METHODS

3.1 MATERIALS

3.1.1 Chemicals and materials

Materials for filtration and dialysis

Centricon 5K, 10K, 30K, 50K	Milipore, Eschborn
MF-milipore membrane filter	Sigma-Aldrich, Taufkirchen
UH 100/10 and 30 Ultrahülsen	Schleicher& Schuell, Dassel
Whatman 3 MM, Filter paper	Maidstone, England
Centrifugation Filter 5K, 10K, 30K	Sigma-Aldrich, Taufkirchen

Chromatography matrices

CNBr-Sepharose 4B	Sigma-Aldrich, Taufkirchen
Glutathion Sepharose 4B	Amersham Pharmacia Biotech, Freiburg
Ni-Nitrilotriacetic Acid (NTA)-Agarose	Qiagen, Hiden
Sepharose-Q (FF)	Sigma-Aldrich, Taufkirchen
Superdex 75 HR 10/30	Amersham Pharmacia Biotech, Freiburg
Superdex 200 HR 10/30	Amersham Pharmacia Biotech, Freiburg
Superdex 200 pg HiLoad	Amersham Pharmacia Biotech, Freiburg

Protein and DNA markers

BenchMark™ Protein Ladder	Life Technologies, Karlsruhe
Protein Ladder, 10-200 kDa	MBI Fermantas, St. Leon Rot
Prestained Protein Ladder, 10-180 kDa	MBI Fermantas, St. Leon Rot
Gene Ruler 100bp Ladder Plus	MBI Fermantas, St. Leon Rot
Gene Ruler 1kb Ladder Plus	MBI Fermantas, St. Leon Rot

Transfer membrane

Hybond-N+

Nylon Transfer Membrane (0,45 µm) Amersham Pharmacia Biotech, Freiburg

PROTRAN

NC Transfer Membrane (0,45 µm) Schleicher& Schuell, Dassel

Imaging film

Amersham Pharmacia Biotech, Freiburg

TM: Kodak, Biomax, USA

3.1.2 Reagents and reactions kits

Big Dye Terminator

Cycle Sequencing RR-Mix Applied Biosystems, Foster City, USA

Desoxynucleotide Set Sigma-Aldrich, Taufkirchen

Freund's Adjuvant (incomplete) Sigma-Aldrich, Taufkirchen

HiSpeed™ Plasmid Midi Kit Qiagen, Hilden

Micro BCA Protein Assay Reagent Kit Pierce, Rockford, USA

Mounting Medium Molecular Probes, Eugene, USA

Polyfect Transfection Reagent Qiagen, Hilden

Protoscript First Strand cDNA Synthesis Kit New England Biolabs

QIAGEN Plasmid Kit (Midi, Maxi) Qiagen, Hilden

QIAGEN Gel Extraction Kit Qiagen, Hilden

Rotiphorese Gel 30 Roth, Kalsruhe

Super Signal West Femto Maximum Sensitivity Substrate Pierce, Rockford, USA

Super Signal West Pico Maximum Sensitivity Substrate Pierce, Rockford, USA

TiterMax Gold, Adjuvant Sigma-Aldrich, Taufkirchen

Trizol® Reagent Life Technologies

3.1.3 Buffers and solutions

ATP: 100 mM ATP, 100 mM Mg(OAc)₂, 20 mM HEPES, pH 7,4

BufferA: 5 mM HEPES-KOH (pH 7.3); 10mM KOAc, 2 mM Mg [OAc]₂, 1 mM DTT

Buffer 1: 6 M Guanidinium/HCl, 0.1 M Na₂HPO₄/NaHPO₄, (pH 6.3) or (pH 8.0)

Blocking Buffer (IF): 2% (w/v) BSA in PBS

Blocking Buffer (WB): 5% (w/v) milk powder in PBS, 0.2% Tween

Coomassie staining: 50% (v/v) Methanol, 10% (v/v) acidic acid, 0.1% (w/v) SERVA Blue R (SERVA)

Coomassie destainer: 50% (v/v) Methanol, 10% (v/v) acidic acid

Carbonate Buffer: 0.2 M Na₂HPO₄ (pH 8.9)

DNA Loading Buffer 6×: 10 mM Tris/HCl (pH 8.0), 50 mM EDTA, 1% (w/v) SDS, 30% (w/v) Glycerine, 0.1% (w/v) Bromophenolblue

Elution buffer: 50 mM Na-Phosphate pH 8.0, 300 mM NaCl, 300 mM Imidazol, 1 mM β-Mercaptoethanol, 1 μg/ml each of AP, L/P

Glutathione Elution Buffer: 50 mM Tris/HCl, 20 mM Glutathione, 150 mM NaCl, pH 8.0

Hypothonic Buffer: 10 mM Tris/HCl (pH 7.9), 10 mM KCl, 0.1 mM EDTA, 0.1 mM EGTA, 2 mM DTT

IP Buffer: 0.1% Triton X-100, 50 mM Tris/HCl (pH 7.4), 300 mM NaCl, 5 mM EDTA

Lysis Buffer: 50 mM Na-Phosphate pH 8.0, 300 mM NaCl, 10 mM Imidazol

P1: 50 mM Tris/HCl, 10 mM EDTA, 100 µg/ml RNase A, pH 8.0

P2: 200 mM NaOH, 1% (w/v) SDS

P3: 3 M K-Acetat, pH 5.5

PFA: 2% (w/v) Paraformaldehyde in PBS, pH 7.4

PBS: 140 mM NaCl, 2.7 mM KCl, 10 mM Na₂HPO₄, 1.8 mM KH₂PO₄, titrate with NaOH pH 7.5

PBS-T: 0.2% (w/v) Tween 20 in PBS

Ponceau S: 0.5% (w/v) Ponceau S, 1% (v/v) acedic acid

Q buffer 1: 50 mM Tris pH 7.5, 50 mM NaCl, 1 mM DTT, 1 µg/ml each of AP, L/P

Q buffer 2: 50 mM Tris pH 7.5, 1 M NaCl, 1 mM DTT, 1 µg/ml each of AP, L/P

RIPA Buffer: 50 mM Tris/HCl, 150 mM NaCl, 1 mM EDTA, 1% (v/v) Nonidet P-40, 0.25% (w/v), Sodiumdeoxycholate, 0.1% (w/v) SDS, pH 7.5

SDS Electrophoresis Buffer: 25 mM Tris, 192 mM Glycine, 0.1% (w/v) SDS

SDS Sample Buffer 10×: 209 mM Tris/HCl (pH 6.8), 41% (w/v) Glycerine, 7.7% (w/v) SDS, 0.2% (w/v) Bromophenolblue, 17% (v/v) β-Mercaptoethanol

SDS Sample Buffer 2×: 100 mM Tris/HCl (pH 6.8), 20% (w/v) Glycerine, 4% (w/v) SDS, 0.2% (w/v) Bromophenolblue, 200 mM DTT

SDS Sample Buffer 1×: 50 mM Tris/HCl (pH 6.8), 10% (w/v) Glycerine, 2% (w/v) SDS, 0.1% (w/v) Bromophenolblue, 100 mM DTT

S200 buffer: 50 mM Tris pH 7.5, 50 mM NaCl, 1 mM DTT, 1 µg/ml each of AP, L/P

TAE, 50×: 2 M Tris, 57.1% (v/v) acetic acid, 0.05 M EDTA, titrate with HCl pH 7.7

Transfer Buffer: 47.9 mM Tris, 38.6 mM Glycine, 0.037% (w/v) SDS, 20% (v/v) Methanol

Transport Buffer: 200 mM HEPES (pH 7.3), 1.1 M KOAc, 20 mM Mg(OAc)₂, 10 mM EGTA, titrate with KOH pH 7.3

Triton X-100 Solution: 0.2% (w/v) Triton X-100 in PBS

Wash Buffer: 10 mM HEPES-KOH (pH 7.3), 110 mM KOAc, 2 mM Mg[OAc]₂

Wash buffer: 50 mM Na-Phosphate pH 8.0, 300 mM NaCl, 20 mM Imidazol, 1 mM β-Mercaptoethanol, 1 µg/ml each of AP, L/P

3.1.4 Cell culture

Components

Dulbecco's Modified Eagle's Medium (DMEM)

with 4,5 g/l Glucose

Life Technologies, Karlsruhe

DMEM plus 4500 mg/ml Glucose

Life Technologies, Karlsruhe

Fetal Calve Serum (FCS)

Sigma-Aldrich, Taufkirchen

L-Glutamin, 100×

Life Technologies, Karlsruhe

Joklik's Medium

Life Technologies, Karlsruhe

Natrium pyruvate, 100×

Life Technologies, Karlsruhe

New Born Calve Serum

Sigma-Aldrich, Taufkirchen

Penicillin/Streptomycin, 100×

Life Technologies, Karlsruhe

Trypsin/EDTA, 10×

Life Technologies, Karlsruhe

3.1.4.2 Cell culture medium

HeLa Suspension Cells

Joklik's Medium plus 2 g/l NaHCO₃,
2.38 g/l HEPES, pH 7.1, 5% (v/v) NCS,

	100 U/ml Penicillin, 100µg/ml Streptomycin 1mM Natriumpyruvate
Adherent cells:	DMEM plus 4.5 g/l Glukose, 10% (v/v) FCS
HeLa, Hs68, 293T	100 U/ml Penicillin, 100µg/ml Streptomycin 1mM Natriumpyruvate

Bacteria expression medium

LB-medium 1%(w/v) Bactotrypton, 0,5% (w/v) Yeast extract, 1% (w/v) NaCl
 Selection medium contain 50 µg/ml ampicilin or 30 µg/ml kanamycin

3.1.5 Antibodies

Primary antibodies

Antibody	Abreviation	Species	Source
anti-Aos1	αAos1	goat	AG Melchior MPI for Biochemistry, Martinsried
anti-clathrin	αclathrin	mouse	BD Transduction Laboratories
anti-EEA1	αEEA1	mouse	BD Transduction Laboratories
anti-ELKS (N-terminal)	αELKS	rabbit	AG Melchior MPI for Biochemistry, Martinsried
anti-ELKS (C-terminal)	αELKS	rabbit	AG Melchior MPI for Biochemistry, Martinsried
anti-GFP	αGFP	rabbit	Santa Cruz Biotechnology, Heidelberg
Anti-GM130	αGM130	mouse	BD Transduction Laboratories
anti-GST	αGST	rabbit	AG Hengst MPI for Biochemistry, Martinsried
anti-LAMP1	αLAMP1 (1D4B)	rat	The Developmental Studies Hybrydoma Bank The University of Iowa, USA
anti-HA (clone 16B12)	αHA	mouse	BAbCo Richmond, USA
anti-His	αHis	rabbit	Santa Cruz Biotechnology, Heidelberg

anti-myc	α Myc	mouse	Alexis Biochemielas
anti-Rab6	α Rab6	rabbit	Santa Cruz Biotechnology, Heidelberg
anti-RanGAP1	α RanGAP1	goat	AG Melchior MPI for Biochemistry, Martinsried
anti-SUMO-1	α SUMO1	goat	AG Melchior MPI for Biochemistry, Martinsried
anti-SUMO-2/3	α SUMO2	goat	AG Melchior MPI for Biochemistry, Martinsried
anti-Uba2	α Uba2	goat	AG Melchior MPI for Biochemistry, Martinsried
anti-Ubc9	α Ubc9	goat	AG Melchior MPI for Biochemistry, Martinsried

Secondary antibodies

Antibody	conjugated with	Species	Source
anti-goat IgG, (H+L)	Peroxidase	Donkey	Jackson Immuno Research Laboratories, West Grove, USA
anti-mouse IgG, (H+L)	Peroxidase	Goat	Jackson Immuno Research Laboratories, West Grove, USA
anti-rabbit IgG, (H+L)	Peroxidase	Goat	Jackson Immuno Research Laboratories, West Grove, USA
anti-mouse IgG, (H+L)	Cyt TM 3	Donkey	Jackson Immuno Research Laboratories, West Grove, USA
anti-rabbit IgG, (H+L)	Cyt TM 2	Donkey	Jackson Immuno Research Laboratories, West Grove, USA
anti-mouse IgG, (H+L)	FITC	Goat	Jackson Immuno Research Laboratories, West Grove, USA
anti-rabbit IgG, (H+L)	FITC	Goat	Jackson Immuno Research Laboratories, West Grove, USA
anti-goat IgG, (H+L)	Alexa Fluor	Donkey	Molecular Probes Oregon, USA
anti-mouse IgG, (H+L)	Alexa Fluor	Goat	Molecular Probes Oregon, USA

3.1.6 Recombinant proteins

CFP-mRanGAP1tail (AS 400-589) pET-11d	AG Melchior, MPI for Biochemistry, Martinsried
GST-hRanBP2 IR1+M (AS 2633-2711) pGEX-2T	AG Melchior, MPI for Biochemistry, Martinsried
GST-hRanBP2ΔFG (AS 2553-2838) pGEX-3x	AG Melchior, MPI for Biochemistry, Martinsried
GST-mELKS (AS 1-3365) pGEX-4T-1	AG Melchior, MPI for Biochemistry, Martinsried
His-hAos1 (AS 1-380) pET-28a	PCR amplification from EST clone DKFZp434J0913 AG Melchior, MPI for Biochemistry, Martinsried
hSUMO1ΔC4 (AS 1-97) pET-11a	AG Melchior, MPI for Biochemistry, Martinsried
hUba2 (AS 1-660) pET-28a	PCR amplification from EST clone DKFZp434D0717 AG Melchior, MPI for Biochemistry, Martinsried
hUba2 (AS 1-660) pET-11d	PCR amplification from EST clone DKFZp434D0717 AG Melchior, MPI for Biochemistry, Martinsried
mUbc9 (AS 1-158) pET-23a	PCR amplification from EST clone IMAGp998A061122 AG Melchior, MPI for Biochemistry, Martinsried
mRanGAP1 (AS 1-589) pET-11d	AG Melchior, MPI for Biochemistry, Martinsried
YFP- hSUMO1ΔC4 (AS 1-97) pET-11d	AG Melchior, MPI for Biochemistry, Martinsried
His-mELKS (AS 1-3365) pET-28a	AG Melchior, MPI for Biochemistry, Martinsried

3.1.7 Plasmids

Eucaryotic expression vectors

HA
His } pCruz
Myc }

Invitrogen, Groningen, Niederlande

pGEX-4T-1

Amersham Pharmacia Biotech, Freiburg

Procaryotic expression vectors

pET-11d

Calbiochem-Novabiochem GmbH, Bad Soden

pET-23a

Calbiochem-Novabiochem GmbH, Bad Soden

pET-28a

Calbiochem-Novabiochem GmbH, Bad Soden

3.1.8 Important oligonucleotides

Cloning of Aosl into pCruzA

Aosl KpnI 5'-GGGGTACCATGGTGGAGAAGGA-3'

Aosl XbaI 5'-ATTGTTAACTCAGTTTTCTTGCCTG-3'

Cloning of ELKS into pCruzA

ELKS NotI 5'-AAAGCGCCGCTACCATGTATGGAAGT-3'

ELKS BglII 5'-AAAAGATCTTCAGGAGGACTCTTCCAG-3'

Cloning of ELKS into pGEX-4-T-1

ELKS EcoRI 5'-GGAATTCATGTATGGAAGTGCTCG-3'

ELKS NotI 5'-AAGCGGCCGCTCAGGAGGACT-3'

Cloning of ELKS into pASK-IBA

ELKSIBA43 SalI 5'-GCCC GCGGTATGTATGGAAGTGCGC-3'

ELKSIBA43 SacII 5'-CTGCAGGTCGACGGAGGACTCTTC-3'

ELKSIBA45 SalI 5'-ATTCCGCGGTAATGTATGGAAGTGC-3'

ELKSIBA45 SacII 5'-ATAGGTCGACCTGGAGGACTCTTX-3'

Cloning of ELKS into pET28a

ELKSforward 5'-AAAGAATTCACCATGTATGGAAGTGCT-3'

ELKSreverse 5'-AAAGCGGCCGCTTCAGGAGGACTCTTC-3'

Cloning of ELKS Fragment 1 into pGEX-4-T-1

ELKS1 EcoRI 5'-AAAGAATTCACCTATGGAAGTGCTCGATCA-3'

ELKS1 NotI 5'-AAAGCGGCCGCTCACTCAATCCTCAGCTCCAT-3'

Cloning of ELKS Fragment 2 into pGEX-4-T-1

ELKS2 EcoRI 5'-AAAGAATTCACCATGACTCAGAAGCAGACCCTA-3'

ELKS2 NotI 5'-AAAGCGGCCGCTCATCGCTCTTCAAGCTGCT-3'

Cloning of ELKS Fragment 3 into pGEX-4-T-1

ELKS3 EcoRI 5'-AAAGAATTCACCATGGTCAAGTCTCTGCAGGCG-3'

ELKS3 NotI 5'-AAAGCGGCCGCTCACTCTTCCACCTGTTTCTC-3'

Cloning of ELKS Fragment 4 into pGEX-4-T-1

ELKS4 EcoRI 5'-AAAGAATTCACCATGCTGTTGATGGCTATGGAG-3'

ELKS4 NotI 5'-AAAGCGGCCGCTCAGGAGGACTCTTCCAG-3'

Cloning of ELKS Fragment 1,1P into pGEX-4-T-1

ELKS1P EcoRI 5'-AAAGAATTCACCTATGGAAGTGCTCGATCA-3'

ELKS1P NotI 5'-AAAGCGGCCGCTCAGCTCCAGAAGGTCTTGAT-3'

Cloning of ELKS Fragment 1,2P into pGEX-4-T-1

ELKS2P EcoRI 5'-AAAGAATTCACCTATGGAAGTGCTCGATCA-3'

ELKS2P NotI 5'-AAAGCGGCCGCTCACTCCCCAGTCCTACTGCT-3'

Cloning of ELKS Fragment 1,3P into pGEX-4-T-1

ELKS3P EcoRI 5'-AAAGAATTCACCTATGGAAGTGCTCGATCA-3'

ELKS3P NotI 5'-AAAGCGGCCGCTCAGGCATTTTCAAATCTCCG-3'

Cloning of ELKS Fragment 1 into pCruzA

ELKS1 NotI 5'-AAAGCGGCCGCTACCATGTATGGAAGTGCTCGATCA-3'

ELKS1 BglII 5'-AAAAGATCTACTCTCAATCCTCAGCTCCAT-3'

Cloning of ELKS Fragment 2 into pCruzA

ELKS2 NotI 5'-AAAGCGGCCGCTACCATGACTCAGAAGCAGACCCTA-3'

ELKS2 BglII 5'-AAAAGATCTACTTCGCTCTTTCAAGCTGCT-3'

Cloning of ELKS Fragment 3 into pCruzA

ELKS3 NotI 5'-AAAGCGGCCGCTACCATGGTCAAGTCTCTGCAGGCG-3'

ELKS3 BglII 5'-AAAAGATCTACTCTTCCACCTGTTTCTC-3'

Cloning of ELKS Fragment 4 into pCruzA

ELKS4 NotI 5'-AAAGCGGCCGCTACCATGCTGTTGATGGCTATG-3'

ELKS4 BglII 5'-AAAAGATCTACTTCAGGAGGACTCTTCCAG-3'

3.1.9 Bacterial strains

BL21(DE3) Stamm Epicurian coli B; F⁻ *dcm ompT hsdS*(r_B⁻m_B⁻)
gal λDE3, Stratagene

DH5α F⁻φ80lacZΔM15 Δ(*lacZYA-argF*)U169 *deoR recA1 endA1*
hsdR17 (r_K⁻m_K⁺) *supE44* λ*thi-1* *gyrA96 relA1*

3.2 MOLECULAR BIOLOGY METHODS

3.2.1 Plasmid DNA purification (miniprep)

Single colonies were picked into 3 ml LB medium containing the appropriate selective antibiotic. Cultures were incubated over night at 37°C with vigorous shaking. 1.4 ml of the culture was transferred into 1.5 ml microcentrifuge tubes. The cells were microcentrifuged (14,000×g) for 30 seconds. The supernatant was discarded; the pellet was resuspended in 300 µl of ice cold buffer P1. Then 300 µl of freshly buffer P2 was added, mixed by gentle inversion and incubated for 5 min at RT. Then 300 µl of buffer P3 was added and mixed. Samples were centrifuged at 14,000×g for 30 min, and supernatants were transferred to new microcentrifuge tubes. 0.7 volumes of isopropanol was added, mixed and centrifuged at 12,000×g for 15 min. Supernatant was carefully discarded and pellets were washed with 70% EtOH and centrifuged at 10,000×g for 5 min. EtOH was removed and pellets were air-dried. DNA was redissolved in a suitable volume of sterile water.

3.2.2 Plasmid DNA (midi-, maxiprep)

Plasmid DNA was prepared using the QIAGEN[®] plasmid midi-, maxi-prep kit according to the procedure described by the manufacturer.

3.2.3 Preparation of chemically competent cells

50 µl of competent DH5α cells were incubated in 5ml LB medium with 0.02 MgSO₄ and 0.01 M KCl and cultured at 37°C overnight. The next day, the 1 ml overnight culture was diluted in 150 ml pre-warmed LB with 0.02 M MgSO₄/0.01 M KCl and grown for around 1.75 h at 37°C until OD₆₀₀ density of 0.3 to 0.4. The culture was kept on ice for 10 min and centrifuged for 10 min at 600 rpm at 4°C. The pellet was resuspended in 37.5 ml TFB I (25 mM KAc, 50 mM MnCl₂, 100 mM RbCl, 10 mM CaCl₂; pH 5.8) sterile filtered; and sterile glycerol added to a final concentration of 15% and kept on ice for 10 min before centrifuging at 6000 rpm for 10 min at 4°C. The pellet was resuspended in 4 ml TFB II (10 mM MOPS pH 7.0, 75 mM CaCl₂, 10 mM RbCl, 15% glycerol,

autoclaved) and cells were aliquoted at 50 μ l or 100 μ l on dry-ice/isopropanol and kept at -80°C.

3.2.4 Estimation of DNA concentration

Concentration of the DNA was estimated using spectrophotometric method by measuring absorbtion at 260 nm. The ratio OD_{260}/OD_{280} was determined in order to assess the purity of the sample. The samples were measured in a spectrophotometer DU 640, Beckman. The values where 1OD= 50 μ g/ μ l.

3.2.5 Digestion of plasmid DNA with restriction endonucleases

Each restriction enzyme requires specific reaction conditions for optimum activity. Enzyme buffers are specifically formulated to provide the salt concentration for optimal enzyme activity. Therefore, the correct buffer solution was used for each particular restriction enzyme. The following procedure was performed.

1. For each digest the following solutions in a microcentrifuge tube were combined.

Item	Amount
deionized water	6 μ l
10x reaction buffer	1 μ l
Plasmid miniprep DNA	3 μ l
Total	10 μ l

2. 0.5 μ l of enzyme solution was added to the mixture from step 1. If digest was with two restriction enzymes (double digest), 0.5 μ l of the second enzyme was added.
3. Incubation at 37° C from 2 h to overnight.
4. Reaction was stopped by adding the 6 \times DNA sample buffer.

3.2.6 DNA purification

Digested DNA fragments were separated on agarose gel and visualized by UV. The DNA fragments were isolated from the agarose gels and purified with QIAquick or QIAEXII Gel Extraction Kit (QIAGEN[®]) according to the procedure described by the manufacturer. Recovery of the DNA fragments was checked on agarose gel.

3.2.7 Ligation of DNA insert into vector DNA

1. In a microcentrifuge tube 5-10 μ l of digested vector DNA (50-400ng) and insert DNA were mixed.
2. Into DNA were added:

10 \times ligation buffer	2 μ l
50% PEG 4000 solution (for blunt ends only)	2 μ l
nuclease free water	to 20 μ l
T4 DNA ligase	1-2u (for sticky ends) 5u (for blunt ends)

3. The tubes were vortexed and centrifuged for 3-5 seconds.
4. The mixture was incubated for 1 hour at 22°C.
5. T4 DNA Ligase was inactivated by heating reaction mixture at 65°C for 10 minutes.
6. The mixture was used for transformation.

3.2.8 Transformation into DH5 α

The ligations were transformed to chemically component E. coli strain DH5 α . 4 μ l ligations were added to 100 μ l competent cells and incubated on ice for 45 min, heat shocked at 42°C for 90 sec and incubated for 2 min on ice. The bacterias were then cultured in 600 μ l LB medium without antibiotics at 37°C for 1 h in a bacteria shaker and plated onto LB plates containing proper antibiotic.

3.2.9 Polymerase Chain Reaction (PCR)

The first five reaction components were combined in the order listed in table below in a thin-walled 0.5ml reaction tube. Mix was gently vortexed in the tube for 10 seconds and briefly centrifuged. Reaction was initiated by adding the template and primers.

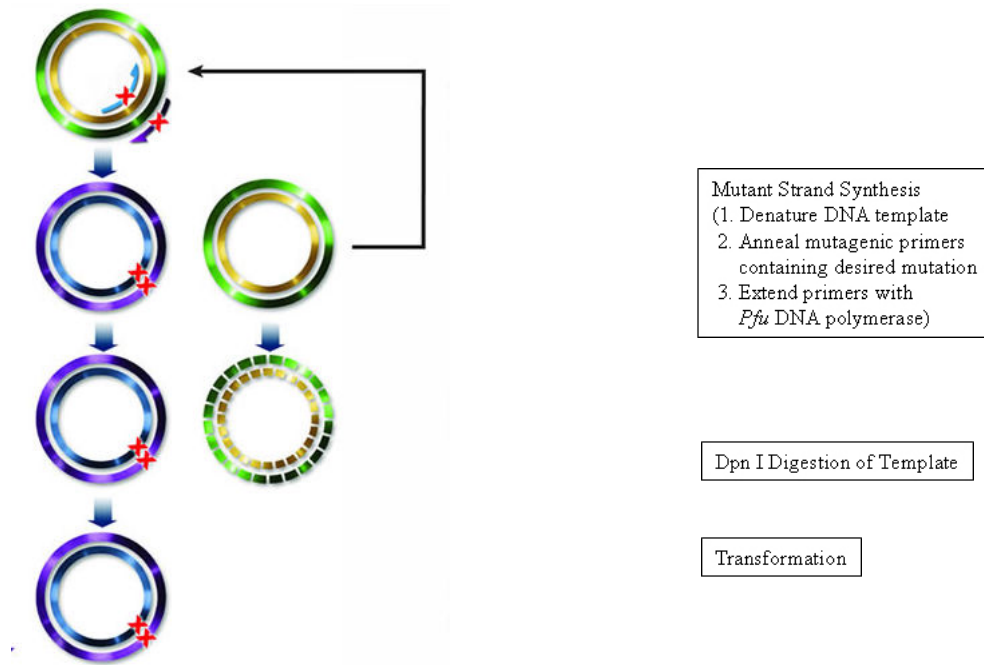
Components	Volume	Final Concentration
Nuclease-Free Water (to a final volume of 50 μ l)	x μ l	
10X Reaction Buffer	5 μ l	1x
dNTP mix (10mM of each dNTP)	1 μ l	0.2 mM each
<i>Taq</i> DNA polymerase (5u/ μ l)	0.25 μ l	0.025 u/ μ l
25mM MgCl ₂	3 μ l	1.5 mM
Downstream Primer	50 pmol	1 μ M
Upstream Primer	50 pmol	1 μ M
Template	Y μ l	

Tubes were placed in a controlled temperature heat block and preceded with the thermal cycling profile chosen for distinct reactions.

PCR reaction products were analysed by agarose gel electrophoresis of a 5 μ l aliquot from

3.2.10 Mutagenesis

Mutagenesis was performed using Stratagene's QuikChange® II site-directed mutagenesis kit.



The point mutants in the SUMO consensus sites of ELKS were introduced using the His-ELKS or HA-ELKS clone (previously verified by sequencing) as a template and with the following primers:

10 K/R (forward):

5' GCTCGATCAGTAGGGAGGGTGGAAACCAAGCAGC 3'

10 K/R (reverse):

5' GCTGCTTGGTTCCACCCTCCCTACTGATCGAGC 3'

444 K/R (forward):

5' GGTAGAGCAACTGAGGGAGGAGCTAAGTTCG 3'

444 K/R (reverse):

5' CGAACTTAGCTCCTCCCTCAGTTGCTCTACC 3'

472 K/R (forward):

5' GTCTGAGATTGGCCAGGTGAGGCAGGAACTGTCCAGAAAGG 3'

472 K/R (reverse):

5' CCTTTCTGGACAGTTCCTGCCTCACCTGGCCAATCTCAGAC 3'

889 K/R (forward):

5' GCTATGGAGAAGGTGAGGCAGGAACTGGAGTCC 3'

889 K/R (reverse):

5' GGACTCCAGTTCCTGCCTCACCTTCTCCTCCATAGC 3'

Reaction mix

Components	Concentration
Plasmid	500 ng
Primer 1	12.5 pmol
Primer 2	12.5 pmol
dNTP-mix	5 nmol
10×Pfu buffer	5 µl
Pfu polymerase	1 µl
H ₂ O sterile	x µl

Cycling Parameters for the mutagenesis

Segment	Cycles	Temperature	Time
1	1	95°C	30 seconds
2	12-18	95°C	30 seconds
		60°C	1 min
		68°C	2 min/kb of plasmid length
		72°C	20 min

After PCR samples were digested with DpnI restriction enzyme (10 U/µl) for 2 h at 37°C. Then 3 µl of the DpnI-treated DNA reaction were transferred to separate aliquots of the DH5α competent cells.

3.2.11 Sequencing

Sequencing was performed using “Big Dye Terminator Cycle Sequencing RR-Mix” from Applied Biosystem. Reaction mix contained: 500 ng plasmid, 4.0 pmol sequencing primer, 4 µl of BD-Mix and H₂O sterile filled up to 10 µl.

PCR program

Segment	Cycles	Temperature	Time
1	1	96°C	2 min
2	40	96°C	30 seconds
		50°C	15 seconds
		60°C	4 min

3.2.12 Organ extracts

Mouse organ extracts for Western blot analysis were prepared by isolating the respective organs from anaesthetized mice, snap freezing them in liquid nitrogen and thawing by resuspension with a plastic homogenizer on ice in cold lysis buffer: 50 mM Tris-HCl 7.5, 1% Triton X-100, 120 mM NaCl, 20 mM NaF, 1 mM sodium pyrophosphate, 1 mM sodium vanadate, 10 µg/ml pepstatin, leupeptin, aprotinin.

3.2.13 RNA isolation

Total RNA was isolated from mouse tissues using TRIzol reagent according to the procedure described by the manufacturer with minor modifications. Briefly, tissue samples were homogenized in TRIzol, 50-100 mg tissue/ml TRIzol. Samples were incubated at RT for 5 min. Chloroform was added to the samples (0.2× the volume of TRIzol used) and vortexed vigorously and centrifuged at 12,000×g at 4°C for 15 min. The upper aqueous phase was extracted with 1 volume phenol pH 4.0/chloroform and centrifuged at 12,000×g at 4°C for 15 min. The RNA in the upper aqueous phase was precipitated with 0.5 volume isopropanol and centrifuged at 12,000×g at 4°C for 15 min. The RNA pellet was washed with 70% ethanol/DEPC-H₂O and quantified at A₂₆₀.

3.2.14 RT-PCR (Reverse transcription polymerase chain reaction)

5 µg RNA in 15 µl of DEPC-H₂O were incubated at 65 °C for 5 min to denature secondary RNA structures, and subsequently placed on ice for 5 min.

The following components were mixed in DEPC-treated Eppendorf tubes:

Reagent	Volume
RNA	15µl
5× first strand buffer (Invitrogen)	5 µl
0.1 M DTT	2 µl
Oligo dT primer (50 pmol/µl)	1 µl
dNTPs (10 mM)	1 µl
Superscript II Reverse Transcriptase (Invitrogen, 200 U/µl)	1 µl
Final volume	25 µl

As a negative control, one reaction was mixed without Reverse Transcriptase. The reaction was carried out at 42 °C for 1 h to allow cDNA synthesis. The samples were diluted 1:2 by addition of 50 µl of DEPC-H₂O and subsequently used for PCR analysis.

3.3 Cell biology methods

3.3.1 Cell lines

The following adherent cell lines were used in this study: 293, Hs68, HeLa. Cells were maintained in standard DMEM medium supplemented with 10% fetal calf serum, 100 units/ml each of penicillin and streptomycin and 2 mM L-glutamine and were usually grown in 10-cm or 15-cm diameter tissue culture dishes. All cells were kept at 37 °C in humidified 5% CO₂ incubator. HeLa cells in suspension were grown in Joklik's medium at 37°C in spinner flask.

Subculturing of the adherent cells was done by trypsinization with 0.25% trypsin, 0.2% EDTA.

Suspension cell lines were grown in 250 ml, 1 l or 3 l tissue culture flasks. Subculturing of suspension cells was done by diluting with fresh medium.

The freezing of cells was done in 90% FCS and 10% (v/v) dimethyl-sulfoxide (DMSO) in a freezing box at -80°C. The frozen aliquots were stored in a liquid nitrogen tank or at -80°C.

Thawing of the cells was done by submerging the frozen vial in a 37 °C water bath. The cells were then washed with medium by centrifugation at 1200 rpm for 3 min. and resuspended in pre-warmed medium before transferring them to culture plates or flasks.

3.3.2 Transient transfection

Cells were transfected with PolyFect according to the procedure described by QIAGEN (“PolyFect Transfection Reagent Handbook”). Briefly, the example of protocol optimized for transient transfection of HeLa cells in 60 mm dishes is given.

The day before transfection cells were seeded 8×10^5 cells per 60 mm dish in 5 ml appropriate growth medium. On the day of the transfection 3 µg DNA was diluted with growth medium containing no serum, proteins, or antibiotics to a total volume of 150 µl. Then 25 µl of PolyFect transfection reagent was added to the DNA solution, vortexed for 10 sec. Samples were incubated for 10 min at RT to allow complex formation. In between, cells were washed once with 4 ml PBS and 3 ml of fresh cell growth medium was added. To the reaction tube containing the transfection complexes, 1 ml of medium was added, mixed and transferred to the cells in the 60 mm dishes. Cells were incubated with the complexes for 24-48 h after transfection to obtain maximal expression levels of the transfected proteins.

3.3.3 Fluorescence microscopy

For indirect immunofluorescence, adherent HeLa cells or Hs68 fibroblasts grown on glass coverslips were fixed for 10 min. with 2% PFA in PBS, 1mM MgCl₂, and permeabilized for 5 min with 0.2% Triton X-100 in PBS, 1 mM MgCl₂. After washing 3 times with PBS, blocking was done with 2 % BSA in PBS+1mM MgCl₂ for 45 min. The coverslips were then incubated with 50 µl primary antibody diluted in 2% BSA, PBS/MgCl₂ for 60 min at RT. Following a 3× washing with PBS, the cells were incubated 45 min. with the secondary antibody, diluted in 2% BSA, PBS/MgCl₂. After a final wash (3× with PBS) the coverslips were mounted on a pre-cleaned microscope slide in mounting medium.

Microscopy was done with a fluorescent microscope (Zeiss, Jena, Germany) equipped with standard DAPI, FITC (or GFP) and Texas Red (or Cy3) filters. Images were acquired with 40×, 63×, 100× objectives, using an Axioskop-II_Fluorescence Microscope (Zeiss, Jena) using MicroMax CCD camera (Princeton Instruments, New Jersey, USA) with IP Lab Software Scientific Image Processing 3.5.5 (Scanalytics, Inc.)

Confocal images were recorded using a Bio Rad Radiance 2000 confocal laser scanning and Nikon TE300 microscope equipped with a 40, 60XI-4, Plan-APO-CHROMAT oil immersion objective

3.3.4 Reporter luciferase assay

Cells were scraped, washed once with 1× PBS and resuspended in 100 µl 1× Reporter Lysis Buffer (Promega, Madison, WI). The cell suspension was frozen in liquid nitrogen and thawed at room temperature. The cell debris were spun down at 13000 rpm for 5 min. 20 µl of the protein extracts were used for measurement of the luciferase activity using the Luciferase assay system (Promega, Madison, WI), following the manufacturer's instructions. The measurement was performed with the luminometer LUMAT LB 9501, Berthold, Wildbad Germany

3.4 Biochemistry methods

3.4.1 Sodium dodecylsulphate polyacrylamide gel electrophoresis (SDS-PAGE)

SDS-PAGE was based on the discontinuous system described by Laemmli (1970). Diverse percentage of the separating gels (depending of the size of the proteins of interest) were cast using a 30% acrylamide/0.8% N, N'-methylene bisacrylamide solution (Roth). For electrophoresis, protein samples were mixed 1:1 with 2× Laemmli buffer, heat denatured for 5 min. at 95 °C and loaded onto the gel. Proteins were separated by applying a current of 20 mA until the front dye had reached the end of the gel. Pre-stained or unstained marker proteins were run in parallel. Following electrophoresis, proteins were stained with Coomassie Brilliant Blue G250, silver staining or subjected to Western blotting (see below).

3.4.2 Coomassie staining

For Coomassie staining of polyacrylamide gels, the gels were incubated for 30 minutes on a slowly rocking platform with Staining solution (50% Methanol, 10% Acetic acid, 0,25 % Coomassie Brilliant Blue G250). To visualize the proteins the gels were incubated overnight in destaining solution (50% Methanol, 10% Acetic acid) until the background was clear. For drying, the gels were soaked in dH₂O containing 20% glycerol, placed between cellophane film and dried over-night at RT.

3.4.3 Silver staining

Gels were fixed for 3 hours in a solution containing 12% acetic acid (v/v), 50% methanol (v/v) and 50 µl (37%) formaldehyde in MilliQ water in a volume of 100 ml. The gels were then rinsed 3 times 5 min in 50% ethanol and soaked for 1 min in a sensitivity-enhancing solution containing 0.2 g/l of freshly sodium thiosulfate in MilliQ water. Gels were rinsed 3 times for 20 sec in dd H₂O and impregnated for 20 minutes with silver solution containing 37 µl of 37% formaldehyde and 0.1 g of silver nitrate per 50 ml of MilliQ water and washed 2 times for 20 sec in dd H₂O. The gels were developed in a

solution containing 3.0g sodium carbonate, 25 μ l of 37% formaldehyde per 50 ml of MilliQ water. Development was stopped when background began to appear. The gels were washed 2 times for 20 sec in dd H₂O and stopped by incubation in stop solution containing 50% MetOH and 12% acetic acid.

3.4.4 Immunoblotting

Proteins were denatured at 95°C and separated by SDS-PAGE and transferred to nitrocellulose membrane for 2 h at 0.8 mA/cm² using a “Semidry”-Blot device in the presence of transfer buffer.

(+) POSITIVE ELECTRODE (ANODE)

***** Plastic cassette
Three Sheets Whatman 3MM
----- Nitrocellulose membrane
----- Polyacrylamide gel
Two Sheets Whatman 3MM
***** Plastic cassette

(-) NEGATIVE ELECTRODE (CATHODE)

The blots were stained with 10 % Ponceau S (Sigma) in order to visualize transfer efficiently and the protein molecular weight marker. The blots were incubated in blocking solution (PBS containing 5 % dried milk and 0.2 % Tween-20) for 1 h at RT. Detection of antigens on nitrocellulose was performed with affinity-purified antibody in 5% milk powder in PBS, 0.2% Tween 20 for 1 h at RT. The blots were washed with PBS, 0.2% Tween-20, 3 times for 10 min each and incubated with secondary antibody diluted in blocking solution for 45 min at RT. The blots were washed with PBS, 0.2% Tween-20, 3 times for 10 min each. Detection was performed by chemiluminescence (ECL from Pierce). Occasionally blots were stripped with stripping buffer (0.1 M Glycine, 0.5 % SDS, pH 2.2) for 2 times 10 min with agitation. The blots were washed with PBS, 0.2% Tween 20, for 10 min and then incubated again in blocking solution and reprobed using other antibodies.

3.4.5 Expression and purification of recombinant proteins

Expression and purification of recombinant SUMO E1 enzyme

The protocol described below uses co-expression of His-tagged Aosl with untagged Uba2. Isolation was normally carried out in four days from a frozen bacterial cell pellet and leads to approximately 0.5-1 mg of SUMO E1 enzyme per liter of bacterial culture.

For protein purification, pET28a-Aosl and pET11d-Uba2 were simultaneously transformed into the *E. coli* strain BL21(DE3), and used to directly inoculate 500 ml of LB with 50 µg/ml ampicillin and 30 µg/ml kanamycin (due to poor growth of the bacteria, selection for single colonies on plates was omitted). After growth for 18 h at 37°C, bacteria were harvested by centrifugation, resuspended in 2 liters of fresh LB medium, and directly induced for protein expression with 1 mM IPTG. The cells are grown for 6 h at 25°C, before harvesting by centrifugation at 4,000 rpm in a Beckman JS5.2 rotor. After resuspension in 50 ml buffer A, the cells were subjected to one freeze-thaw cycle (-80°C). Once thawed, 1 mM β-Mercaptoethanol, 0.1 mM PMSF, 1 µg/ml each of AP, L/P, and 50 mg lysozyme (SIGMA) were added, and the bacterial suspension incubated on ice for 1 h. Bacterial debris were removed by centrifugation at 1 h 100,000g, 4°C, in a 45Ti rotor. His-Aosl and associated Uba2 are enriched from the supernatant by batch incubation for 1 h at 4°C (slow rotation) with 6 ml Probond resin (Invitrogen) equilibrated in lysis buffer including protease inhibitors and β-mercaptoethanol. After harvesting by centrifugation, resin was transferred into a column and washed extensively with cold wash buffer until no more protein elutes from the column (protein detection by OD280 or by Ponceau S staining on nitrocellulose membrane). Proteins were eluted with 3 volumes elution buffer (gravity flow), and 2 ml fractions were collected. Protein containing fractions were combined and concentrated to 2 - 5 ml using a centrifugal device (e.g., 30K-Millipore-concentrator). After filtration of the concentrate through 0.2 µm low protein binding filter, it was applied to an FPLC S200 preparative gel filtration column equilibrated in S200 buffer. 5 ml fractions were collected and analysed by SDS-PAGE. His-Aosl was expressed in large excess, and smeared over many column fractions. Only fractions that contain both His-Aosl (migrates at 40 kD) and Uba2 (note that it migrates at 90 kD despite a predicted size of 72 kD) were combined and applied

for further purification on a 1ml MonoQ anion exchange column (Pharmacia FPLC, 1 ml). Elution from the MonoQ column involved a linear gradient from 50 to 500 mM NaCl (generated from Q buffers 1 and 2). 0.5 ml fractions were collected, and analysed by SDS-PAGE. Fractions containing approximately equimolar levels of His-Aos1 and Uba2 were combined and dialyzed against TB. The enzyme was aliquoted (5 μ l aliquots), frozen in liquid nitrogen, and stored at -80°.

Expression and purification of recombinant ELKS

His-ELKS was transformed into the *E. coli* strain BL21(DE3), and plate out on LB plate plus kanamycin. The next day single colony was selected to inoculate 100 ml over night pre-culture. After growth for 18 h at 37°C, bacteria were harvested by centrifugation, resuspended in 2l fresh LB medium, and directly induced for protein expression with 1 mM IPTG. The cells were grown for 5 h at 25°C, before harvesting by centrifugation at 4,000 rpm in a Beckman JS5.2 rotor. Pellet was resuspended in 30 ml of lysis buffer containing 50 mM Na-Phosphate, pH 8.0, 300 mM NaCl, 10mM imidazol, protease inhibitors and β -mercaptoethanol. Than the cells were subjected to one freeze-thaw cycle (- 80°C). Once thawed, lysozyme was added to a final concentration 1 mg/ml, and the bacterial suspension was incubated on ice for 1 h. Further the cells were sonicated and bacterial debris were removed by centrifugation for 1h at 100,000 \times g; 4°C, in a 52.2 Ti rotor. The supernatant was incubated for 1 h at 4°C (slow rotation) with 3 ml Probond resin equilibrated in lysis buffer including protease inhibitors and β -mercaptoethanol. After harvesting by centrifugation, the resin was transferred into a column and washed extensively with cold wash buffer (50 mM Na-Phosphate, pH 8.0, 300 mM NaCl, 20mM imidazol, protease inhibitors and β -mercaptoethanol) until no more protein elutes from the column (protein detection by OD₂₈₀ or by Ponceau staining on nitrocellulose membrane). Proteins were eluted with 3 volumes elution buffer (50 mM Na-Phosphate, pH 8.0, 300 mM NaCl, 350 mM imidazol, protease inhibitors and β -mercaptoethanol, gravity flow), and 0.5 ml fractions were collected. Protein containing fractions were combined and concentrated to 2-5 ml using a 30K-Millipore-concentrator. After centrifugation for 30 min at 100,000 \times g, the concentrate was applied to an FPLC S200 analytical gel filtration column equilibrated in buffer containing 50 mM Na-Phosphate,

pH 8.0, 150 mM NaCl, protease inhibitors and DTT. Fractions were analyzed by SDS-PAGE and only those containing His-ELKS were combined and dialyzed against TB.

3.4.6 Measurement of protein concentration

Protein concentration was determined using a Coomassie Brilliant Blue G-250-based protein assay reagent (Biorad) or “Micro BCA Protein Assay Reagent” kit (Pierce).

3.4.7 *In vitro* SUMOylation.

For *in vitro* sumoylation, 500 ng of substrate (ELKS), 1 mM ATP, 150 ng Ubc9 (28 nM), 150 ng E1 (68 nM), 500 ng SUMO1 (2.2 μ M) and 20 ng BP2 fragments (31 nM BP2 Δ FG, 109 nM IR1+M,) or \cong 1 μ g PIAS1 were incubated in a total volume of 20 μ l transport buffer supplemented with protease inhibitors, 1 mM DTT, 0.05% (v/v) Tween and 0.2 mg/ml ovalbumin grade VI (Sigma) at 30°C for 30 min. Reactions were stopped by addition of an equal volume of (SDS) sample buffer.

Thioester reactions were performed in 20 mM Tris (pH 7.6), 50 mM NaCl, 10 mM MgCl₂, protease inhibitors, and 0.1 mM DTT. Reactions were terminated by 1:1 dilution with 2 \times nonreducing sample buffer (50 mM Tris [pH 6.8], 2%SDS, 4 M urea, 10% glycerol).

3.4.8 Fluorescence Resonance Energy Transfer (FRET)-based SUMO assay

FRET is a process by which the excited state energy of a fluorescent donor molecule is transferred emission free to an acceptor molecule. The consequence of this is a significant reduction in donor - and a concomitant appearance of acceptor - emission. Efficient energy transfer not only requires overlapping emission and excitation spectra, it also requires very close proximity (less than 10 nm) of the donor and acceptor molecules. FRET is therefore widely used as an indicator for inter- or intramolecular protein interactions.

The principle of FRET based sumoylation assay developed in our laboratory is depicted in Figure 1A. As a model target, we have chosen RanGAP1, as it is the most efficient

SUMO target known to date. Fusion proteins of YFP with SUMO and CFP with the 20 kDa C-terminal domain of RanGAP1 (GAPtail) are used for conjugation. CFP and YFP represent a well characterized donor and acceptor pair for *in vivo* and *in vitro* FRET applications (Pollok and Heim, 1999; Tsien, 1998). Isopeptide bond formation between these components enables FRET directly, hence secondary reagents for analysis are not required. YFP-SUMO, CFP-GAPtail, and the required enzymes Aos1/Uba2 and Ubc9 can be expressed and purified well from bacteria (Figure 1B), and are functional in ATP dependent isopeptide bond formation (Figure 1C). The strong FRET signal that can be observed upon YFP-SUMO and CFP-GAPtail conjugation makes this assay a very useful platform for kinetic analysis of the basic sumoylation machinery.

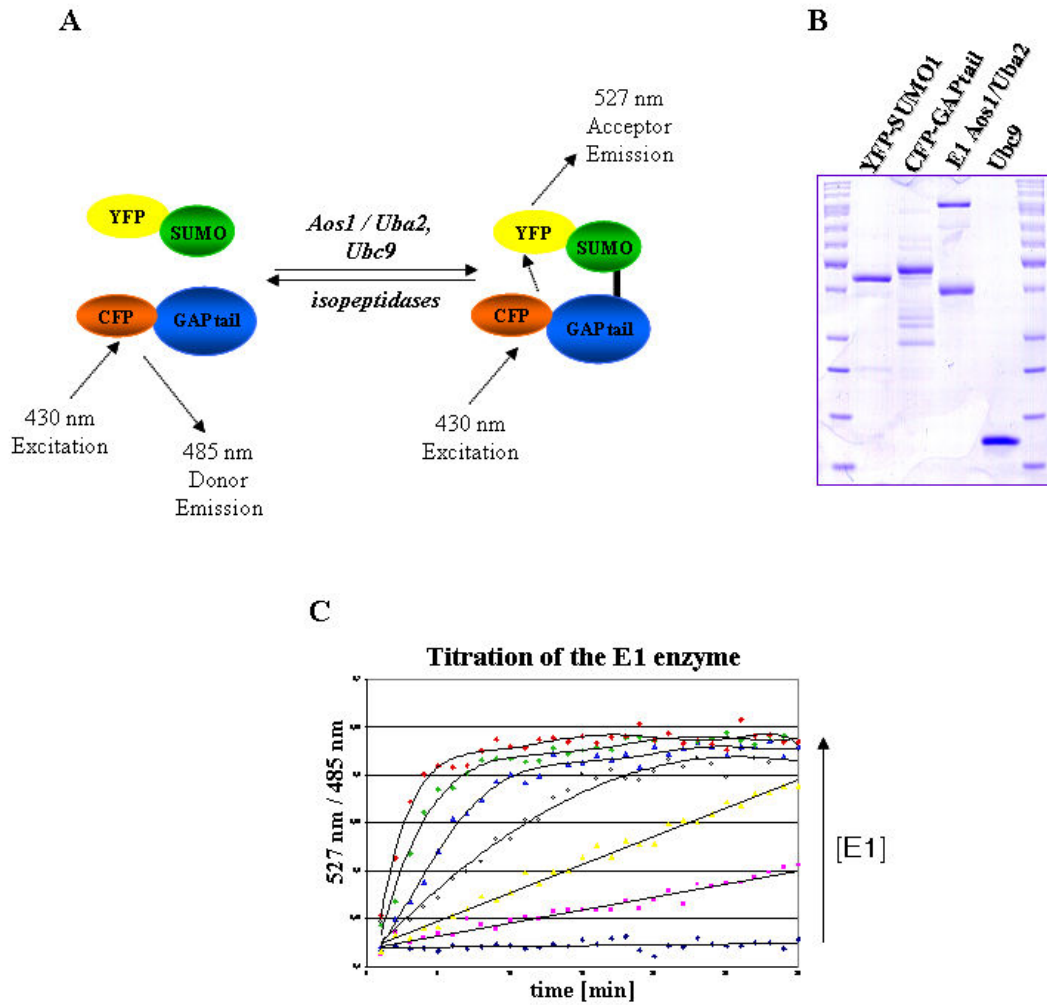


Figure 1 A FRET-based sumoylation assay. A. Principle of the FRET assay. When YFP-SUMO and CFP-GAPtail are not conjugated, excitation of CFP at 430 nm results in strong emission at 485 nm. Upon addition to the conjugating enzymes (Aos1/Uba2, Ubc9) and ATP, YFP-SUMO is covalently conjugated to CFP-GAPtail. This allows FRET to take place. As a consequence, emission at 485 nm is reduced and emission at 527 nm increases. B. Purified components used in the FRET-based assay. Coomassie staining of recombinant YFP-SUMO1, CFP-GAPtail, Aos1/Uba2 and Ubc9. C. Titration of the E1 activating enzyme Aos1/Uba2. Reactions included YFP-SUMO1, CFP-GAPtail, Ubc9, and increasing concentrations of Aos1/Uba2. The reaction was started by the addition of ATP and was monitored over 30 min. An ATP control was included to provide a baseline.

3.4.9 Generation and purification of rabbit or goat polyclonal antibodies

α ELKS antibodies were raised in rabbit; α Uba2, antibody were raised in goat. Rabbits or goat were injected with 500 μ g of protein (Gst-ELKS C-term, Gst-ELKS N-term, or His-full length Uba2) emulsified with Titermax Gold. Boosts were with 500 μ g emulsified with incomplete Freund's adjuvant. To obtain a good titer three injections were sufficient. Once blood was received from animal facility, it was stirred with a glass rod for approx. 1 min, then was let at RT for 1 hour, stirred again and stored at 4°C over-night. The next day, blood was stirred again, and then centrifuged for 30 min at 4000 rpm in Beckmann J6B centrifuge. Supernatant was collected, aliquoted, and stored at -20°C.

For testing the titer, immunoblots were carried with a fixed amount of antigen (10ng) in each strip, and serial dilution (1:100-1:10000) of the serum. To control for nonspecific background, the antigen was applied as a mix with total HeLa cell extract, and for each antibody dilution two samples were loaded, one with and one without antigen in the HeLa extract. Antibodies were affinity purified from serum by adsorption of affinity columns containing the corresponding recombinant proteins. Briefly, the recombinant protein was extensively dialyzed against Carbonate buffer (0.2 M, pH 8.9), with buffer change, over-night. CNBr beads were prepared and the protein (0.5 mg protein/ml beads) was added. Incubation was performed for 3 h at RT. To determine the coupling rate, the OD at 280 nm was checked before and after coupling. Then the beads were washed 2 times with carbonate buffer and incubated with 100 mM Ethanolamine for 1 h at RT to block all remaining coupling sites and then beads were washed again 3 times and equilibrated with 500 mM NaCl in PBS. Those beads were then used for affinity purification of serum. 1-2 ml of matrix was incubated with 30 ml serum and 20 ml PBS in a falcon tube at 4°C

over-night. On the next day beads were washed two times with 50 ml PBS + 500mM NaCl and transferred into a column. Wash was continued until no more protein in flow through was detected. Then, elution buffer (0.2 M acetic acid, pH 2.7, 500 mM NaCl) was carefully applied onto column. Antibodies were eluted with approximately 10 column volumes. Fractions (0.5 ml) were collected and immediately 100 μ l of 1M Tris base was added to neutralize the pH. Fractions with antibodies were combined and concentrated to approx. 1 ml. Buffer was changed to PBS and antibodies were mixed with 1 vol of 87 % glycerol and stored in aliquots at -20°C .

3.4.10 Immunoprecipitation

Immunoprecipitation using HeLa cells in suspension lysed with a nondenaturing detergent solution for Mass Spectrometry.

HeLa cells pellet, 25 ml (TZ 1008, 5E9 zellen/Röhrchen) was thawed or HeLa cell culture in suspension from about 10 l, were resuspended in 25 ml of nondenaturing buffer [1% (w/v) Triton X-100, 50 mM Tris-Cl, pH 7.4, 300 mM NaCl, 5 mM EDTA, 0.02% (w/v) sodium azide]. Immediately before use 10 mM iodoacetamide, 1 mM PMSF and 2 μ g/ml L/P were added. Suspension was incubated on ice for 30 min and centrifuged for 10 min at 1000 rpm. The supernatant was used for the following centrifugation steps: 6000 \times g for 10 min, 20000 \times g for 10 min, 100,000 \times g for 1 h. Pellet was resuspended in 1 ml nondenaturing buffer. Final pellets for IP: 20000 \times g and 100000 \times g were centrifuged at 6000 \times g for 15 min (wash step) before use. Extract was pre-cleared for 60 min with IgG cross-linked at 2 mg/ml to Ultralink Immobilized Protein G/A Plus beads (Pierce Chemical Co.). Affinity-purified antibodies (Aos1, Uba2, ELKS) or control IgGs cross-linked at 2 mg/ml to Ultralink Immobilized Protein G Plus beads were incubated with extracts for 120 min at 4°C . Beads were washed three times in wash buffer [0.1% (w/v) Triton X-100, 50 mM Tris-Cl, pH 7.4, 300 mM NaCl, 5 mM EDTA, 0.02% (w/v) sodium azide] and boiled in 2 \times SDS-Laemmli loading buffer. Proteins were separated by SDS-PAGE: 5-20 % gradient gel. Then gels were incubated for 2 h in Coomassie solution and destained over-night.

3.4.11 His-SUMO pull down

293T cells were transfected with PolyFect reagent according to the procedure described by QIAGEN, with either HA-ELKS and His-SUMO2, or pCruz empty vector and His-SUMO2 (control). 42 h after transfection cells were washed once with 1×PBS and harvested in lysis buffer containing 8 M Guanidinium-HCl, 100 mM Na₂HPO₄/NaH₂PO₄, 10 mM Tris-HCl (pH 8.0), 0.05% Tween 20, 10 mM B-mercaptoethanol, 20 mM imidazole, and 20 mM NEM. Cell lysates were sonicated and His₆-SUMO-2 conjugates were enriched on Ni²⁺ beads for 3 h at 4°C. Beads were successively washed at room temperature with 10 column volumes of lysis buffer, then buffer A (8 M urea, 100 mM Na₂HPO₄/NaH₂PO₄, 10 mM Tris-HCl (pH 6.3), 0.2% Triton X-100, and 10 mM B-mercaptoethanol), then buffer A lacking Triton X-100, then buffer A plus 0.2% Triton X-100, and finally buffer A lacking Triton X-100. Conjugates were eluted at room temperature with 2×SDS-Laemmli loading buffer. Samples were run on 6% gel and subjected to immunoblot with ELKS antibody.

3.4.12 Mass spectrometry

First, the gel was stained for 2-3 h in Coomassie, and then the gel background was destained overnight to visualize the proteins. Gel digestion was followed by protocol adapted by Shevchenko et al. (1996). Briefly, after the gel pieces were excised and shrunk by dehydration in acetonitrile, which was then removed; they were dried in a vacuum centrifuge. A volume of 10 mM DTT in 100 mM NH₄HCO₃ sufficient to cover the gel pieces was added, and the proteins were reduced for 1 h at 56 °C. After cooling to RT, the DTT solution was replaced with roughly the same volume of 55 mM iodoacetamide in 100 mM NH₄HCO₃. After 45 min incubation at ambient temperature in the dark with occasional vortexing, the gel pieces were washed with 50-100 µl of 100 mM NH₄HCO₃ for 10 min, dehydrated by addition of acetonitrile, swelled by rehydration in 100 mM NH₄HCO₃, and shrunk again by addition of the same volume of acetonitrile. The liquid phase was removed, and the gel pieces were completely dried in a vacuum centrifuge. The gel pieces were swollen in a digestion buffer containing 50 mM NH₄HCO₃, 5 mM CaCl₂, and 12.5 ng/µl of trypsin (sequencing grade) in an ice cold bath.

After 45 min, the supernatant was removed and replaced with 5-10 μ l of the same buffer, but without trypsin, to keep the gel pieces wet during enzymatic cleavage (37°C, overnight). Peptides were extracted by one change of 20 mM NH_4HCO_3 and three changes of formic acid in 50% acetonitrile (20 min for each change) at RT and dried down. Samples were re-dissolved in 5% formic acid and then desalted by Poros microcolumns for MALDI Mass Spectrometry analysis.

4 RESULTS

4.1 Part1: Characterisation of an Uba2 splice variant

4.1.1 Identification of Uba2 splice variant

As described below, our lab identified serendipitously an Uba2 splice variant in which 50 amino acids are missing (Figure 11). As this suggested the existence of distinct sets of SUMO E1 enzymes, it was my aim to characterise the splice variant.

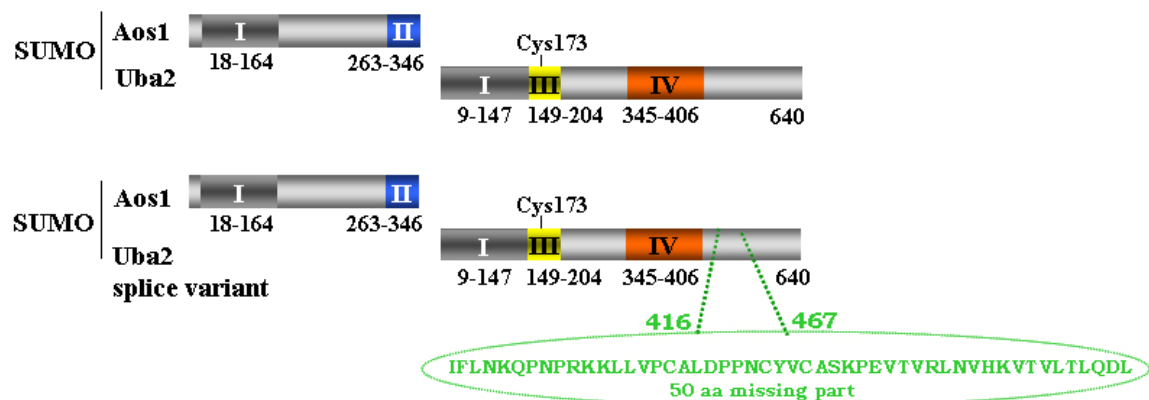


Figure 11. Schematic representation of homologous domains in SUMO-1 activating enzymes, Aos1/Uba2 and Aos1/Uba2 variant. Domain I includes a potential nucleotide-binding motif, domain III contains the active site cysteine (173) residue which forms a thioester with the C-terminus of SUMO.

Ulrike Gärtner, a technician in the group, noticed that one of the two cDNA's obtained from the RZPD contained different length open reading frames for Uba2 (Figure 12a). The cDNAs corresponding to both open reading frames were further sequenced. The shorter fragment encoded an Uba2 variant which lacked amino acids 416 to 467, suggesting that the shorter form was a splice variant of Uba2. Both full length and splice variant of Uba2 were subcloned into the bacterial expression vector pET28a (His-Uba2). Once I took over the project, I also cloned both isoforms of Uba2 into mammalian

expression vector pCruz A (HA-Uba2). HeLa cells were transfected with plasmids of Uba2 full length and splice variant, and analysed by immunoblotting with anti HA antibodies. Uba2 wild type and splice variant were migrating differently on SDS-PAGE due to their difference in the size (Figure 12b). The same result was obtained by using the bacterial expression plasmid (His-Uba2). After expression and purification of both Uba2 forms in bacteria (as described in Materials and Methods) the recombinant proteins of Uba2 full length and Uba2 splice variant were subjected to 6% SDS-PAGE and stained with Coomassie blue solution (Figure 12c). As expected the Uba2 splice variant migrated faster than Uba2 full length protein.

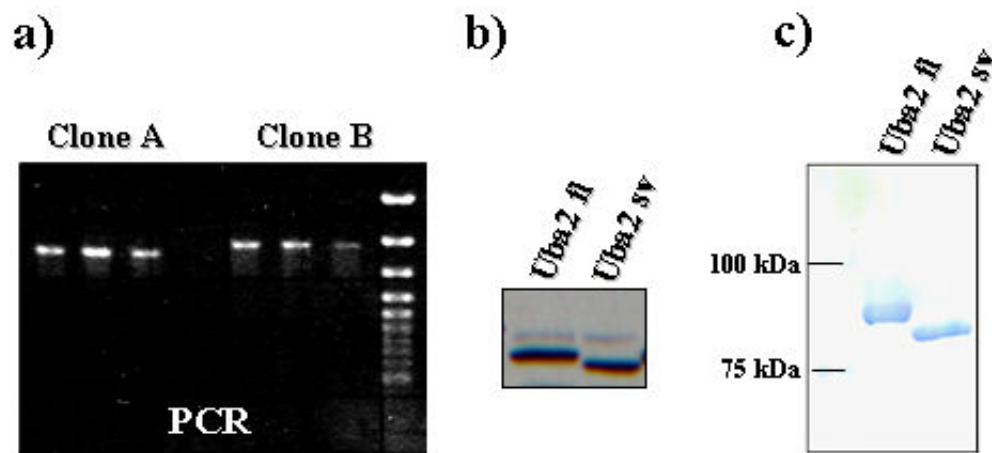


Figure 12 a) Carried out by Ulrike Gärtner: two PCR products containing two isoforms of Uba2, clone A=Uba2 splice variant (sv), clone B=Uba2 full length (fl), b) Western blot showing transfected Uba2 full length and splice variant in HeLa cells c) Recombinant proteins of Uba2 full length and splice variant were run on 6% SDS PAGE and stained with Coomassie.

To confirm that the short form of Uba2 was due to alternative splicing, the cDNA sequence was compared to the genomic sequence of Uba2. This revealed that one complete exon (exon 13, which consists of 150 base pairs) was missing in the shorter open reading frame (Figure 13).

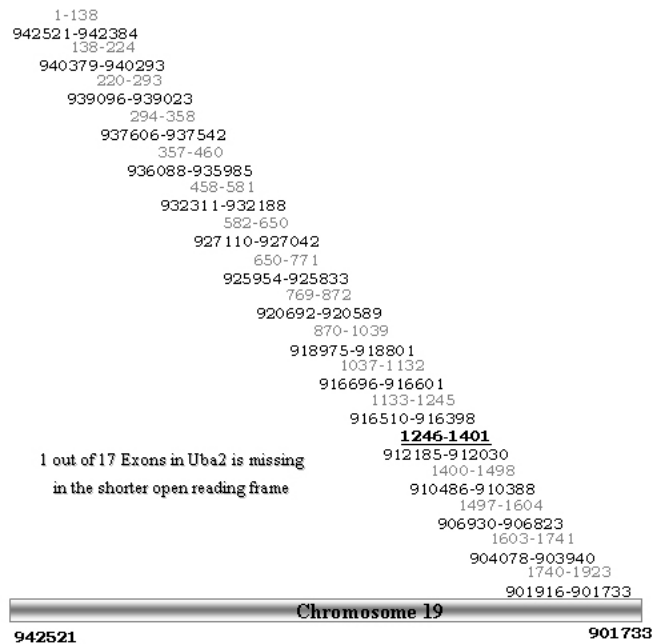


Figure 13. The human Uba2 gene consists of 17 exons. Exon 13 (black underline) is missing in the Uba2 splice variant. Numbers indicated start and end of each exon and refer to genomic sequence (top) and open reading frame (bottom) respectively.

4.1.2 Generation and characterisation of Uba2 polyclonal antibody in goat

For further characterization of expression and localization of Uba2 proteins, antibodies were required. For this purpose, His-Uba2 full length recombinant protein was expressed and purified (see Materials and Methods). After three times injection of a goat with 500 µg of purified His-Uba2 full length, 950 ml of blood was obtained and the antibodies were affinity purified as described in detail in Materials and Methods. In brief, 2.1 mg of His-Uba2 full length was coupled to 1.2 g CNBr beads. After incubation of the column material with 50 ml of serum, elution with acetic acid was performed. 500 µl fractions were collected and protein-containing fractions were concentrated to 1 ml. Antibodies were mixed with one vol of 87 % glycerol and aliquotes were stored at -20°C.

Using HeLa cell lysates I could show by western blotting that affinity purified Uba2 antibody recognized a single band at the molecular weight corresponding to 90 kDa (Figure 14a). This is the expected size, because the 72 kDa protein Uba2 is known to migrate aberrantly (Figure 12c). Uba2 antibody also worked well on cell immunostaining of human skin fibroblast cells (Hs68). Uba2 protein was distributed throughout nuclei (Figure 14b). This result was consistent with a previous study that showed that SUMO-1 enzyme resides in the nucleus (Azuma et al. 2001).

Affinity purified antibodies were further characterized by immunoprecipitation. For this, 500 μ g of total HeLa cell extract was incubated with 10 μ g α Uba2 or unspecific IgG's. The immunoprecipitates were analysed by immunoblot with anti-Uba2 antibodies and showed specific pull down of Uba2 protein (Figure 14c).

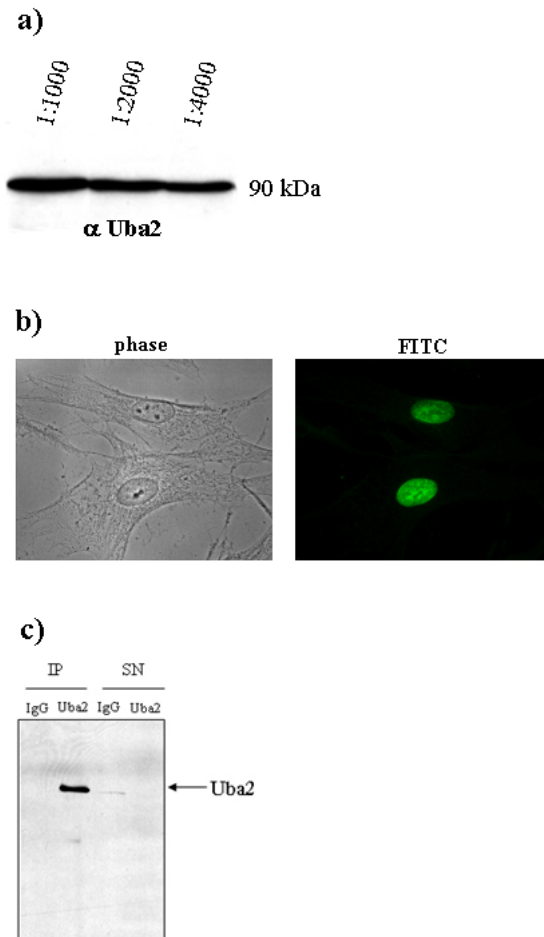


Figure 14. a) Western blot analysis with Uba2 antibody. Uba 2 antibody specifically recognized a single band in HeLa cells extract. b) Hs68 cells were stained with antibodies directed against Uba2 and visualized with FITC coupled secondary antibody, c) Immunoprecipitation of Uba2 from HeLa cell lysate and detection with Uba2 immunoblotting.

Uba2 antibodies were tested in western blot, immunoprecipitation assays and cell immunostaining. Results are summarized in Table 1.

Table 1 Working conditions of Uba2 antibodies

Uba2 antibodies	
<i>yield</i>	4.1 mg/ 50 ml of serum
<i>concentration of glycerol stock</i>	2.1 mg/ml
<i>dilution for Western blot</i>	1:6000
<i>dilution for immunoprecipitation</i>	1:100
<i>dilution for immunofluorescence</i>	1:100

4.1.3 *In vivo* and *in vitro* analysis of the Uba2 splice variant

The Uba2 splice variant is ubiquitously expressed

To determine the tissue distribution of the Uba2 splice variant, RNA from different mouse organs was isolated, and RT-PCR was performed using specific oligonucleotides (Figure 15).

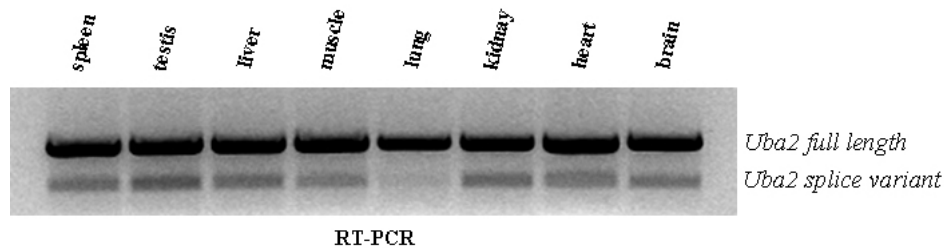


Figure 15 RT-PCR analysis of tissue distribution for Uba2 full length and splice variant mRNA. RT-PCR picture showed abundant expression of Uba2 full length and Uba2 splice variant in selected mouse organs.

RT-PCR of total RNA showed that both Uba2 full length and splice variant were detected in all selected mouse organs with no apparent tissue specificity of expression, indicating that the Uba2 splice variant is present in most organs. However, Uba2 splice variant was expressed only at about 10 % of total Uba2 full length mRNA. Furthermore, in lung, the Uba2 splice variant showed reduced expression compared to full length Uba2.

Subcellular localisation of Uba2 splice variant in HeLa

I then investigated, whether the Uba2 splice variant would have a different localization compared to Uba2 full length protein. Transfection of HeLa cells with HA-Uba2 splice variant showed predominantly nuclear distribution in these cells (Figure 16)

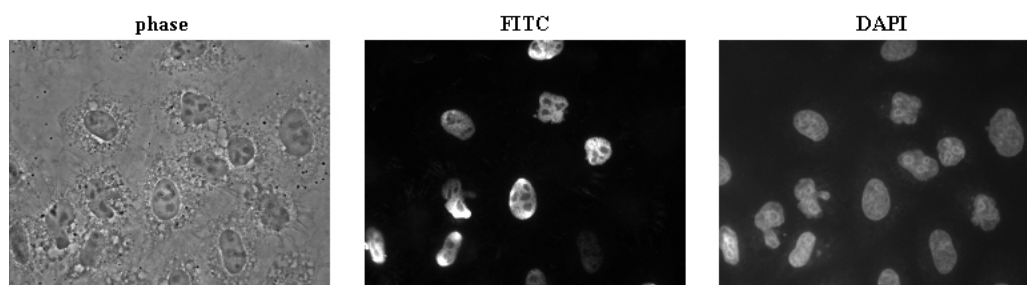


Figure 16. Localisation of the Uba2 splice variant. HeLa cells were fixed with 2% PFA, permeabilized with 0,2% Triton X-100, stained with antibodies directed against Uba2, and visualized with FITC coupled secondary antibody (middle picture). Picture on the left shows phase contrast and picture on the right shows staining of DNA with DAPI.

This localisation was identical to that observed for full length Uba2 (Azuma et al. 2001 Azuma et al., 2001; Pichler et al., 2002 and Figure 14b). Consequently, the Uba2 splice variant shows no obvious differences in localisation compared to Uba2 full length protein.

Uba2 splice variant forms a complex with Aos1

To gain insights into a potential difference between full length and variant Uba2, I first tested if the Uba2 splice variant was still able to interact with Aos1 to form the SUMO E1 enzyme. Recombinant His-Aos1 and recombinant His-Uba2 (full length or splice variant) were incubated in a 1:1 molar ratio on ice in TB buffer for 30 minutes. After incubation, samples were applied to gel filtration on an analytical FPLC S200 column, and 0.5 ml fractions were collected. 20 μ l of each fraction was mixed with 2 \times SDS sample buffer and analysed on 8% SDS-PAGE and stained with Coomassie blue.

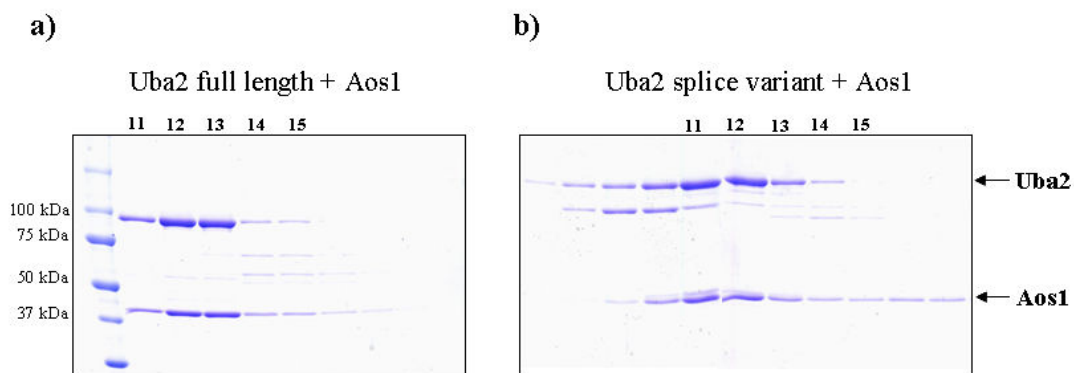


Figure 17. Coomassie staining of different fractions of Aos1-Uba2 full length (a) and Aos1-Uba2 splice variant (b) analysed after S200 analytical gel filtration column.

As shown by their co-elution, both Uba2 full length and Uba2 splice variant formed a stable heterodimer with Aos1 (Figure 17a, b). They also co-eluted on Mono Q (data not shown), which supports the notion that these proteins are stably complexed with each other. Therefore, no difference in Aos1 binding could be observed between Uba2 full length and Uba2 splice variant.

Enzymatic activity of variant Uba2 protein

As mentioned earlier, the splice variant of Uba2 lacks amino acid 416-467 (green arrows in Figure 18). In full length Uba2, this area is part of a stretch that connects the SUMO binding region with an ubiquitin like domain. This domain has been implicated as an Ubc9 binding site (Lois and Lima, 2005).

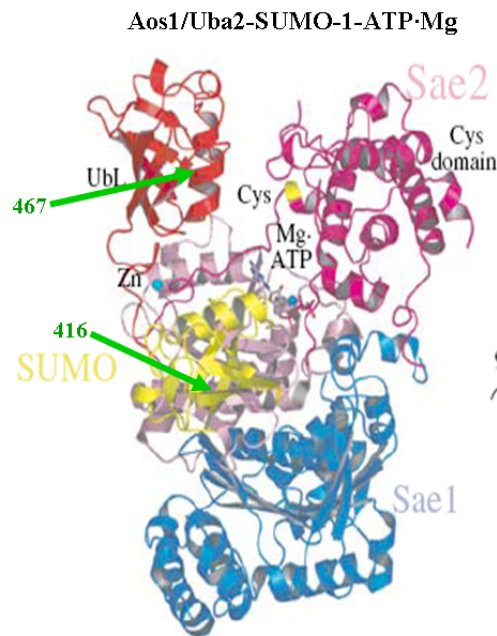


Figure 18. Ribbon diagram of the Aos1/Uba2-SUMO-1 complex. SUMO is colored yellow. Catalytic domain and UbL domains are labeled. The active site cysteine is labeled and colored yellow. E1 with deletion in Uba2 is indicated on left with the green arrows from 416-467 (From Lois and Lima, 2005).

SUMO-1 is recognized exclusively by residues emanating from Uba2, as no direct interactions are observed between SUMO-1 and the Aos1 subunit so far. According to the

structure presented by Lois and Lima 2005 the deletion in the Uba2 variant protein would alter the SUMO binding surface significantly and disrupt the Ubl domain. The question whether SUMO conjugating activity is affected in the splice variant was addressed through comparing the enzymatic activity of both proteins.

For the comparison of enzymatic activity of both proteins, His-tagged Aosl with untagged Uba2 (full length) or Uba2 (splice variant) were co-expressed in the *E. coli* strain BL21 DE3 and purified. Purified recombinant proteins were run on a 5-20 % gel and stained with Coomassie blue (Figure 19 a).

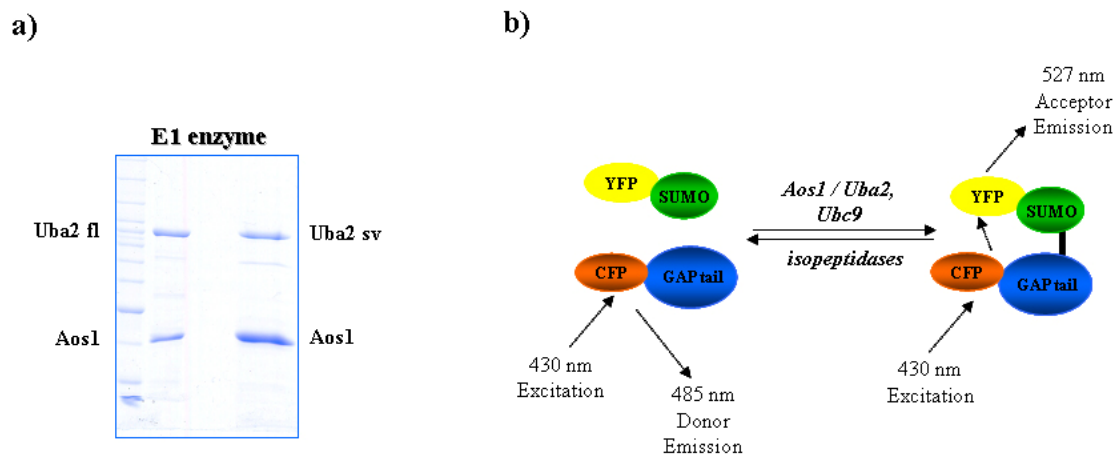


Figure 19. FRET based sumoylation assay. a) Purified E1 enzymes. Coomassie staining of recombinant Aosl/Uba2 full length and Aosl/Uba2 splice variant. b) Principle of the FRET assay. When YFP-SUMO and CFP-GAPtail are not conjugated, excitation of CFP at 430 nm results in strong emission at 485 nm. Upon addition of the conjugating enzymes (Aosl/Uba2 and Ubc9) and ATP, YFP-SUMO is covalently conjugated to CFP-GAPtail. This allows FRET to take place. As a consequence, emission at 485 nm is reduced and emission at 527 nm increases.

Those purified components were used in a FRET based assay that allows kinetic analysis of RanGAP1 sumoylation. The principle outline is shown in Figure 19b. Measurements were carried out in 384 well plates, using a fluorescence microtiter plate reader (Fluoroscan Ascent; Labsystems). Reactions were performed using equimolar amounts of CFP-GAPtail and YFP-SUMO1 (200 nM each), Ubc9 (163 nM) and variable E1 enzyme concentrations, ranging from 0.36 to 36.4 nM. FRET buffer, in which all proteins were diluted, contained 0.05 % Tween 20 and 0.2 mg/ml ovalbumin to prevent nonspecific

adsorption of the proteins. After 5 min preincubation at 30°C, reactions were started automatically by addition of ATP (5 μ l of a 5 mM solution, supplied by a sample dispenser). At desired time points, samples were excited at 430 nm, and fluorescence emissions at 485 nm and 527 nm were recorded with an integration time of 20 ms. After addition of ATP, the ratio of emissions (527 nm/485 nm) increased linear over time, until it reached a stable plateau. The maximal value (0.6-0.7) is reached, when nearly 100% of the substrates are conjugated (verification by immunoblotting, not shown). Linear rates over the whole time of the experiment were observed with low enzyme concentrations. Doubling the E1 enzyme concentration approximately doubles the reaction rate.

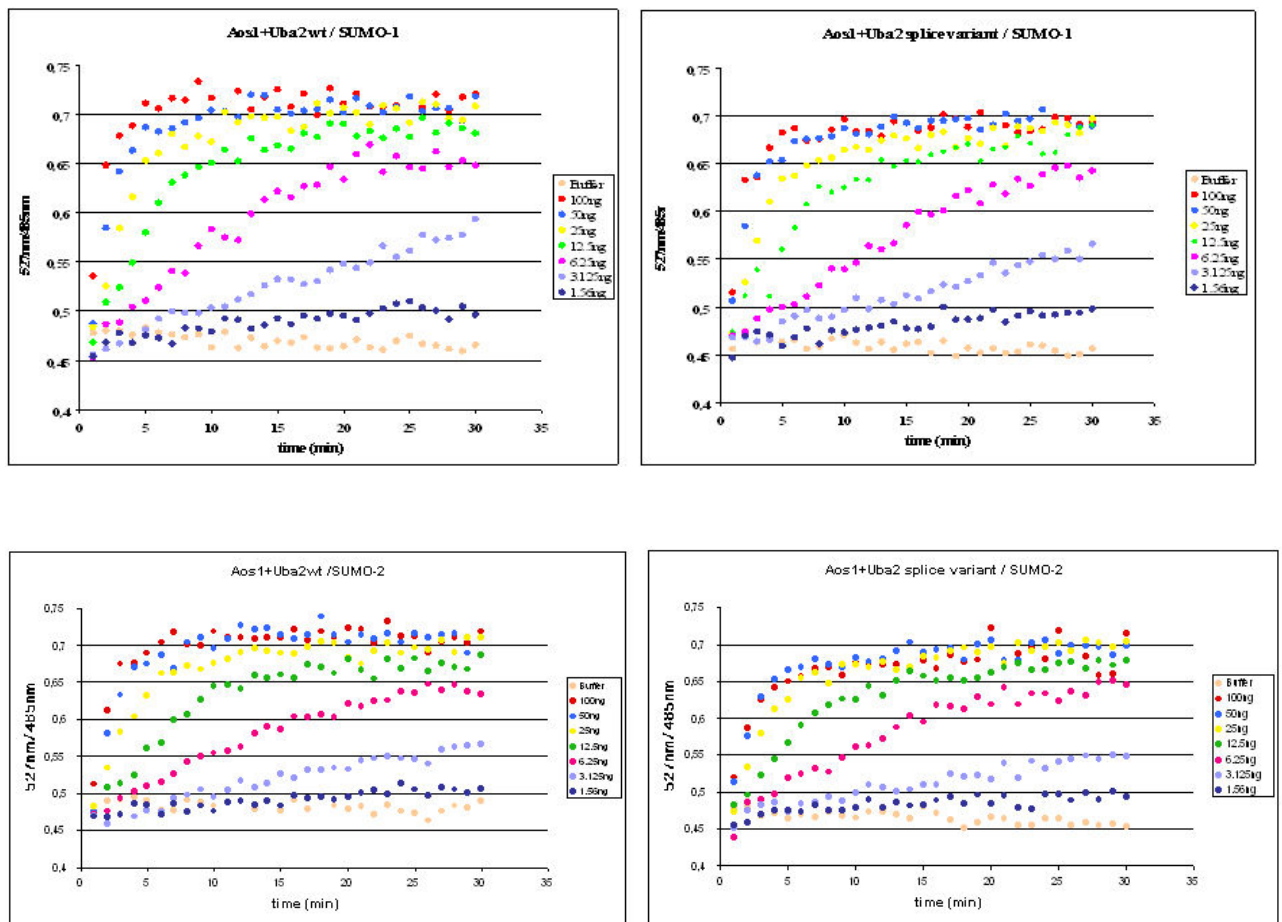


Figure 20. SUMO E1 enzyme containing either full length or variant Uba2 were compared for enzymatic activity using SUMO1 or SUMO2 in a FRET assay.

Surprisingly, full length and variant protein were equally active in reactions involving SUMO1 (Figure 20, top panels). I next addressed the question whether there may be a difference in activity when SUMO2 rather than SUMO1 was used as a substrate. Full length Aos1/Uba2 is known to show no preference (Lois and Lima, 2005). As shown in Figure 20, bottom panel, again, no difference could be observed. Taken together, these findings demonstrate that amino acids 416 to 467 in Uba2 are dispensable for E1 activity.

4.1.4 Finding new binding partners for Uba2 full length and Uba2 splice variant

One possible difference between Uba2 wild type and Uba2 variant proteins could be the proteins they interact with. Therefore I began to search for binding partners of human Uba2 full length and Uba2 splice variant. To identify new interacting proteins, pull downs experiments were performed. 20 g HeLa cells (commercially available) was thawed and resuspended in 50 ml TB buffer supplemented with protease inhibitors and 1 mM DTT. Cells were homogenized in a dounce homogenizer by 30 passages and centrifuged down at 10000 rpm for 15 min. Supernatant was ultracentrifuged at 100,000×g for 1 h (sup 1) and was frozen at -70°C. The pellet was resuspended in two volumes of TB containing protease inhibitors and 1 M NaCl, homogenized, ultracentrifuged at 100000×g for 1 h (pellet 1) and frozen at -70°C. The supernatant was dialyzed over night in TB buffer, spun down at 100000×g for 1 h (sup 2) and frozen. Uba2 full length and Uba2 splice variant were coupled to CNBr beads (see protocol in Material and Methods). 200 µl of beads with Uba2 wild type or Uba2 splice variant or empty beads as a control, were placed in columns, washed once with TB plus 1 M NaCl, and once with TB. To each column 7 ml of supernatant 1 was added and incubated for 2 h on the rotator in the cold room. After incubation, beads were washed five times with TB and bound proteins were eluted with increasing amount of salt: first with 600 µl of TB plus 200 mM NaCl, second with 600 µl TB plus 500 mM NaCl and third with 600 µl TB plus 1 M NaCl. 30 µl of each fraction was loaded on a gradient gel (5-20%) and stained with Coomassie Blue (Figure 21b). Bands marked from 1 to 10 were cut out and analysed by mass spectroscopy. Sample preparation including trypsin digest (Materials and Methods) was

carried out by myself. Mass spectrometry analysis was carried out by Dr. Marjaana Nousiainen (group of Dr. Körner, MPI in Martinsried).

I could not identify any binding partner(s) specific for either Uba2 splice variant or Uba2 full length protein. The results of mass spectrometry analysis are in appendix part. Further experiments will be needed to determine if some of the identified proteins are real Uba2 interactors.

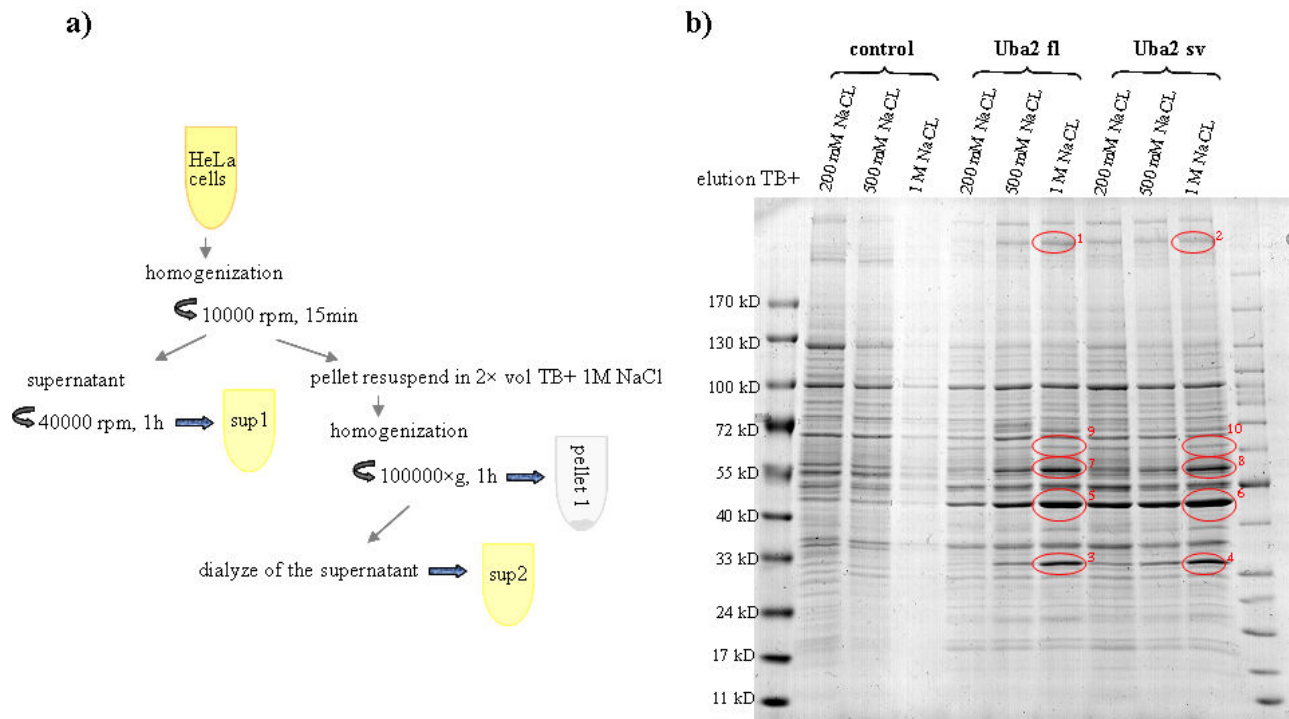


Figure 21. a) Schematic representation of Uba2 pull down. HeLa cells were harvested, homogenized and centrifuged. Supernatant was ultracentrifuged for 1h at 40000 rpm (sup 1), pellet was resuspended in double volume of TB contained 1 M NaCl, homogenized and ultracentrifuged for 1h at 100,000×g (pellet 1). Supernatant was dialyzed against TB over night (sup 2). b) Coomassie stained gel showing three elutions with increasing amount of NaCl for IgG, Uba2 fl and Uba2 sv. Bands numbered from 1 to 10 were cut out and analysed by mass spectrometry analysis.

As conclusion, here I could show that a variant Uba2 protein that lacks amino acids 416 to 467 compared to full length Uba2 is expressed in all mouse tissues analysed. The splice isoform it localises similar to the full length protein – predominantly in the nucleus, and based on pull down experiments it shows no striking differences in binding. Surprisingly, it is fully active; although 50 amino acids are missing that seem to play an important structural role.

RESULTS

4.2 PART 2: Identification of a novel SUMO target

Another part of my project consisted in the study of Aos1, one of the two subunits of the SUMO E1 enzyme.

4.2.1 Affinity purification and characterisation of Aos1 polyclonal antibody

Generation of Aos1 antibodies and purification of the third obtained blood from goat was carried out by Dr. Andrea Pichler. This antibody was used for earlier studies. However, I needed large quantities of Aos1 antibody for my studies, and I affinity purified final blood (boost 8) of Aos1 serum (see Materials and Methods). Briefly, 2.0 mg of His-Aos1 full length was coupled to 1.1 g CNBr beads. Upon incubation of the column material with 50 ml of serum, elution with acetic acid was performed. 500 µl fractions were collected and protein-containing fractions were concentrated to 1 ml. Antibodies were mixed with one vol of 87 % glycerol and aliquotes were stored at -20 °C.

HeLa cell lysates were used for characterisation of the Aos1 antibodies. Aos1 protein was recognized specifically by anti-Aos1 antibodies on immunoblot at the right molecular weight corresponding to 39 kDa (Figure 22a).

Human skin fibroblast or HeLa cells were used for the characterisation and localisation of Aos1 in indirect immunofluorescence using the affinity purified antibodies. As published,

the antibodies decorate predominantly the nucleus and gives faint staining in the cytoplasm (Pichler et al., 2002). As shown in Figure 22c and d, Aosl is predominantly localized in the nucleus, with a diffuse staining in the cytoplasm. Surprisingly, our purified antibodies from the third bleed stain membrane like structures around the nucleus (Figure 22c, d). However, affinity purified Aosl antibody from the final bleed not always decorates membrane structure (Figure 22e). Purified antibodies of Aosl were further characterized by immunoprecipitation of cell lysate made with RIPA buffer (Figure 22b). HeLa cell lysates were incubated with affinity purified Aosl antibody or preimmune serum as a control. The immunoprecipitates were analysed by Western blotting with anti-Aosl antibody. Figure 22b shows that the produced antibodies are able to immunoprecipitate Aosl.

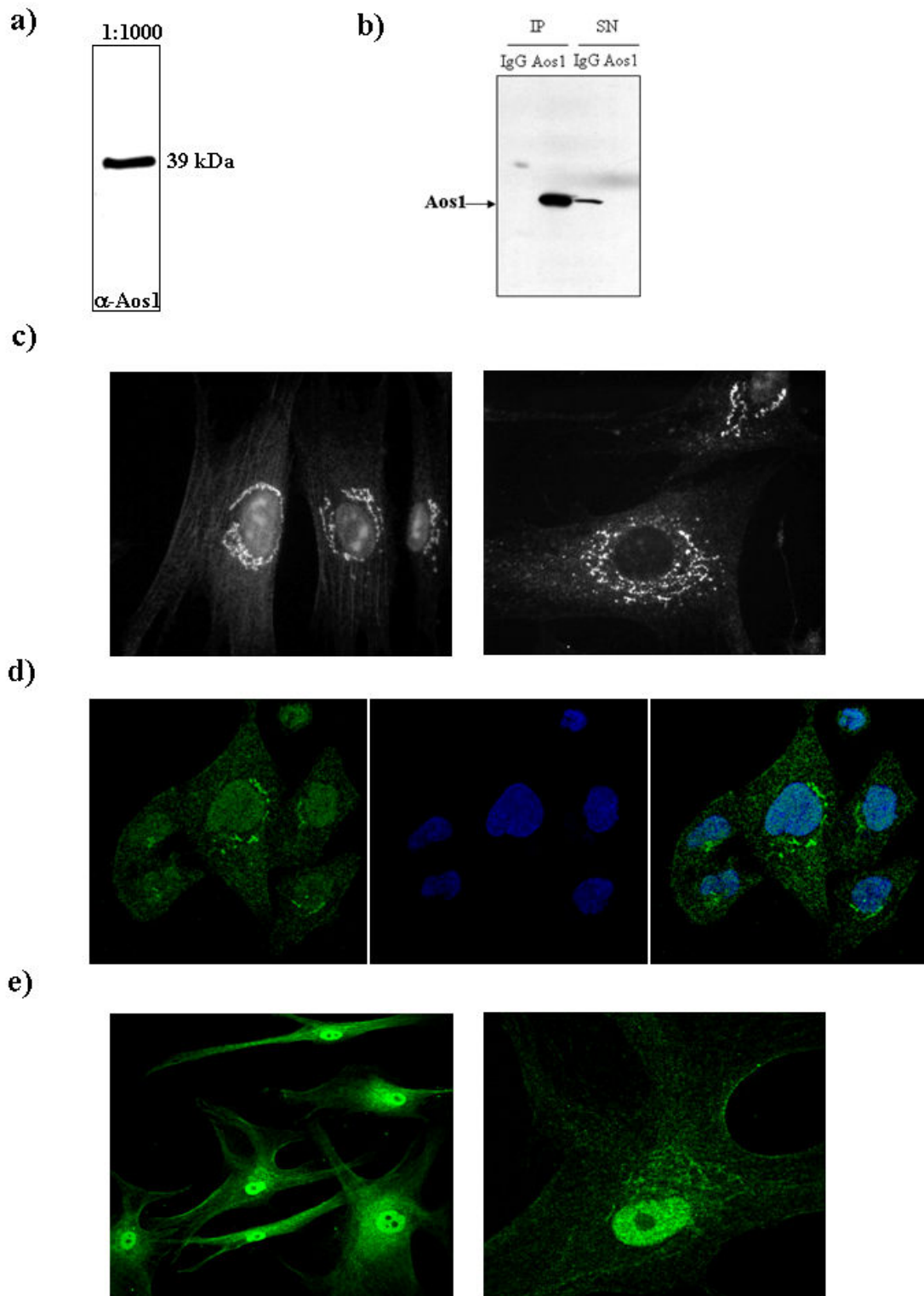


Figure 22. Characterisation of affinity purified Aosl polyclonal antibodies. a) Western blot analysis of Aosl antibodies (terminal bleed). Aosl antibodies specifically recognized a single band in HeLa cells extract. b) Immunoprecipitation of Aosl in HeLa cells lysed in RIPA buffer. c) Indirect immunofluorescence with Aosl antibodies (third blood) was done with Hs68 cells. Picture on the left side shows cells permeabilized with 0,2% Triton X-100, and picture on the right panel shows cells permeabilized with 0,001% digitonin, d) HeLa cells were fixed with 2% PFA, permeabilized with 0.2% Triton X-100 and stained with antibodies directed against Aosl (third blood) and visualized with FITC coupled secondary antibodies, e) Hs68 cells were fixed with 2% PFA, permeabilized with 0.001% digitonin and stained with antibodies directed against Aosl (final blood) and visualized with FITC coupled secondary antibodies.

The working conditions of Aosl antibodies are summarized in Table 2. Aosl antibodies work in immunoblot, in immunoprecipitation assays and also work well for cell immunostaining. Antibodies derived from third and terminal blood are comparable in Western and IP, but show some difference in IF.

Table 2 Working conditions of Aosl antibodies (terminal bleed)

Aosl antibodies		
<i>yield</i>	2.6 mg/50 ml of serum	
<i>concentration of glycerol stock</i>	1.3 mg/ml	
<i>dilution for Western blot</i>	1:1000	
<i>dilution for immunoprecipitation</i>	1:65	
<i>dilution for immunofluorescence</i>	1:50 (third blood)	1:100 (final blood)

4.2.2 α Aos1 antibodies decorate the nucleus and Golgi structures

To visualize the cytoplasmic localization of Aos1 a bit further, indirect immunofluorescence was performed using a specific marker for Golgi structure. Using confocal microscope and double immunofluorescence labeling with anti-GM130 antibodies (a *cis*-Golgi matrix protein marker) and anti-Aos1 (third bleed), I could detect costaining of Aos1 with Golgi in Hs68 cells (Figure 23). The same results were also obtained using HeLa cells (data not shown).

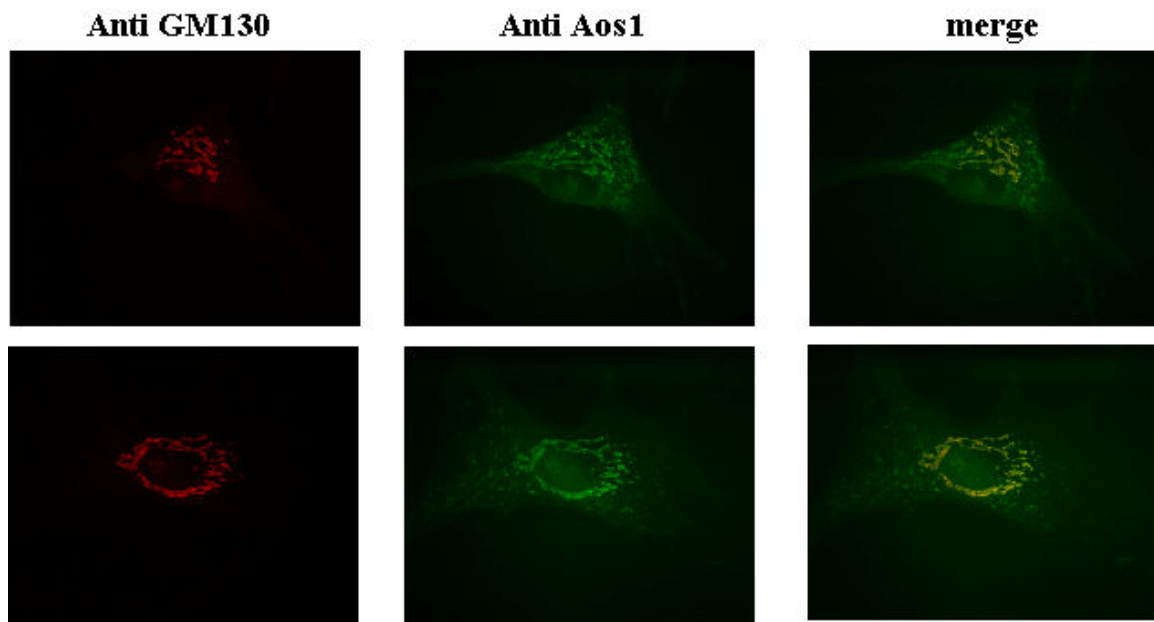


Figure 23. α Aos1 antibodies decorate the Golgi apparatus. Hs68 cells were fixed with 2% PFA, permeabilized with 0.001% digitonin, stained with antibodies directed against Aos1 (third bleed), GM130 and finally visualized with FITC or Cy3TM coupled secondary antibodies

4.2.3 A small fraction of Aos1 and Uba2 are present in insoluble pellet fractions

To address the question whether the Golgi staining observed with one of the two affinity purified antibodies was due to an artifact or indeed reflected some enrichment of Aos1 on membranes, I carried out cell fractionation. Here, I noticed that a small fraction of both Aos1 and Uba2 could be found in insoluble fractions as well. Briefly, HeLa cells were

homogenized in buffer A (5 mM HEPES-KOH (pH 7.3); 10mM KOAc, 2mM Mg [OAc]₂, 1mM DTT). The nuclei and cell debris were removed from the homogenate by centrifugation at 900 rpm for 10 min at 4 °C. Cell lysates were then fractionated by a series of differential centrifugation steps designed to separate organelles and particles on the basis of size, density, and sedimentation properties (Table 3 and Figure 24). Aox1 and Uba2 were predominantly located in the cyto-soluble fraction (100,000×g), but they were also enriched in some of the insoluble membrane fractions like the 3000×g pellet, which contains amongst others plasma membrane fractions, the 6000×g pellet which is enriched in lysosomes, peroxisomes and intact Golgi, and the 100,000×g pellet, containing vesicles, plasma membrane and endosomes. As a control for the purity of the cellular fractions, proteins with a well-known subcellular distribution were also tested on the same western blot. Figure 24 shows that cytoplasmic proteins like RanGAP1 and Ubc9 were only present in the cyto-soluble fractions, as expected.

RCF (G_{AV})TIME	CONTENT^A
1,000g × 10 min	nuclei, heavy mitochondria, plasma membrane sheets
3,000g × 10 min	heavy mitochondria, plasma membrane fragments
6,000g × 10 min	mitochondria, lysosomes, peroxisomes, intact Golgi
10,000g × 10 min	mitochondria, lysosomes, peroxisomes, Golgi membranes
20,000g × 10 min	lysosomes, peroxisomes, Golgi membranes, large and dense vesicles (e.g., rough ER)
100,000g × 10 min	all vesicles from ER, plasma membrane, Golgi, endosomes etc.

Table 3. Definition of differential centrifugation pellets. ^A In practice, the pellets may show more cross-contamination of particles than suggested. Plasma membrane fragments may be of a variety of sizes that sediment at all speeds. The majority of mitochondria should be in 3,000×g and 6,000×g pellets, the majority of lysosomes and peroxisomes in 10,000×g pellet. (From Deltry and Rickwood, 1992).

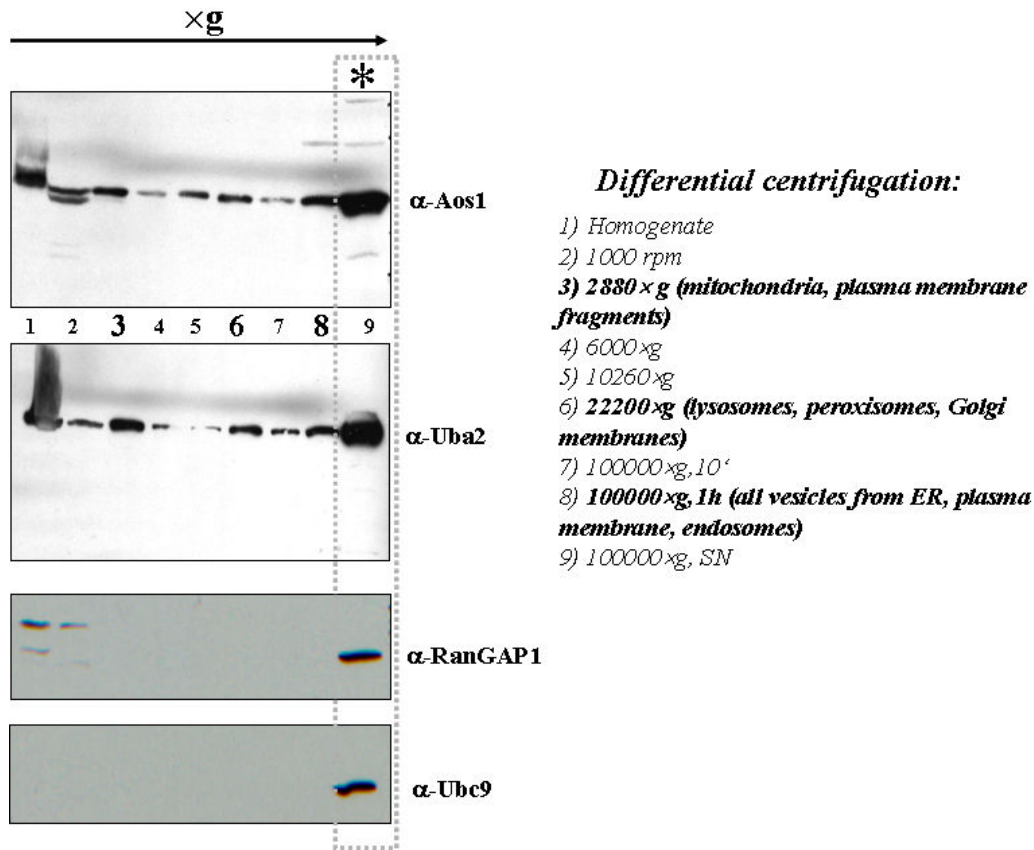


Figure 24. HeLa cells were harvested and subcellular fractions were analysed by western blot analysis using antibodies against: Aos1, Uba2, RanGAP1 and Ubc9. Subcellular fractions (Table 3) were separated by SDS-PAGE, blotted and stained with anti-Aos1, anti-Uba2, anti-RanGAP1 or anti-Ubc9.

To obtain information about association and complex formation between Aos1 and Uba2, proteins from the cytosolic fraction were separated by gel filtration column. Briefly, HeLa cells in suspension were harvested, washed with PBS and resuspended in 2 volumes of TB buffer supplemented with protease inhibitors. Cells were resuspended, treated with 0.001% digitonin for 5 min and centrifuged for 1 h at 100,000 $\times g$. Proteins from the cytosol were applied and separated on an FPLC S200 analytical column (Figure 25a). Immunoblotting with anti Uba2 and anti Aos1 antibodies of individual fractions showed that both proteins co-migrated at the expected size (Figure 25b).

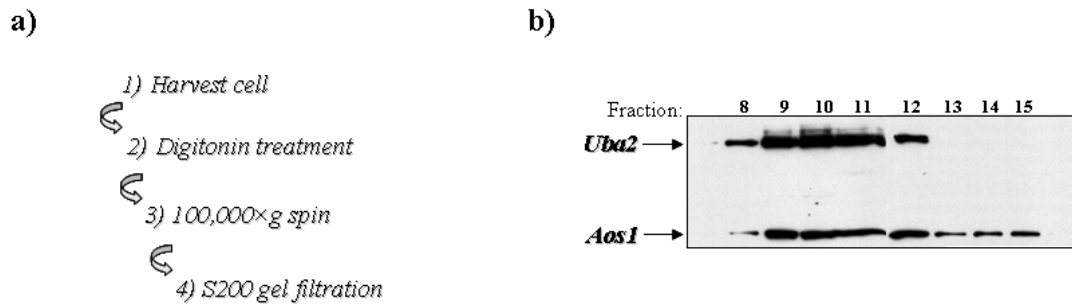


Figure 25. Aos1 and Uba2 run as a complex in HeLa cytosol. a) Schematic representation of the experiment, b) Western blot with α -Aos1 and α -Uba2 antibodies of the corresponding fractions.

This finding is consistent with recent published work by others (Azuma et al., 2001), and demonstrates that Aos1 and Uba2 exists predominantly as a herodimeric stable complex.

4.2.4 Aos1/Uba2 is present in Golgi fraction

Based on the cell fractionation experiment and immunofluorescence, which showed that a small amount of Aos1 and Uba2 were present in pellet fractions that could correspond to Golgi membranes or endoplasmatic reticulum, Golgi fraction isolation from cultured cells by flotation through a discontinuous sucrose gradient was performed. Briefly, HeLa cells were pelleted and resuspended in 3 ml of homogenization medium containing 0.25 M sucrose, 10 mM Tris, pH 7.4, and homogenized in a Dounce homogenizer. 1.4 M homogenate was made by adding 2 vol of 2.0 M sucrose gradient solution. The final gradient was constructed by overlaying the 3 ml of 1.6 M sucrose, next the 3 ml of homogenate, and then the sample was overlaid with 3 ml of 1.2 M sucrose gradient solution and 3 ml of 0.8 sucrose gradient solution. Samples were centrifuged for 2 h in an ultracentrifuge at 110,000×g, 4°C. During centrifugation, the Golgi membranes, which have a much lower density than those of the other membrane particles (with the exception of the trans-Golgi network and possibly the plasma membrane), float upwards to band at the 1.2 M/0.8 M sucrose interface (Figure 26a). Fraction corresponding to Golgi was

collected and loaded on 5-20 % gel and analysed by western blot with antibodies against Aos1, Uba2, Ubc9 and GM130 (Golgi marker); (Figure 26b). In addition, all of the fractions were loaded on a gradient gel and subjected to immunoblot with anti-Aos1 antibody. As it shows in Figure 26, indeed, Aos1 was enriched at the Golgi fraction. The enrichment of Aos1 at the Golgi was confirmed using isolated Golgi fraction from rat liver, kindly obtained from Dr. F. Barr (data not shown).

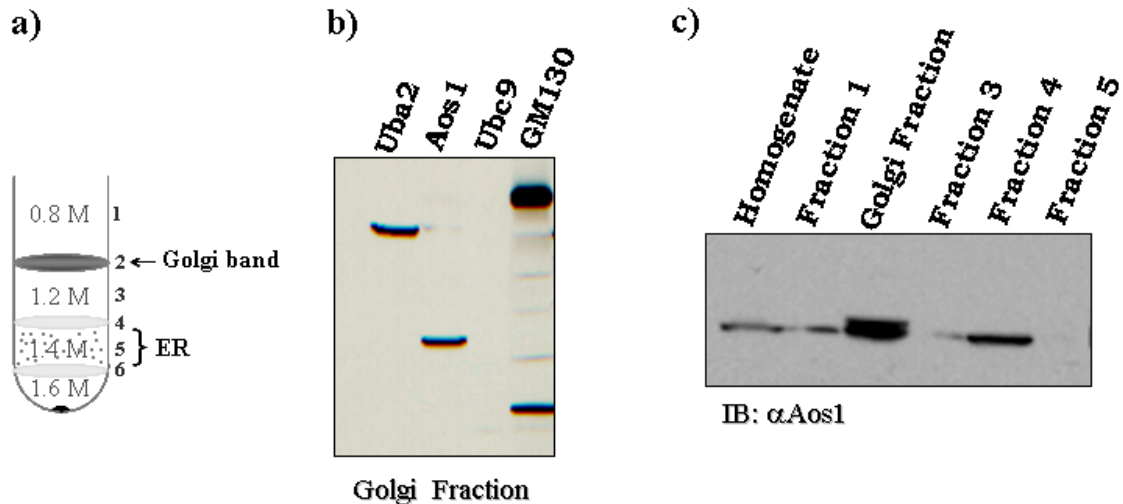


Figure 26. a) Illustration of the purification procedure used to isolate the Golgi fraction from HeLa cells, b) Western blot showing Aos1 and Uba2 proteins were detected in the Golgi fraction. Golgi fraction was analysed by western blots using antibodies directed against: Uba2, Aos1, Ubc9 and GM130, c) Different fractions (1-5) were analysed by western blots using antibodies against Aos1.

4.2.5 Identification of a new binding partner (ELKS) for Aos1

So far I could clearly demonstrate that Aos1/Uba2 is not only a soluble heterodimer, but is associated with other cellular structures, possibly with the Golgi. This raised the question whether additional binding partner for Aos1/Uba2 could be identified. As it was shown earlier, both anti Aos1 and anti Uba2 antibodies worked nicely in immunoprecipitation and are thus a good tool for the identification of such proteins. Immunoprecipitation under nondenaturing conditions was performed (see Materials and Methods). In brief, 10 l HeLa suspension cells were harvested by centrifugation, washed 1 time in ice cold PBS, and resuspend in nondenaturing buffer [1% (w/v) Triton X-100, 50 mM Tris-Cl,

pH 7.4, 300 mM NaCl, 5 mM EDTA, 0.02% (w/v) sodium azide]. Suspension was incubated on ice for 30 min and centrifuged for 10 min at 1000 rpm. Soluble lysate was generated by centrifugation at 6000×g for 10 min, then at 20000×g for 10 min, and used for immunoprecipitation. Affinity-purified antibodies or control IgGs cross-linked at 2 mg/ml to Ultralink Immobilized Protein G Plus beads were incubated with extracts for 120 min at 4°C. Beads were washed four times in nondenaturing buffer and boiled in 2×SDS-Laemmli loading buffer. Samples were run on a gradient gel (5-20%) and stained with Coomassie blue (Figure 27). Bands were cut out and were analysed by mass spectrometry to identify the proteins. Samples preparation including trypsin digest was carried out by me, mass spectrometry analysis was carried out by Dr. Marjaana Nousiainen (group of Dr. Körner, MPI in Martinsried).

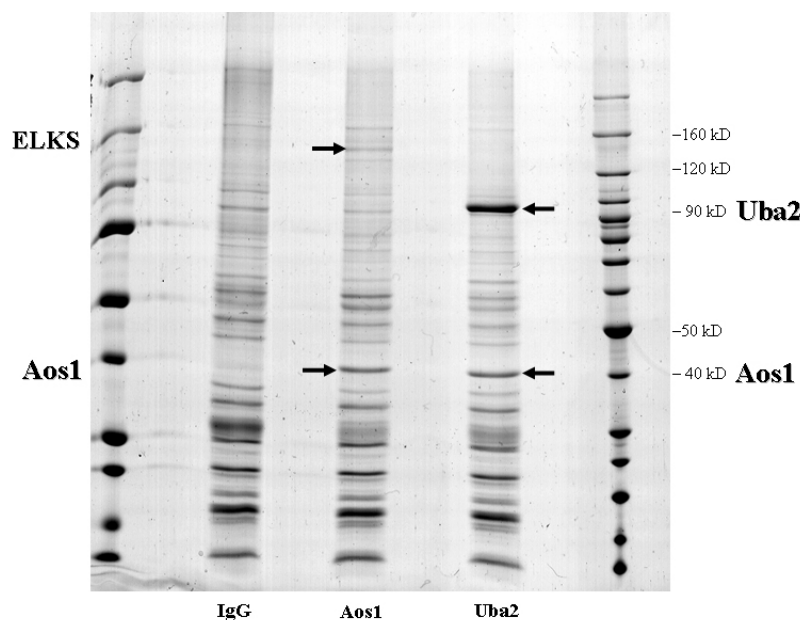


Figure 27. Identification of ELKS as a new binding partner for Aos1. Coomassie blue stained gel, shows immunoprecipitation from HeLa cell extract under nondenaturing conditions. First lane: IgG-control, second lane: IP-Aos1, third lane: IP-Uba2.

Several bands which were distinct compared to the control lane were cut out and analysed. A 130 kDa band which was found in the anti Aos1 immunoprecipitation showed high homology to the sequence of a protein called ELKS. These experiments showed that ELKS specifically associates with the Aos1 subunit, but not with Uba2. It is however possible that all three proteins form a complex under physiological buffer

conditions. Aos1 and Uba2 co-fractionated in differential centrifugation, and in gel filtration, but 1 % Triton disrupts also the association of recombinant Aos1 and Uba2.

4.2.6 Published functions of ELKS

ELKS was originally identified as a gene with its 5'-terminus fused to the RET tyrosine kinase oncogene in a papillary thyroid carcinoma (Nakata et al., 1999). The name ELKS is derived from the relative abundance of its constitutive amino acids: glutamic acid (E), leucine (L), lysine (K), and serine (S). Secondary structure prediction of the ELKS sequence indicates coiled-coil motifs throughout the protein and a leucine zipper at the C terminus (Figure 28b). The protein sequence of ELKS is hydrophilic, and the majority (except the first 143 residues of the N terminus, and a short segment located between residues 993 and 1060) is predicted to be α -helical containing heptad repeats characteristic of coiled-coil domains (Figure 28a).

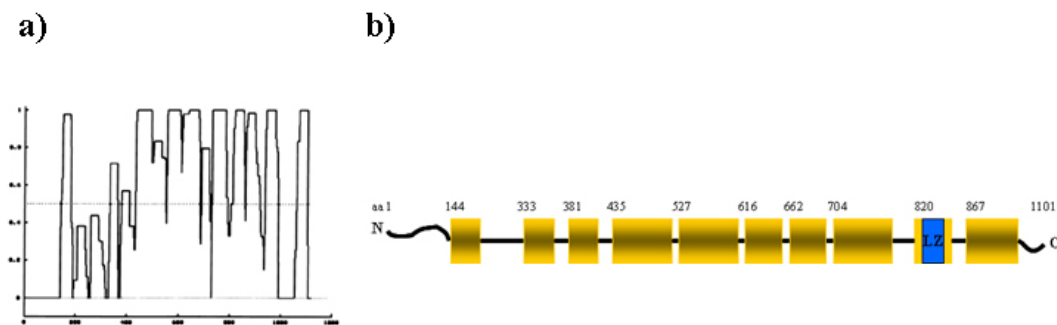


Figure 28. Sequence of ELKS protein. a) Prediction of the coiled-coil regions of ELKS (based on “Coils”), b) Schematic diagram of the secondary structure prediction for ELKS using PAIRWISE residue correlations. Boxes indicate the predicted coiled-coil domains, including the leucine zipper (LZ) motif (From Sigala et al., 2004).

ELKS involvement in nuclear factor kappa B (NF κ B) signaling

ELKS was also identified as an essential regulatory subunit of the IKK complex (Ducut Sigala et al., 2004); (Figure 29). Silencing ELKS expression by RNA interference blocked induced expression of NF κ B target genes, including the NF κ B inhibitor I κ B α ,

proinflammatory genes such as cyclo-oxygenase 2 and interleukin (IL)-8. These cells were also not protected from apoptosis in response to cytokines. ELKS functions by recruiting I κ B α to the IKK complex and thus serves a regulatory function for IKK activation. ELKS, as it was suggested, may serve a regulatory function in the NF κ B-activation (Ducut Sigala et al., 2004).

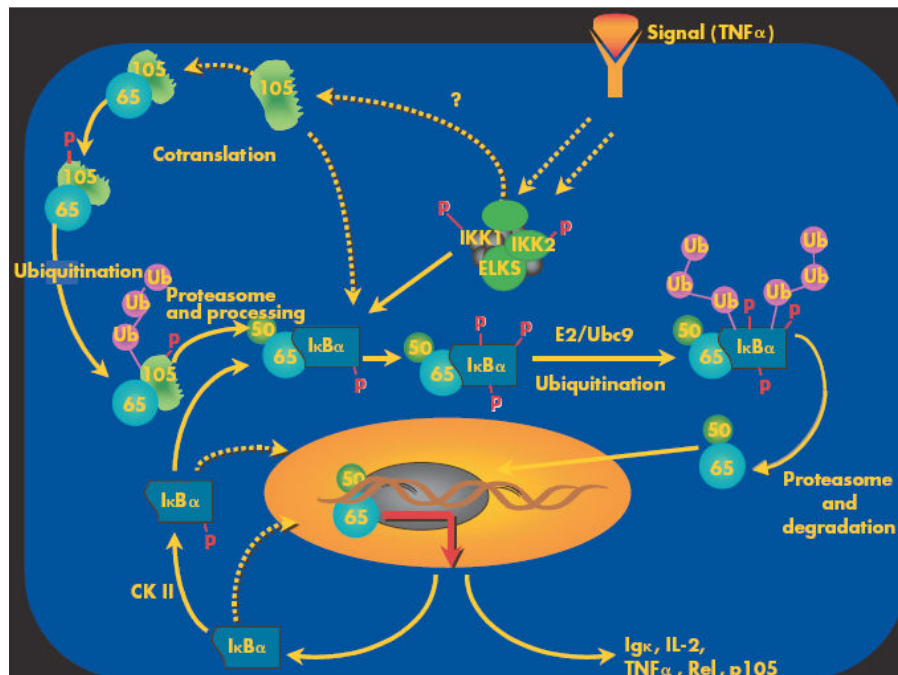


Figure 29. Schematic illustration on NF κ B activation. Induction with TNF α causes IKK complexes to phosphorylate I κ B α , which leads to its degradation and allows NF κ B dimers to enter the nucleus, where they bind to cognate DNA binding sites and deactivate transcription of genes including I κ B α . I κ B α can then either translocate to the nucleus and remove the NF κ B proteins bound to DNA or translocate to the cytoplasm to prevent further activation. At the same time new p50 is generated by processing of p105. ELKS is believed to function by recruiting to IKK complex (adapted from Verma IM 2005).

The importance of ELKS in vesicular transport

ELKS has also been identified as a Rab6-interacting protein 2 (Monier et al., 2002). Monier et al., reported two novel proteins, Rab6IP2A and Rab6IP2B (ELKS) that specifically interact with GTP-bound forms of Rab6A and A'. ELKS, which is a cytosolic protein, is recruited to Golgi membranes in a GTP-dependent manner and is likely to function in endosomes to Golgi transport.

ELKS appears to be involved in intracellular membrane traffic in several tissues (Monier et al., 2002; Wang et al., 2002) and notably, ELKS is a component of active zones in the brain that binds RIMs (presynaptic active zone proteins that regulates neurotransmitter release), (Wang et al., 2002; Deguchi-Tawarada et al., 2004). These data suggest that ELKS have at least two principal functions, one that is ubiquitously executed in the cytosol and one that is synapse-specific and associated with the active zone (Wang et al., 2002).

Very recently, another study demonstrated that ELKS is involved in the regulation of insulin exocytosis (Imaizumi et al., 2005). ELKS was expressed in rat pancreatic islets and in an insulin-producing clonal cell line, MIN6 β cells, where it colocalized with both insulin granules and syntaxin 1. The data obtained indicated that ELKS regulated insulin exocytosis.

4.2.7 Generation of recombinant ELKS

Purification of recombinant ELKS (full length and small fragments) for antibody generation and in vitro studies

A GFP-ELKS construct containing the full length open reading frame could be obtained from Dr. S. Monier (Institute Curie, Paris). To generate recombinant full length ELKS protein, the open reading frame of ELKS sequence was amplified by PCR and cloned into three different bacterial expression vectors encoding different affinity-purification tags: pGEX-4T-1 (EcoRI, NotI sites), pASK-IBA43 (SacII, SalI sites) and pET28 a (EcoRI, NotI sites), (Figure 30a, b). Whereas GST-ELKS was insoluble and His-ELKS-strep was highly degraded, His-ELKS could be purified to satisfactory levels.

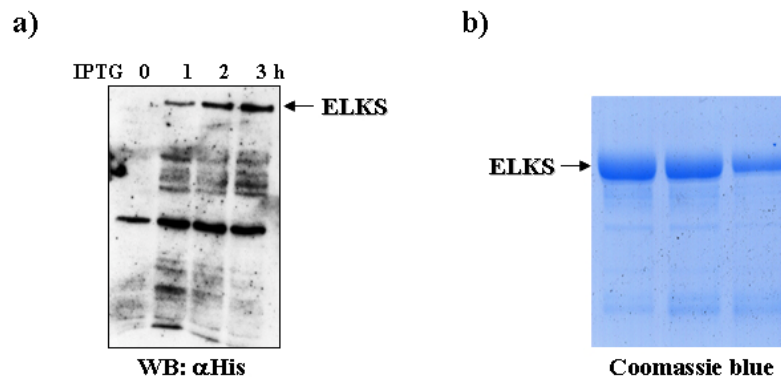


Figure 30. Expression of full length ELKS. a) ELKS was cloned into the bacterial expression pASK-IBA 43 system and the protein was expressed and purified (see Materials and Methods). Supernatants of *E. coli* cell lysates from 0-3h IPTG induced cultures were analysed by SDS-PAGE and immunoblot against His antibodies. Specific bands are indicated by arrows. b) ELKS full length was cloned into the bacterial expression vector (pET28a) and the protein was expressed and purified (see Materials and Methods). Picture showed Coomassie staining of three harvested fractions of His-ELKS after S200 gel filtration column.

In addition, seven short fragments were generated as GST fusion proteins: (Fragment 1, contained 1-888 aa; Fragment 2, residues 889-1800; Fragment 3, residues 1801-2640; Fragment 4, residues 2641-3361; Fragment 1, 1P residues 1-573; Fragment 1+ Fragment 2, residues 1-1800 and Fragment1, 3P, residues 1-1113) (Figure 31a, Table 4).

These fragments were also cloned into the mammalian expression vector pCruz and tested for expression after transient transfection. Figure 31b shows that fragments one, two, and three were highly expressed in HeLa cells while fragment four were expressed at lower level.

ELKS constructs	amino acids	solubility
ELKS full length in pGEX-4T-1	1-1101	–
ELKS full length in pASK-IBA43	1-1101	–
ELKS full length in pASK-IBA45	1-1101	–
ELKS full length in pET28a	1-1101	+
Fragment 1 in pGEX-4T-1	1-290	–
Fragment 1,1P in pGEX-4T-1	1-192	+
Fragment 1,3P in pGEX-4T-1	1-372	+
Frag.1+Frag.2 in pGEX-4T-1	1-600	+
Fragment 2 in pGEX-4T-1	290-600	+
Fragment 3 in pGEX-4T-1	600-880	+
Fragment 4 in pGEX-4T-1	880-1101	+

Table 4. Generation of ELKS expression constructs.

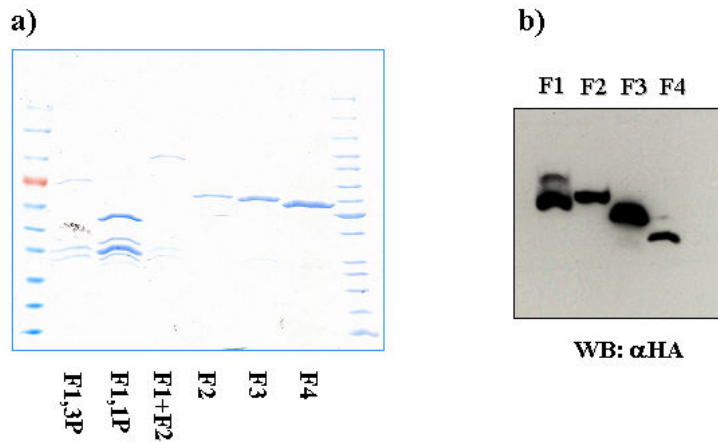


Figure 31. Expression of ELKS deletion fragments. a) Selected recombinant ELKS fragments separated on a 5–20% (w/v) SDS gel and stained by Coomassie blue. b) Expression of HA-ELKS-fragments in HeLa cells. ELKS fragments were cloned into the mammalian pCruz A expression vector and were transfected in HeLa cells for 48 hours (as described in Materials and Methods). Cells were harvested in 2×SDS Laemmli loading buffer and subjected to anti HA western blot.

4.2.8 Generation and characterisation of ELKS polyclonal antibodies

To find the connection between ELKS and SUMO E1 enzyme, it was necessary to generate antibodies against ELKS. For the production of polyclonal antibodies against ELKS, two recombinant GST-tagged ELKS fusion proteins were used (Frag.1+Frag.2 and Fragment 4, see table 4; Figure 32). For the generation of polyclonal antibodies, each of the recombinant fusion proteins were used to immunize a rabbit (see Material and Methods) and the resulting immune sera, α -N-terminus and α -C-terminus antibodies, were then affinity purified.

```

1 MYCSARSVGR VEPSSQSPGR SPRLPSPRL CHRRTNSTGC SSGNSVCGCS
51 GKTLSMHNQ SLMAYATSC PHYLSDHENW GARTPKSTMT LGRSGGRLPY
101 GVRMTAMGSS PMLASSGVAS DTIAFGHHH PPVSMASTVP HSLRQARDNT
151 IMDLQTLKE VIRENDLLEK DVEVKESKLS SSMNSIKTFW SPFLKKEKAL
201 RFDKASKTI WKREYRVVQE ENQHMHTIQ ALQDELRIQR DLNLQFQDQS
251 SSRTCEPCVA ELTEENFQRL HARHERQAKR LFLLEKTLLE MELRIETQRQ
301 TLMARDESIR KLEMLQSKC LSAKATEEDH ERTRRARAE MHVHLESLL
351 EQKRENNML REEMHRRFEN APDSARTKAL QTVIRMRDSE ISSMERGLD
401 LEEETQMLKS NGALSSEERE EEMFQMEVYR SHSKFMKRV EQLKEELSSK
451 DAQCEELKRR AACLQSEIQG VRQELSRKDT ELLALQTKLE TLTNQFSDSK
501 QHI EVLKESL TAKEQRAAIL QT EVDALRLR LEEKETMLNK KTRQIQDMAE
551 EKCQAQRIH DLRDMLDVEE RYVWVLOKCI EMLQEQLEPK EKQMSSLKER
601 VKSIAQDTN TDTALTTLEE ALADKERTIE ELKEQRDRDE RENQEKIDTY
651 KKDLEKLEK VSLQGLSE KEASLDTKE HRS SLASSGL KKSRLKTLK
701 TALEKKEEC LKME SQLKKA HEKTLKRRAS PEMSDRIQQL EREI SRYKDE
751 SSKMQTEVDR LLEKLEVEN EKNDKDKKIA ELE SLT SRV KQNKVAVNL
801 KHKEQVEKKK SQMLKEARR REDSLSDSQQ QLQDSLKKKD DRIEELEKAL
851 RESVQITRER EMVLRQEEEA RTNAENQVEE LLMANERKVKQ ELESKAKLS
901 STQQSLARKK THLTMLRAER RKHLE EVL RM FQBALLAATS EFDANIALLE
951 LSSSEKKTQE EVAALKRERD RLVVQLRQQT QNRMKLMADN YEDDHFSSR
1001 SNQTNHKPSP DQIIQPLLEL DQNSKSLKLY IGHILTALCHD RDPLILRGLT
1051 PPASTYNADGE QAANENE LQQ MTQEQQLQNEL ERVCEQNAEL QEFANTILQQ
1101 IADHCPDILE QVWNALEESS

```

} *N-terminus fragment*

} *C-terminus fragment*

Figure 32. Protein sequence of human ELKS. N-terminal antibodies were raised against sequence of first 600 amino acids, and C- terminal antibodies against last 221 amino acids.

To evaluate the specificity of the purified antibodies directed against ELKS, the antiseras were examined in western blots of HeLa cell extracts containing 10 ng of recombinant full-length ELKS. Both antiseras selectively recognized the recombinant ELKS in Western blots and endogenous ELKS present in the HeLa cell extracts (Figure 33a). Purified antibodies of ELKS N- and C-terminus were further characterized by immunoprecipitation under nondenaturing conditions (Figure 33b). Both of the antibodies work well in immunoprecipitation

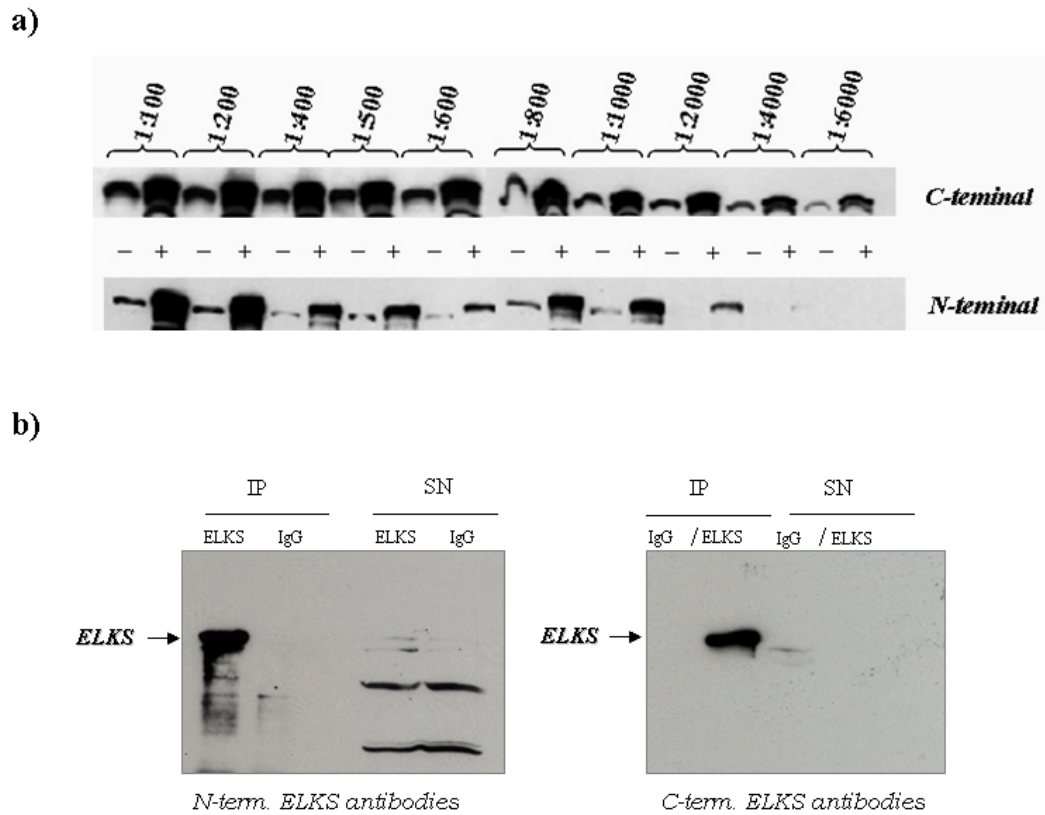


Figure 33. Characterization of ELKS antibodies. a) ELKS (N- and C- terminus) antibodies specifically recognized a single band in HeLa cells extract. (-) 10×10^4 HeLa cells or (+) 10×10^4 HeLa cell + 10 ng of recombinant full length ELKS were used for testing the ELKS antibodies on western blot. b) Immunoprecipitation using ELKS N- and C-terminal antibodies in HeLa cells lysate under nondenaturing conditions.

ELKS antibodies were tested in western blot, immunoprecipitation assays and cell immunostaining (as shown below). Results are summarized in Table 5.

Table 5 Working conditions of ELKS antibodies

ELKS antibodies		
	ELKS N-terminal	ELKS C-terminal
<i>yield</i>	1 mg/ 15 ml of serum	2.49 mg/ 15 ml of serum
<i>concentration of glycerol stock</i>	0.5 mg/ml	1.47 mg/ml
<i>dilution for Western blot</i>	1:1000	1:6000
<i>dilution for immunoprecipitation</i>	1:50	1:100
<i>dilution for immunofluorescence</i>	1:100	1:300

4.2.9 Conformation of ELKS-Aos1 interaction

I originally identified ELKS by mass spectrometry in immunoprecipitation experiment performed under nondenaturing conditions, with the lysis buffer containing Triton X-100 (see Material and Methods). To confirm these results, whether Aos1 and ELKS can bind to each other co-immunoprecipitation assays in HeLa cell extracts from the same buffer were performed using my own ELKS antibodies (Figure 34). Affinity-purified antibodies or control IgGs cross-linked at 2 mg/ml to Ultralink Immobilized Protein G Plus beads (for Aos1) or Protein A (for ELKS, C-terminal antibodies) were incubated with HeLa cells extracts for 120 min at 4°C. Beads were washed four times in nondenaturing buffer and boiled in 2×SDS-Laemmli loading buffer. Samples were run on a gradient gel (5-20%), and the immunoprecipitates were analyzed by immunoblotting against Aos1 or ELKS.

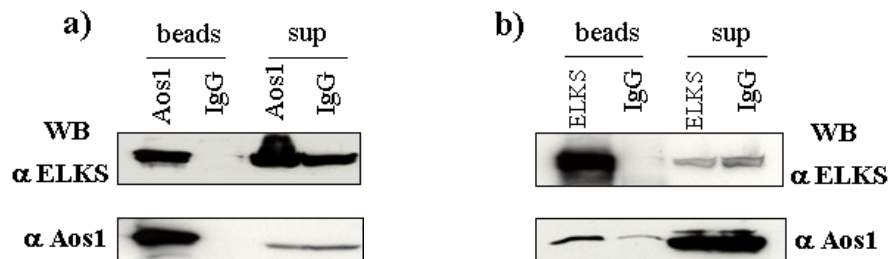


Figure 34. Co-immunoprecipitation of Aosl and ELKS in HeLa cell extracts. a) using Aosl antibodies ELKS protein was coimmunoprecipitated, while in b) Aosl was coimmunoprecipitated using ELKS antibodies.

Immunoprecipitation of endogenous Aosl demonstrated that Aosl strongly interacts with ELKS (Figure 34a) and the other way around, in ELKS immunoprecipitation Aosl was pulled down (Figure 34b). These results suggest that Aosl is able to interact with ELKS *in vivo* and also that this interaction is specific.

ELKS does not form a stable complex with Aosl in cytosol

To characterise the cellular distribution of ELKS, differential centrifugation was performed (see Figure 24 and Table 3). Here, I noticed that ELKS could be found in insoluble fractions (Figure 35a), especially enriched in 22000×g pellet as well as Aosl (Figure 35a and see Figure 24). Additionally, a fraction of ELKS could be detected in cytosol, which was in line with previous study (Monier et al., 2002).

To further determine whether Aosl, Uba2 and ELKS could form a complex, HeLa cell cytosol was run on a S200 gel filtration column. HeLa cells were harvested, washed one time in cold PBS and resuspend in hypotonic swelling buffer. Cells were lysed by homogenization and centrifuged to remove the nuclei. Lysate was ultracentrifuged for 1 h at 100,000×g and supernatant was applied on S200 analytical column. Fractions were harvested and run on a gradient gel and finally blotted against Aosl, Uba2, or ELKS (Figure 35b).

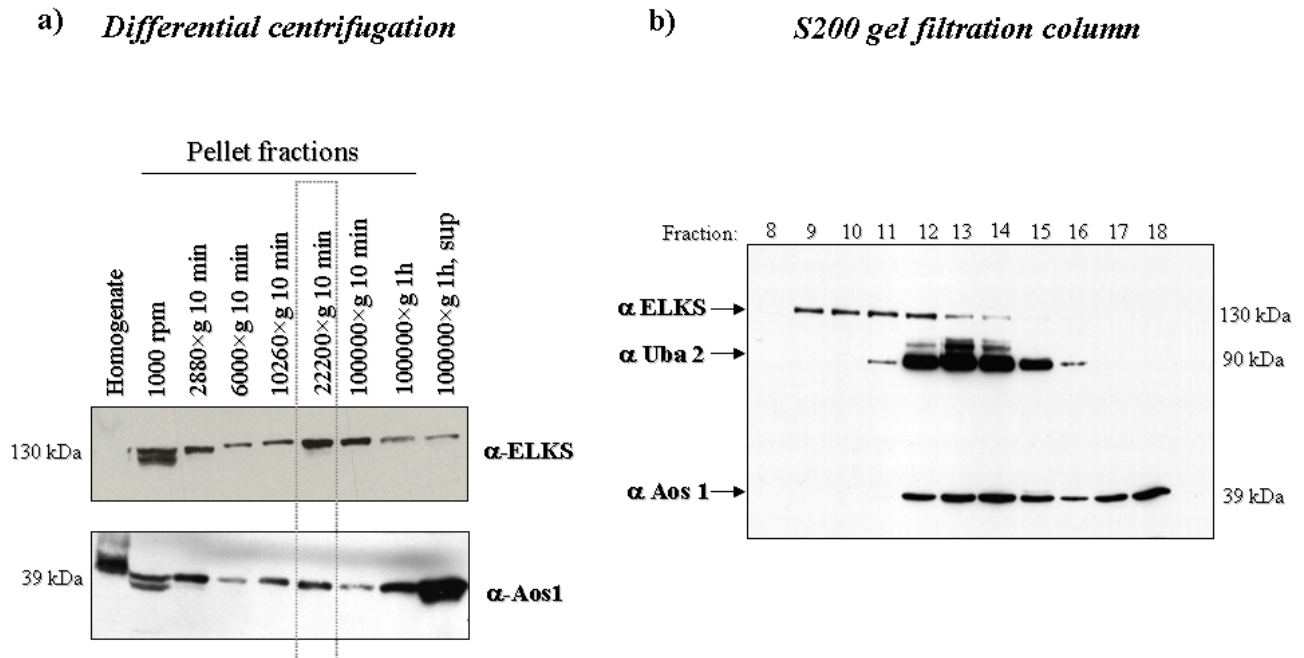


Figure 35. Differential centrifugation. a) HeLa cells were harvested and subcellular fractions were analysed by western blot analysis using antibodies against: Aos1 and ELKS. Subcellular fractions (Table 3) were separated by SDS-PAGE, blotted and stained with anti-Aos1 or anti-ELKS. b) Profile of Aos1, Uba2 and ELKS after Sephadex 200 analytical run. Cytosol fraction of HeLa cells in hypotonic swelling buffer was injected onto column and these fractions were analysed by western blot against Aos1, Uba2 and ELKS antibodies was performed.

As it is shown in Figure 35b I could not detect significant association between ELKS/Aos1-Uba2. Therefore, Aos1, Uba2 and ELKS proteins do not form a stable complex in HeLa cytosol under physiological salt conditions.

4.2.10 Subcellular localisation of ELKS

Immunofluorescence was used next to gain further insights into ELKS localisation. As shown in Figure 36 ELKS localised exclusively in the cytoplasm to discrete punctuate structure and this localisation was in line with previous studies (Monier et al., 2002; Ducut Sigala et al., 2004; Imaizumi et al., 2005).

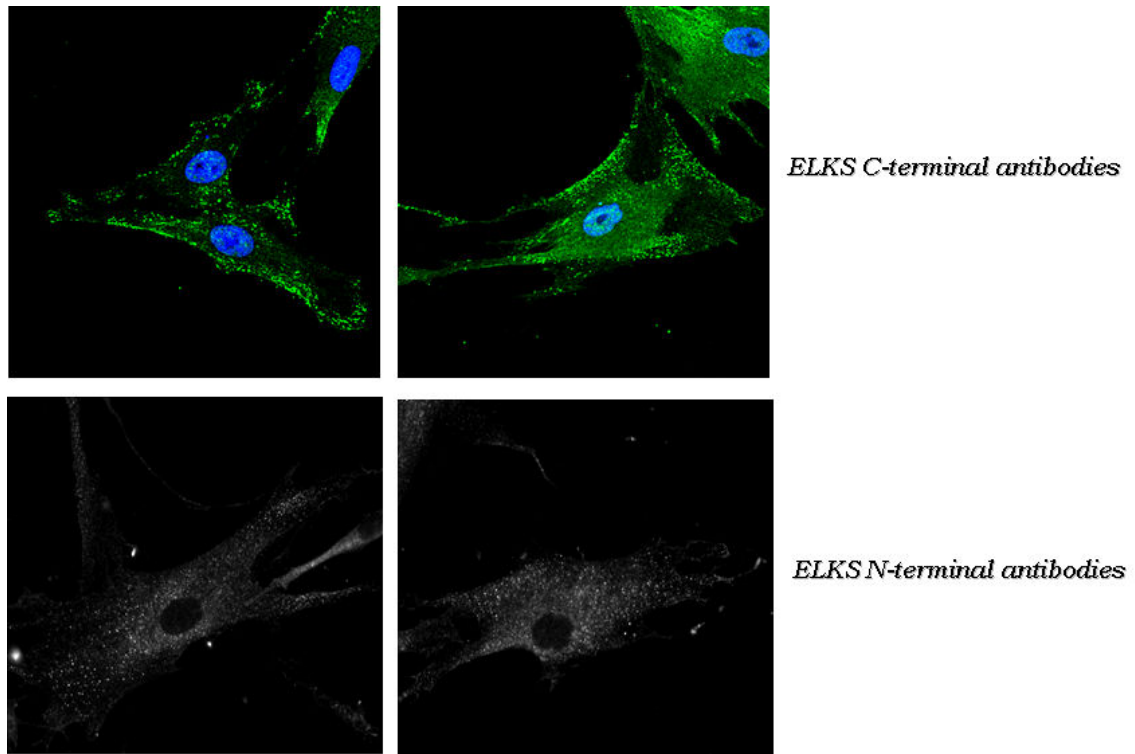


Figure 36. Subcellular localisation of ELKS using confocal microscope. Hs68 cells were stained for endogenous ELKS, with C-terminal or N-terminal antibodies, (secondary antibody Cy3TM) and Hoechst.

ELKS colocalises with late endosomes

To gain insights into the nature of the punctate structures stained by anti-ELKS antibodies, co-staining with different vesicle specific antibodies, labeling early endosomes (EEA1), clathrin and late endosomes (anti-LAMP-1) was performed (Figure 37).

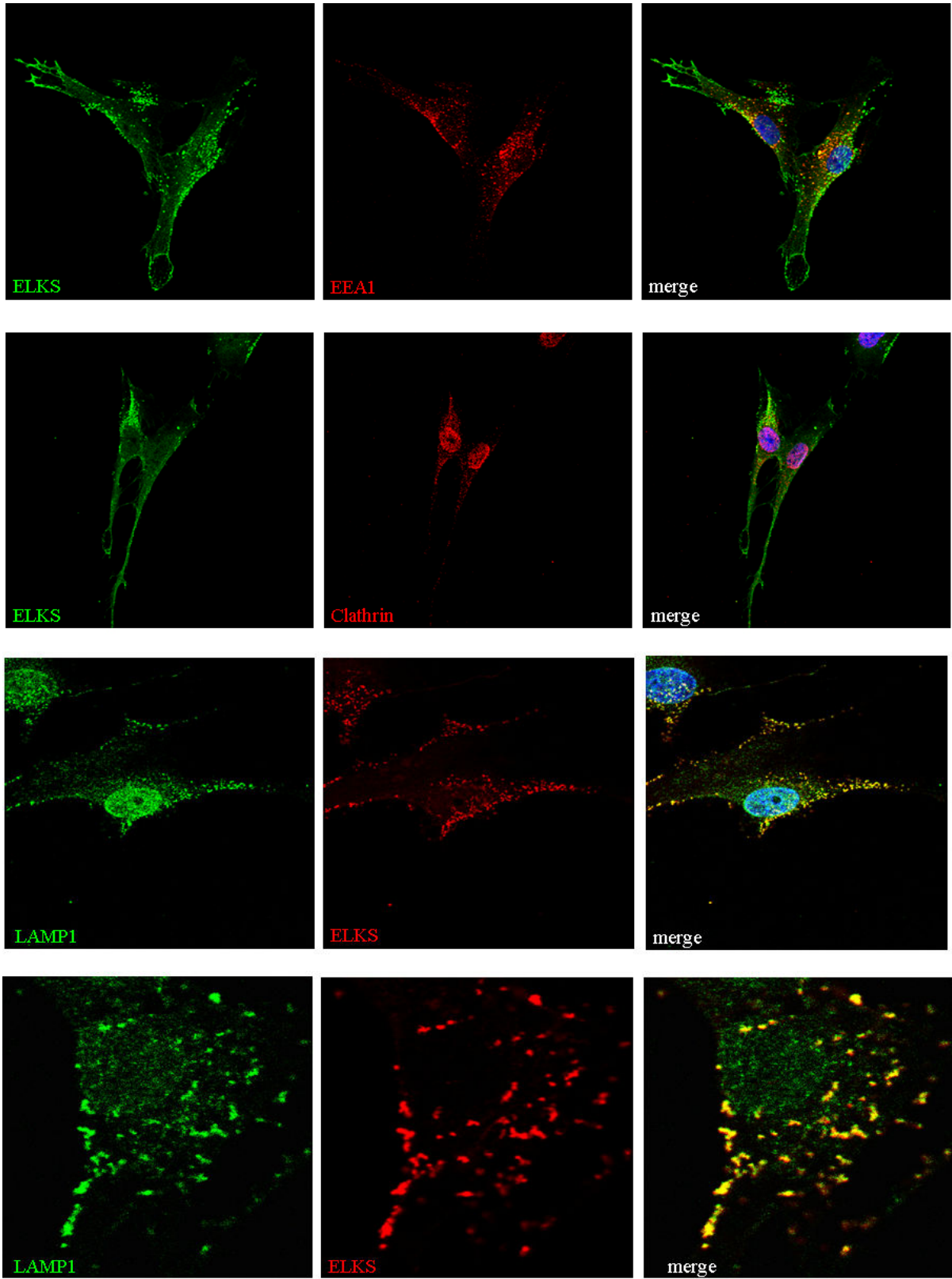


Figure 37. Subcellular localisation of ELKS using confocal microscopy. The localization of endogenous ELKS protein was analysed in Hs68 cells. Hs68 cells were fixed with 2% PFA, permeabilized with 0.2% Triton X-100, and stained with antibodies directed against early endosomes (EEA1), clathrin, late endosomes (LAMP1), and finally visualized with FITC or Cy3TM coupled secondary antibodies. DNA was stained with Hoechst.

The results shown in Figure 37 strongly suggest that ELKS colocalises with late endosomes (LAMP1) but not with early endosomes (EEA1), nor clathrin. The question that remained to be addressed is, if Aosl also colocalises with late endosomes (work in progress for finding the best conditions for immunofluorescence).

4.2.11 Recombinant of ELKS and Aosl do not bind

Co-immunoprecipitation experiments using cell lysate do not exclude the possibility that additional cellular factors may be involved in the binding. To study whether the interaction between the Aosl and ELKS is direct, pull down assays using all purified deletion fragments or full length ELKS and Aosl were performed (data not shown). However, no interaction between Aosl and ELKS was observed. While this could be due to improper folding or lack of a eukaryotic posttranslational modification, an alternative interpretation is that a bridging factor is required. One candidate is Rab6.

4.2.12 Rab6 is not the binding factor between ELKS and Aosl

Rab6 GTPases regulate intracellular transport at the level of the Golgi complex (Goud et al., 1990). Rab6 has been described as a binding partner for ELKS based on a yeast two-hybrid interaction and *in vivo* colocalisation (Monier et al., 2002). Direct interaction between these two proteins had however not been shown so far.

A Rab6 bacterial expression constructs were obtained from Dr. S. Monier (Institute Curie, Paris). I expressed and purified them (Figure 38a), and test for direct interaction between ELKS and Rab6. Pull down experiments using glutathione-S transferase (GST) fusion proteins with Rab6A, Rab6A' and Rab6B coupled to glutathione-Sepharose 4B

were performed (Figure 38a). ELKS was incubated in the presence of the GST-Rab6 fusion protein loaded with GTP γ S. ELKS was found to bind directly all three GST-Rab6 isoforms in their GTP conformation (Figure 38 b). As a control, GST alone was used, which did not bind ELKS.

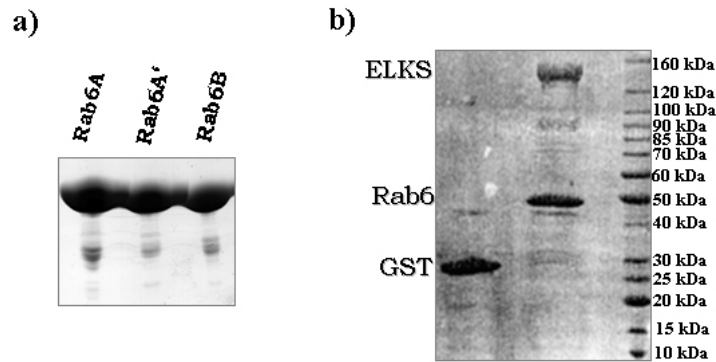


Figure 38. ELKS binds directly to Rab6. a) Recombinant Rab6 proteins (Rab6A, Rab6A', Rab6B) separated on a 5–20% (w/v) SDS gel and stained by Coomassie blue, b) Ponceau S staining showed direct interaction between Rab6A' and ELKS (for Rab6A and B data not shown).

Since ELKS binds directly to the GTP bound form of Rab6, one could speculate that Rab6 mediates the interaction between ELKS and Aosl. GST pull down experiments using recombinant GST-Rab6A', GST alone, His-Aosl and His-ELKS were performed (Figure 39). Unfortunately, specific association between ELKS, Aosl and Rab6 could not be detected, suggesting that Rab6 is not a bridging factor between Aosl and ELKS.

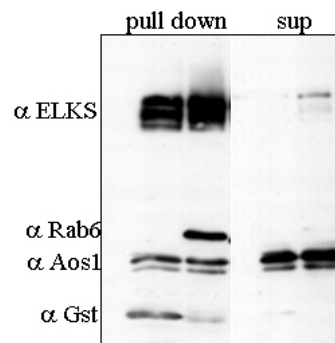


Figure 39. ELKS does not associate directly to Aosl and Rab6A' *in vitro*. The fusion protein GST-Rab6A', or the GST protein alone were coupled to Sepharose 4B glutathione beads, loaded with GTP γ S and incubated in the presence of full length His-ELKS and His-Aosl. After SDS-PAGE and blotting, the nitrocellulose membrane was cut and incubated with anti-ELKS antibody, or with anti-GST or anti-Aosl.

4.2.13 ELKS does not interact directly with SUMO *in vitro*

As Aosl is part of a SUMO E1 enzyme, I next tested if SUMO could be a bridging factor between Aosl and ELKS. For this, 1 μ g purified SUMO1 or SUMO2 proteins were mixed on ice with 1 μ g of His-ELKS in TB containing protease inhibitors, and then bound to Ni²⁺ beads. The beads were washed five times in TB and eluted with 2 \times SDS sample buffer. Samples were subjected to 5-20% SDS gel and analyzed by immunoblotting with SUMO1, SUMO2, or ELKS antibodies. As figure 40 shows, ELKS does not interaction with SUMO-1 or SUMO-2, at least *in vitro*. It is therefore unlikely that SUMO is the bridging factor between ELKS and Aosl.

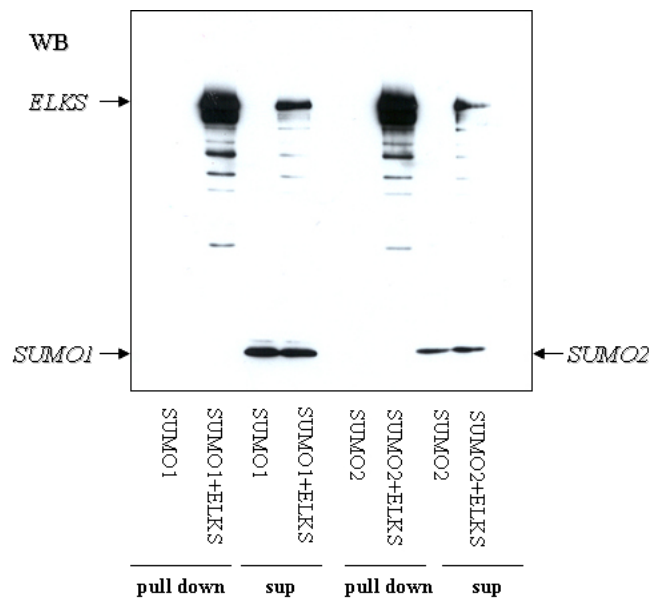


Figure 40. ELKS does not associate with SUMO1 and SUMO2. The fusion protein of SUMO1 or SUMO2 were incubated in the presence of His-ELKS full length. After SDS-PAGE and blotting, the nitrocellulose membrane was cut it and incubated with either anti-ELKS antibodies, anti-SUMO1 or with anti-SUMO2 antibodies.

4.2.14 Identification of binding partner candidates for Aos1 and ELKS

To identify protein/s which could have served as bridging factors between Aos1 and ELKS, large scale immunoprecipitation with HeLa cells was performed. In brief, cell pellet from 9 L HeLa suspension cells was washed 1 time in ice cold PBS, pellet was resuspend in nondenaturing buffer containing 1% (w/v) Triton X-100 (see Material and Methods) and lysate was generated for immunoprecipitation. After crosslinkage of affinity purified antibodies anti Aos1 and anti ELKS or control IgG to ultralink immobilized protein G or protein A, respectively, HeLa cell extracts were incubated with these beads for 120 min at 4°C. Beads were washed five times in nondenaturing buffer and boiled in 2×SDS-Laemmli loading buffer. Samples were run on a gradient gel (5-20%) and stained with Silver staining (Figure 41). All bands that are marked with stars were cut out and were analysed by mass spectroscopy. Samples preparation including trypsin digest was carried out by me, mass spectrometry analysis was carried out by Dr. Marjaana Nousiainen (group of Dr. Körner, MPI in Martinsried).

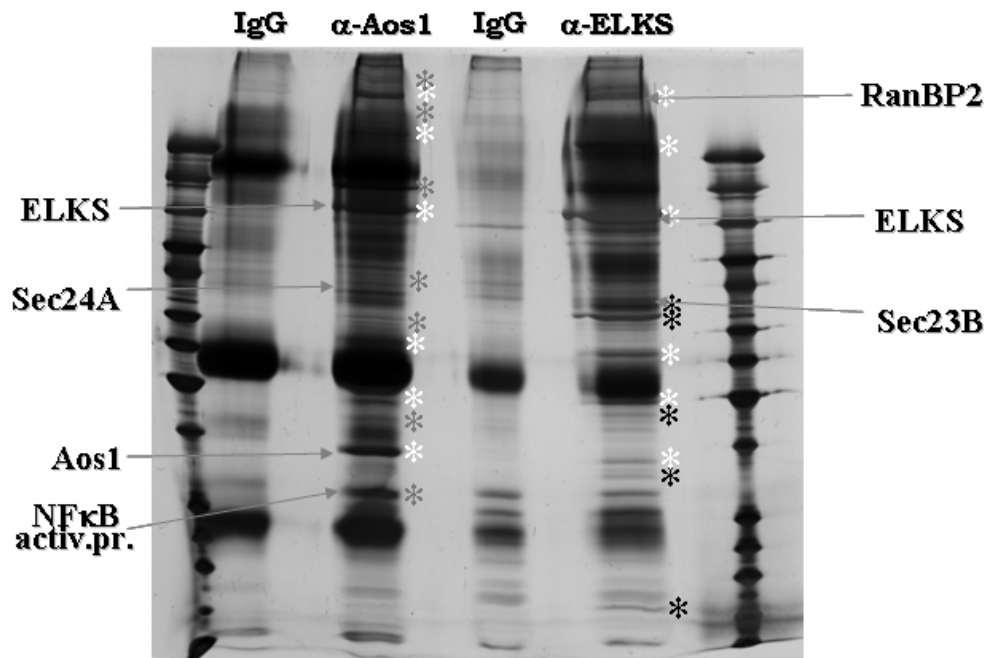


Figure 41. Silver stained gel showing α Aos1 and α ELKS immunoprecipitation. Aos1 and ELKS were immunoprecipitated from HeLa cells extract with anti-Aos1 and anti-ELKS antibody. The precipitates were fractionated by 5-20% SDS-PAGE and stained with silver staining. The bands marked with stars were cut out and analysed by mass spectrometry. White stars showed bands common for Aos1 and ELKS, and grey and black stars illustrate the bands characteristic for Aos1 and ELKS respectively.

Interestingly, Sec24A/Sec23B proteins were found to bind specifically to both Aos1 and ELKS. The Sec24A/Sec23B proteins are important in vesicle formation and they are involved in the ER to Golgi transport pathway. The established route for secretory proteins from the ER to the Golgi is via COPII coated vesicles (Bednarek et al., 1996; Schekman and Orci, 1996). Formation of COPII vesicles requires the ordered assembly of the coat built from the cytosolic components Sar1, Sec23–Sec24 and Sec13–Sec31 (Barlowe et al., 1994; Antonny et al., 2001).

Among other interesting proteins which were analyzed by mass spectrometry in the Aos1 immunoprecipitation was also a putative NF κ B activating protein (Figure 41), and in the ELKS immunoprecipitation was RanBP2, a nucleoporin with SUMO E3 ligase activity (Pichler et al., 2002).

In addition to the silver gel, 5 μ l of each samples were run on a 5-20% gel and immunoblotting was performed with specific antibodies against Aos1, Uba2, Ubc9, ELKS and RanBP2 (Figure 42a, b). RanBP2 was identified by mass spectrometry from the anti-ELKS immunoprecipitation. To test whether it was also present in the anti-Aos1 immunoprecipitation, immunoblot with RanBP2 was carried out. Indeed, RanBP2 was present in this immunoprecipitation, even much stronger (Figure 42a). As expected from known stable interaction of RanBP2 with Ubc9 (Pichler et al., 2004), Ubc9 was also found in the anti-Aos1 immunoprecipitation (Figure 42a).

As relative intensities of RanBP2, Ubc9 and Uba2 varied significantly between both immunoprecipitations this indicated that only a subpopulation of ELKS is in a complex with Aos1 (Figure 42a, b).

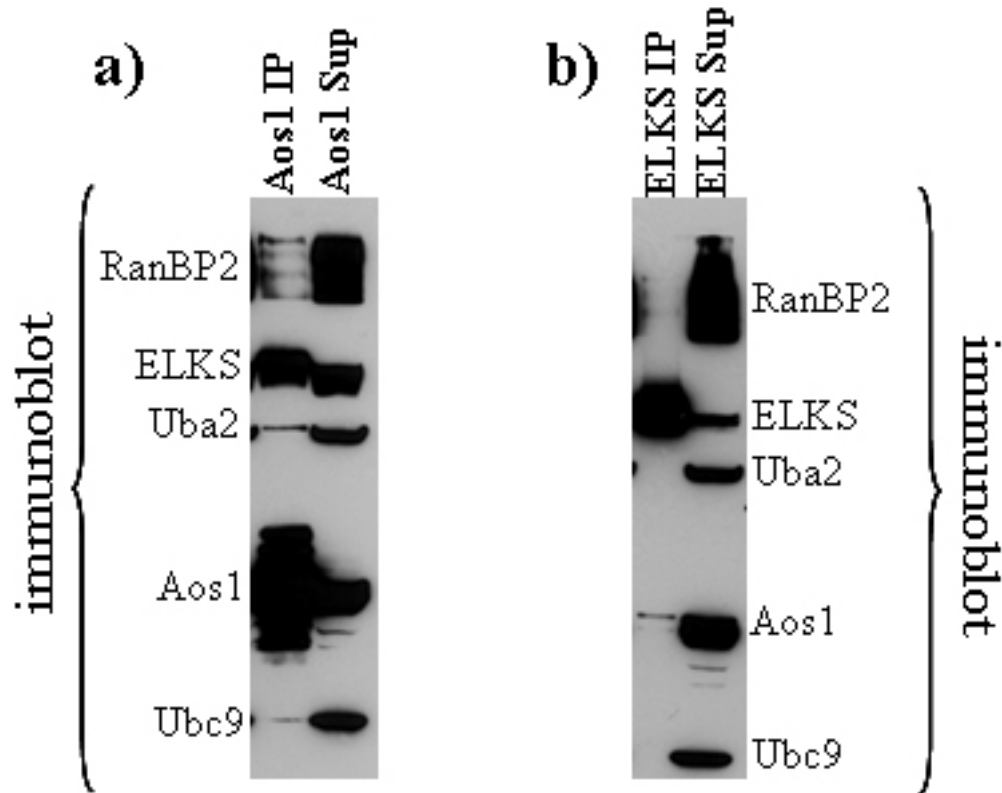


Figure 42. Immunoprecipitation of Aosl and ELKS. Aosl and ELKS were immunoprecipitated from HeLa cells using a) anti-Aosl antibody, b) anti-ELKS antibody. The precipitates were subjected to SDS-PAGE (5-20%) and detected with specific antibodies against: Ubc9, Aosl, Uba2, ELKS, RanBP2.

4.2.15 ELKS interacts with RanBP2 in interphase cell extract

To gain further evidence for RanBP2/ELKS interaction, nocodazole extracts were included, because a large pool of soluble RanBP2 is available in the extracts. Surprisingly, however, a small amount of RanBP2 co-precipitated only from interphase extracts (Figure 43).

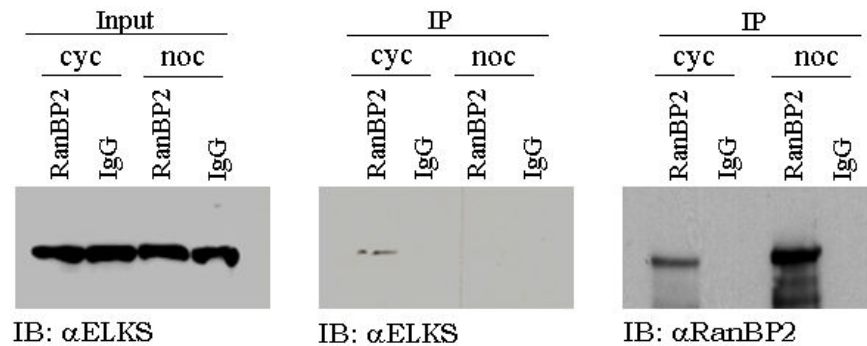


Figure 43. ELKS interacts with RanBP2 in the interphase extract. α RanBP2 immunoprecipitates from cycling cells or nocodazole extract were analyzed for the presence of ELKS by immunoblotting. IgG was from the respective preimmune sera and served as specificity control. Experiment was performed by Annette Flotho and membrane was obtained from her and probed with anti-ELKS antibodies.

As will be shown below (Figure 52) the weak interaction detected here could indeed be physiologically meaningful.

4.2.16 ELKS does not interact directly with BP2 Δ FG *in vitro*

As we had a small fragment of 358 kDa protein RanBP2 available in the lab, I could test whether it bound directly to ELKS. This fragment is the SUMO E3 ligase domain described previously (Pichler et al., 2002), consists of two internal repeats (IR1 and IR2) separated by the 25-residue M domain, and N- and C-terminal flanking regions. BP2 Δ FG contains residues from 2553 to 2838 aa. Recombinant GST or GST-BP2 Δ FG proteins were mixed on ice for 1 h with His-ELKS and His-Aos1 in nondenaturing buffer containing protease inhibitors. The mixture was incubated with 20 μ l of Glutathion Sepharose 4B beads for 90 min at 4°C. After washing five times with nondenaturing buffer, proteins associated with the beads were separated on 5–20% SDS-PAGE, and analysed by immunoblotting with anti-ELKS, anti-Aos1 and anti-GST antibodies (Figure 44). ELKS was unable to interact directly with BP2 Δ FG fragment of RanBP2. Altogether, this suggests that RanBP2 (at least the fragment used in this experiment) is

not the bridging factor between Aosl and ELKS. It will be important to repeat the experiment in the presence of Ubc9.

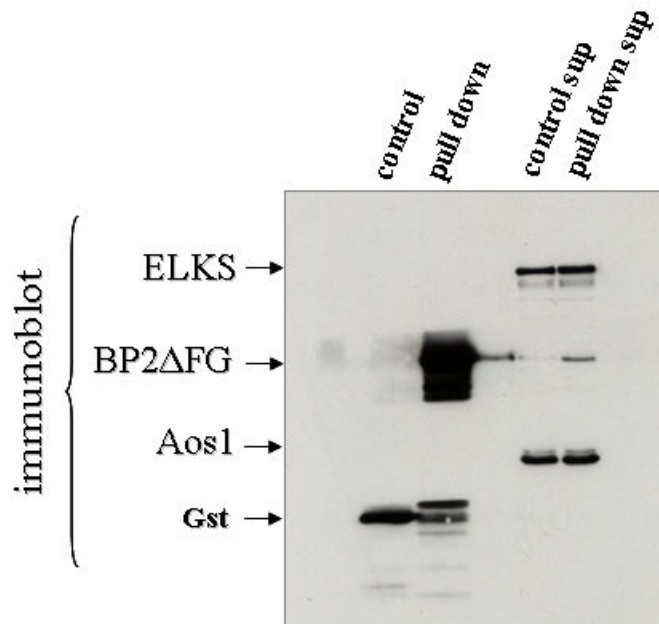


Figure 44. Fragment BP2 Δ FG of RanBP2 does not interact directly with ELKS in vitro. Recombinant His-ELKS, His-Aosl, GST-BP2 Δ FG and GST were subjected to GST pull down assay. Samples were analysed by immunoblotting with the indicated antibodies.

4.2.17 ELKS does not inhibit sumoylation

ELKS does not inhibit formation of thioester between E1 and SUMO

Even though a stable direct interaction between Aosl and ELKS could not be observed, this did not exclude the possibility of a transient interaction. I therefore wondered whether ELKS could affect SUMO activation. In the initial step, SUMO-activating enzyme (Aosl/Uba2) utilizes ATP to adenylate the SUMO C-terminus, which is then transferred to a conserved Cys residue in the catalytic subunit of the E1 (Uba2), yielding SUMO-E1 thioester, AMP and pyrophosphate.

I first tested the possibility that ELKS affects the thioester formation between SUMO and Uba2. E1-SUMO1 thioester formation was induced in the presence of E1, SUMO1 and

ATP, with or without a molar excess of ELKS at 30°C. Reaction was stopped at indicated time points with a nonreducing buffer (-DTT) or with a reducing buffer (+DTT). Samples were separated on a 6% SDS gel and analyzed by immunoblotting with α Uba2 antibody (Figure 45).

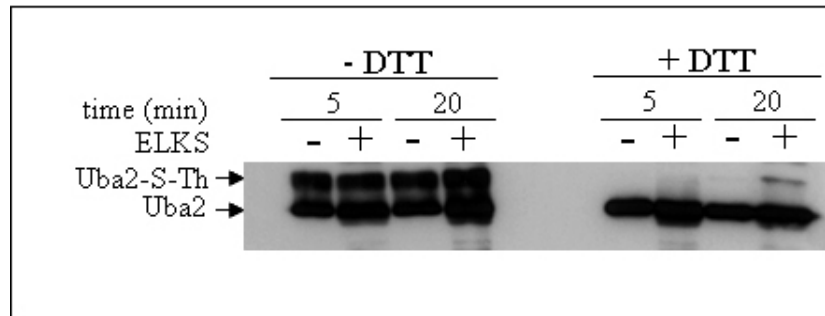


Figure 45. Uba2-SUMO1 thioester formation in the presence or absence of ELKS.

As shown in Figure 45, SUMO-E1 thioesters were formed very efficiently with or without ELKS, indicating that ELKS does not affect SUMO activation.

ELKS does not inhibit RanGAP1 sumoylation

To address the question whether ELKS inhibits a later step, i.e. transfer of SUMO from the E1 to Ubc9 or transfer of SUMO from Ubc9 to a target protein, a Fluorescence Resonance Energy Transfer (FRET) based sumoylation assay (described in Material and Methods) was performed. Briefly, 20 μ l reaction mixes without ATP were set up in 384 well plates. They included YFP-SUMO1 or YFP-SUMO2, CFP-GAPtail, Aos1/Uba2, Ubc9, and increasing concentrations of ELKS (from 0.012-10 pmol). FRET buffer, in which all proteins were diluted, contained Tween20 and ovalbumin to prevent nonspecific adsorption of the proteins. The reaction was started by addition of ATP (1mM) and was monitored over 30 min (Figure 46b; a)). As expected, linear rates over the whole time of the experiment were observed with low enzyme concentrations. Even increasing the ELKS concentration in the reaction did not change the reaction speed,

indicating that ELKS does not have any influence on the basic SUMOylation machinery. The FRET assay was also performed using SUMO1 and SUMO2 as a substrate, but again no difference was observed (Figure 46a&b).

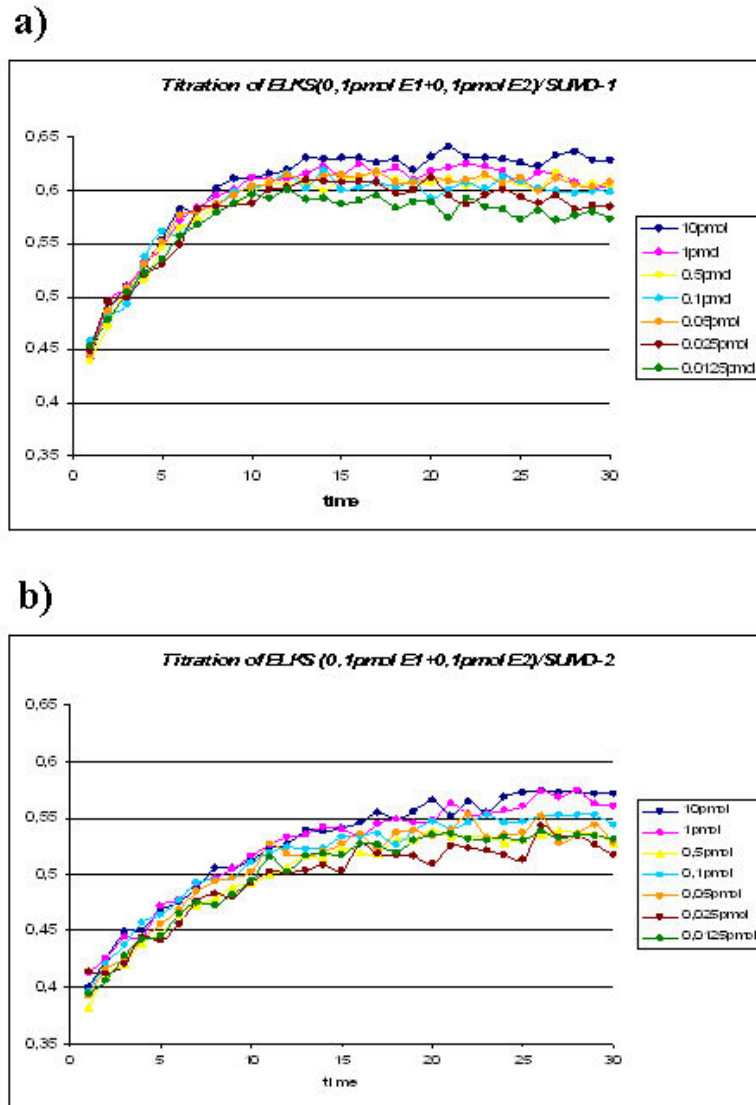


Figure 46. Effect of ELKS on RanGAP1 SUMO conjugation. The FRET based assay included YFP-SUMO1(a) or YFP-SUMO2 (b) , CFP-GAPtail, Aos1/Uba2, Ubc9, and increasing concentrations of ELKS (1×10^{-8}). The reaction was started by addition of ATP and was monitored over 30 min.

4.2.18 ELKS is SUMO modified on 3 distinct lysine residues

The immunoprecipitation experiment clearly showed that ELKS is a binding partner for Aos1 (SUMO E1 activating enzyme). Moreover, a small amount of the SUMO E3 ligase RanBP2 was found to co-precipitate. One explanation for these interactions could be that ELKS is a novel SUMO substrate. I first checked whether ELKS sequence contains possible acceptor lysines for sumoylation, which would be part of the SUMO consensus motif (Φ KXE), in which Φ is a large hydrophobic residue and K is the lysine to which SUMO is added (Rodriguez et al., 2001). As shown in figure 47 eight lysines are part of predicted SUMO consensus sequences.

```

1  MYGSARSVGK VEPSSQSPGR SPRLPRSPRL GHRRTNSTGG SSGNSVGGGS
51  GKTLSMENIQ SLNAAAYATSG PNYLSDHENV GAETPKSTMT LGRSGGRLPY
101 GVRMTAMGSS PNIASSGVAS DTIAFGEHHL PPVSHASTVP HSLRQAFQMT
151 IMDLQTLKE VLRENDLLRK DVEVKESKLS SSMNSIKTFW SELKKERAL
201 RKDEASKITI WKEQYRVVQE ENQHMQNTIQ ALQDELRIQR DLNQLTQDS
251 SSRTGEPVVA ELTEENFQRL HAEHERQAKE LFLLRKTLLE MELRIETQKQ
301 TLNARDES IK KLEMLQSKG LSAKATEEDH ERTRRLAEAE MHVHLESLL
351 EQKEKENNML REEMHRRFEN APDSAKIKAL QTVIEMKDSK ISSHERGLRD
401 LEEEIQLKLS NGALSSEERE EEPKQMEVYR SHSKFMKNKV EQLKEELSK
451 DAQGEELKKR AAGLQSEIGQ VKQELSRKDT ELLALQTKLE TLTNQFSDSK
501 QHIEVLKE SL TAKEQRAAIL QTEVDALRLR LEEKETMLMK KTKQIQDMAE
551 EKGTQAGE IH DLKDMLDVKE RKNVVLQKKI ENLQEQLRDK EKQMSLKER
601 VKSLQADTTN TDTALTTLEE ALADKERTIE RLKEQRDRDE FEMQEE IDTY
651 KKDLKDLREK VSLEQDLSE KEASLLDIKE HASSLASSL KKDSLKTLTLE
701 IALEQKKEEQ LKMESQLKKA HEATLEARAS PEMSDRIQQL EREISRYKDE
751 SSKAQTEVDR LEELKEVEN ENKDKDKKIA ELESLSRQV KQMKKVAML
801 KHKEQVEKKK SAQMLEEARR REDSLSDSQ QLQDSLERKD BRIELEAL
851 RE SVQITAEER EMVLAQEEA RTNAEKQVEE LLMAMEVKQ ELESNKAKLS
901 STQQLAEKE THLTNEFAER RKHLEEVLEM KQEQALLAATS EKDANIALLE
951 LSSSKKKTQE EVALKKREKD RLVQQLKQQT QNRMKLMADN YEDDHFRSSR
1001 SNQTNHKP SP DQIIQPLEL DQNRSKLKLY IGHLTALCHD RDPLILRGLT
1051 PPASYNADGE QAAWENELQQ MTQEQLQNEL EKVEGDNAEL QEFANTILQQ
1101 IADHCPDILE QVWNALEESS

```

Figure 47. Protein sequence of ELKS with marked SUMO consensus sites calculated by the SUMO prediction program (<http://www.abgent.com/doc/sumoplot>).

ELKS is sumoylated in vivo

Is ELKS a SUMO substrate? His-SUMO pull down was performed to determine if ELKS is SUMO modified *in vivo*. 293T cells were transfected with either HA-ELKS and His-SUMO2 or pCruz empty vector, and His-SUMO2 (control). 42 h after transfection cells were harvested. SUMO conjugates were enriched under denaturing conditions according to protocol (see Material and Methods). Samples were run on a 6% gel and subjected to immunoblotting with ELKS antibodies. Indeed a band corresponding to covalently

modified ELKS with the 12 kDa small ubiquitin like modifier (SUMO), was enriched specifically in bound fraction (Figure 48). Some unmodified ELKS was also detected in the bound fraction. This could be due either to some unspecific binding, or due to residual activity of SUMO isopeptidases in the experiment.

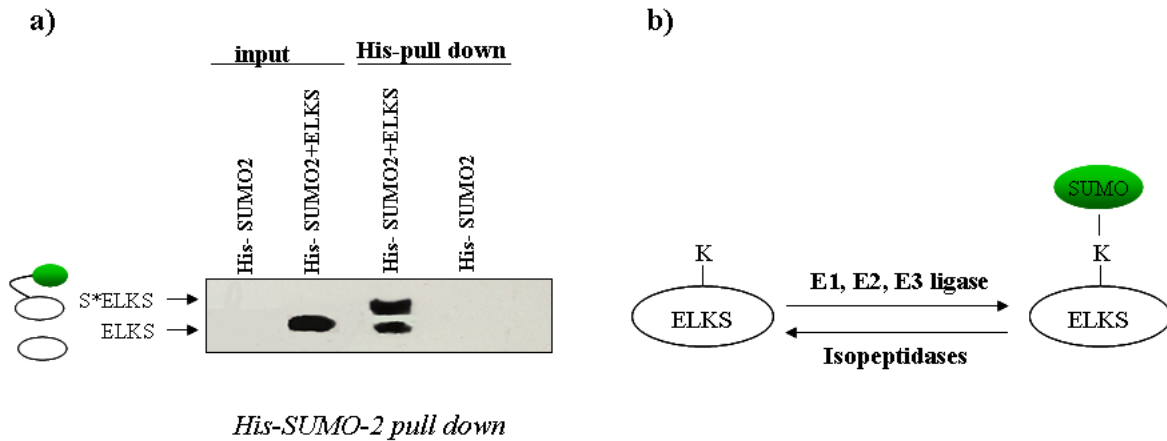


Figure 48. ELKS is sumoylated *in vivo*. a) His-SUMO-2 conjugates were purified on Ni²⁺-agarose, separated by SDS-PAGE, transferred to a membrane, and probed with antibody to detect ELKS. Some unspecific binding of ELKS occurs (see line third from the left), b) The SUMO conjugation pathway. After SUMO is proteolytically processed by C-terminal hydrolases, it serves as the substrate for an isopeptide bond formation between the free carboxyl group of the C-terminal glycine in SUMO and the ϵ -amino group of a lysine (K) in the acceptor protein. The catalytic reaction is mediated by the E1 activating enzyme: Aos1/Uba2, the E2 conjugating enzyme Ubc9, and an E3 ligase, which confers the substrate specificity. The cleavage of the isopeptide bond is mediated by isopeptidases.

Sumoylation of endogenous ELKS

To test whether endogenous ELKS is sumoylated as well, stable HeLa cell lines expressing His₆SUMO-1 or His₆SUMO-2 (kindly provided by Prof. Dr. Ronald Hay) were used. HeLa, HeLa Sumo1 or HeLa Sumo2 cells were lysed in denaturing conditions and sumoylated proteins were purified on Ni²⁺ beads according to protocol (see Material and Methods). Western blot analysis of purified substrates with ELKS antibodies showed that endogenous ELKS is indeed conjugated to SUMO-2 (Figure 49). The extremely low level of sumoylated endogenous ELKS is not unusual, as this has been observed for many SUMO targets.

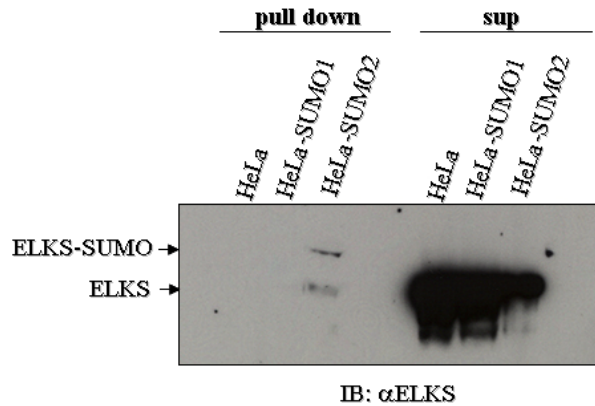


Figure 49. Ni²⁺-pull down under denaturing conditions from wild type HeLa cells or HeLa cells stably expressing His-SUMO1 or His-SUMO2. Immunoblotting was done with ELKS antibody.

Small deletions fragments of ELKS are modified in vitro by SUMO

Analysis of the ELKS sequence revealed eight putative SUMO acceptor sites (Figure 47). To determine whether these sites in ELKS are the actual sites of modification, I decided to analyse sumoylation of small deletion fragments of ELKS (see figure 31, Table4). GST-fragments of ELKS were tested in an *in vitro* SUMO conjugation system, consisting of purified proteins (Pichler et al., 2002). Incubation of recombinant GST-ELKS fragments with SUMO1, the E1 activating enzyme Aos1/Uba2, the E2 conjugating enzyme Ubc9 and ATP resulted in significant SUMO conjugation of ELKS-fragment four (2641-3361 aa) (Figure 50a). Most SUMO targets require E3 ligases for efficient modification. In light of my finding that a small fraction of RanBP2 coprecipitated with ELKS, I included the minimal catalytic domain of RanBP2 (IR1+M) in one reaction. Addition of IR1+M (domain of RanBP2, SUMO E3 ligase) led to multiple conjugation of SUMO1 to all ELKS deletion fragments (Figure 50b).

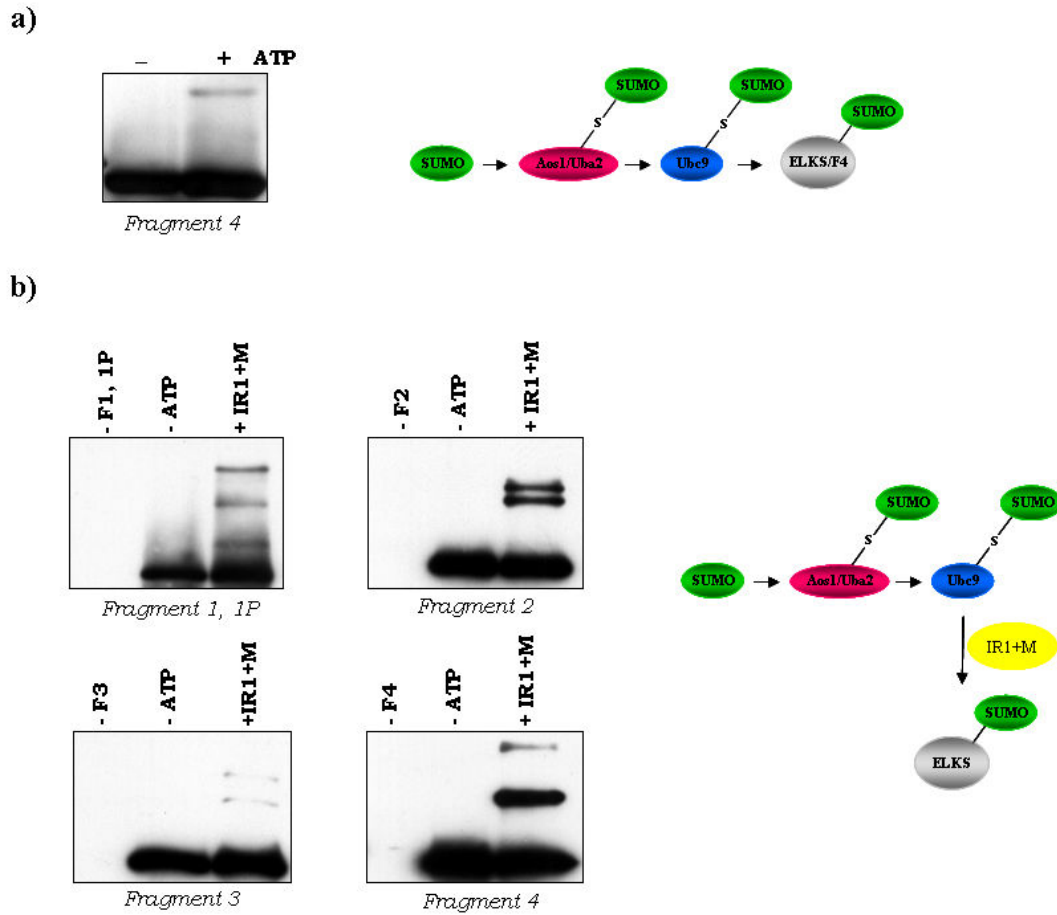


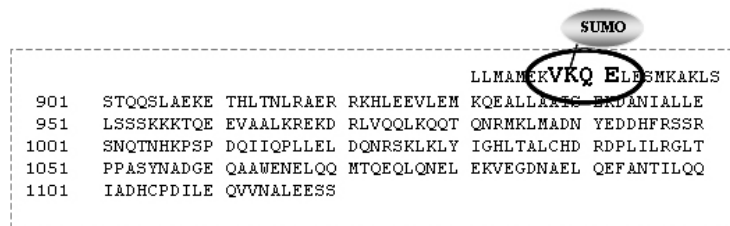
Figure 50. IR1+M stimulate SUMO conjugation to ELKS *in vitro*. a) Purified GST- tagged ELKS-F4 was subjected to *in vitro* SUMO1 modification in the presence of purified E1 enzyme (Aosl/Uba2 heterodimer), E2 enzyme (Ubc9), SUMO1 and ATP. b) Four GST-ELKS fragments were subjected to *in vitro* SUMO1 shift with addition of IR1+M for 30 min at 30 °C. Samples were analysed by immunoblot with GST antibody.

Of all fragments, fragment 4 was the most efficiently modified. I performed large scale *in vitro* SUMO conjugation to identify the conjugation site by mass spectrometry. Mass spectrometry analysis was carried by Dr. Marjaana Nousiainen (group of Dr. Roman Körner). The result obtained by mass spectrometry showed that lysine at position K889 was the site of SUMO attachment.

Sumoylation of full length ELKS *in vitro*

To examine if lysine 889 was also modified by SUMO in full length ELKS, the mutation of lysine 889 to arginine was introduced in the full length ELKS protein. WT and mutant ELKS were tested for modification in *in vitro* shift. Unfortunately, immunoblot analysis indicated the same pattern of modification in the mutant and in the wild type ELKS protein (Figure 51b). Lysine K889 was therefore not SUMO modified in full length ELKS. Using fragments for the identification of the acceptor site was thus misleading. The lysine identified in fragment four was strongly preferred by SUMO probably because this lysine residue was highly exposed within the fragment. However, creating the mutation in a full length protein did not abolish modification by SUMO, indicating that lysine K889R might be hidden in the context of the full length protein.

a)



b)

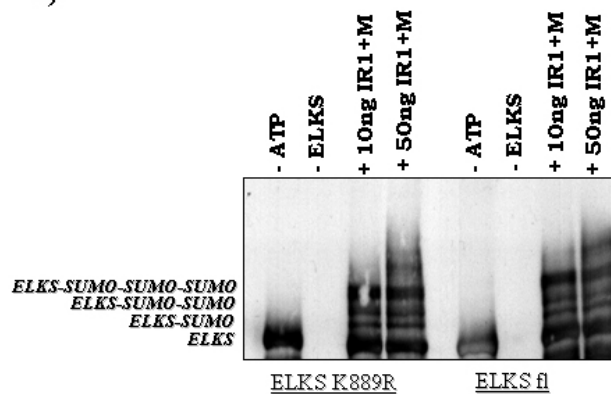


Figure 51. Lysine K889 is not the SUMO acceptor site in ELKS. a) SUMO consensus site marked in the sequence of ELKS fragment 4. b) Western blot showed SUMO shift of ELKS K889R mutant and ELKS full length.

Therefore, sumoylation had to be studied again in the context of full length protein. To determine whether sumoylation of full length ELKS protein is specifically enhanced with RanBP2 or one of the members of the PIAS family of SUMO E3 ligases, SUMO1 modification assays were performed using these proteins. Reactions were incubated at 30°C and were stopped by addition of 2×Laemmli-buffer. This assay demonstrated that in the absence of E3 ligase, ELKS full length protein is not sumoylated *in vitro* (Figure 51a). However, with the notable exception of RanGAP1, SUMO modification with only Aosl/Uba2 and Ubc9 is rather inefficient, and additional components are usually required to accelerate the conjugation reaction. I was therefore interested in testing the different SUMO E3 ligase for ELKS sumoylation. Different PIAS family members as well as small fragments of RanBP2 (IR1+M and BP2ΔFG) (Figure 51a, b, c) were tested for E3 activity on ELKS in the *in vitro* SUMOylation assay.

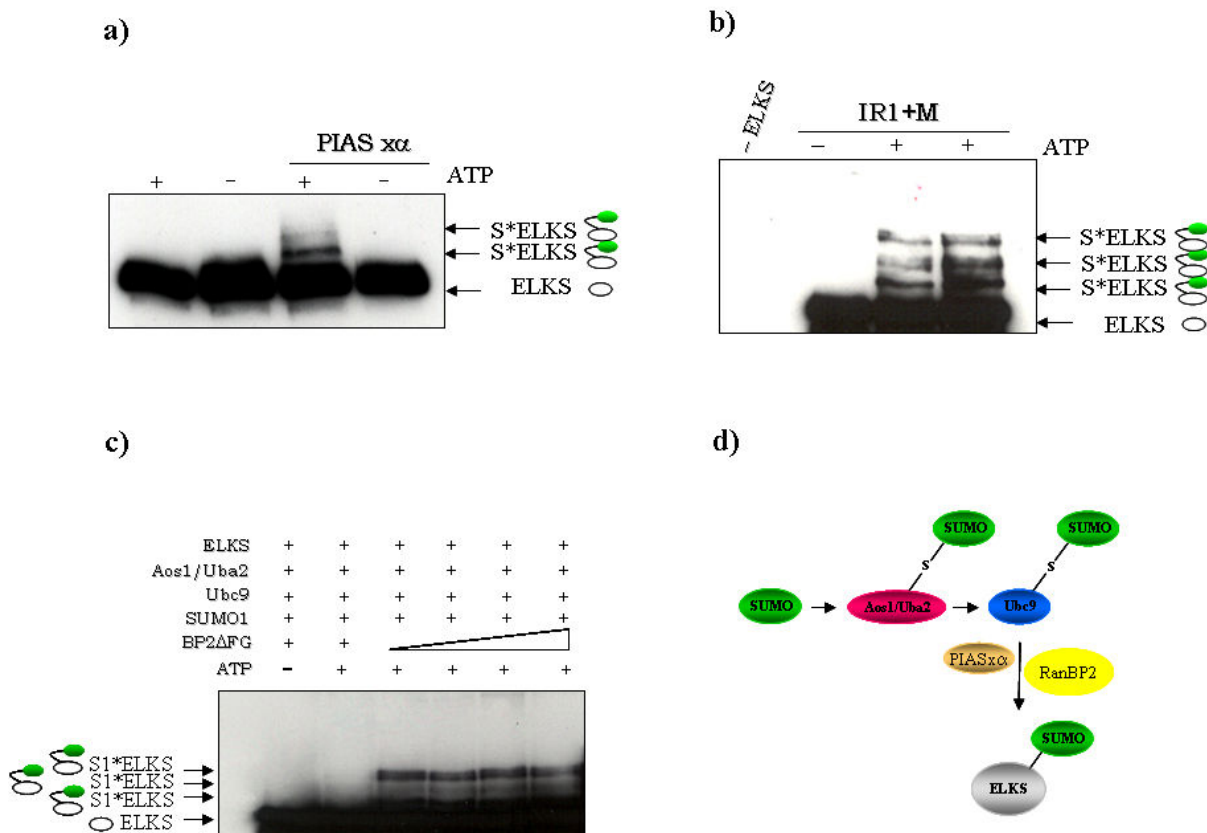


Figure 52. PIAS $x\alpha$ and RanBP2 stimulate SUMO conjugation to ELKS *in vitro*. a) Purified His-tagged ELKS was subjected to *in vitro* SUMO1 modification in the presence of purified E1 enzyme (Aosl/Uba2 heterodimer), E2 enzyme (Ubc9), SUMO1 and a) GST-PIAS $x\alpha$, b) or with increasing amounts GST-IR1+M, or c) GST-BP2ΔFG. Reactions were incubated for 30 min and proteins were detected by anti-

ELKS immunoblot analysis. d) Schematic representation of the conjugation pathway leading to SUMO modification of ELKS. PIASx α or RanBP2 act as an E3 ligase for the sumoylation of ELKS.

Significant ELKS modification was observed with PIASx α , IR1+M domain and BP2 Δ FG fragment. Small fragments of RanBP2 stimulated SUMOylation of ELKS more strongly compared to PIASx α (compare Figures 51a and b). All other PIAS family members (PIASy, PIAS x β , PIAS1, PIAS3) were tested in the *in vitro* SUMO shift assay, but they did not show any specificity for sumoylation of ELKS (data not shown).

ELKS contains 3 SUMO acceptor lysines

To identify the SUMO acceptor sites in full length ELKS, recombinant protein was modified at large scale. Standard *in vitro* modification assays using the recombinant enzymes were performed in the presence of Aos1/Uba2, Ubc9, SUMO-1, His-ELKS and IR+M. These reactions, in the presence of ATP, were incubated at 30°C for 60 min and terminated by addition of 2 \times sample buffer. Samples were separated on 6% gel and stained with Coomassie blue (Figure 52) and analysed by mass spectrometer (analysis was carried out by Dr. Marjaana Nousiainen, MPI, Martinsried)

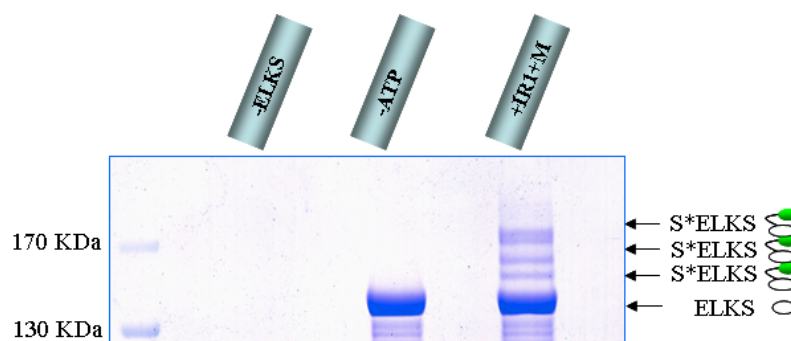


Figure 53. Coomassie blue stained gel of *in vitro* SUMOylated ELKS.

Mass spectrometry analysis could identify three peptides containing one lysine each bound covalently to SUMO. Figure 54 shows a distribution of the modified lysines on the ELKS sequence.

```

1 MYGSARS GK10VE SPGR SPRLPRSPRL GHRRTNSTGG SSGNSVGGGS
51 GKTLSEME YATSG PNYLSDHENV GAETPKSTHT LGRSGGRLPY
101 GVRMTAMGSS PNIASSGVAS DTIAFGEHHL PPVSMASSTVP HSLRQARDNT
151 IMDLQTQLKE VLRENDLLRK DVEVKESKLS SSMNSIKTFW SELKKERL
201 RKDEASKITI WKEQYRVVQE ENQHMQMTIQ ALQDELRIQR DLNQLEPQDS
251 SSRTGEPVVA ELTEENFQRL HAEHERQAKE LFLLRKTLEE MELRIETQKQ
301 TLNARDES IK LLEMLQSKG LSAKATEEDH ERTTRLAEAE MHVHHLESLL
351 EQKEKENMML REEMHRRFEN APDSAKTKAL QTVIEMKDSK I LK444EE
401 LEEEIQLMKS NGALSSEER YR SHSKFMKNKV I
451 DAQGEELKKR AAGLQSEIQ VK472QE DT ELLALQTKLE TH
501 OHIEVLKESL TAKEQRAAL RLR LEEKETMLNK KTKQIQDMAE
551 EKGQTAGE IH DLKDMLDVKE RRVVVLQKKI ENLQEQLRDK EKQMSLKER
601 VKSLQADTTN TDTALTLEE ALADKERTIE RLKEQRDRDE REMQEE IDTY
651 KKDLDLREK WLLQGLSE KEASLLDIKE HASSLASSL KKD SALKTLE
701 IALEQKKEEG LKME SQLKKA HEAT LEARAS PEMSDRIQQL ERE ISRYKDE
751 SSKAQTEVDR LE FLKEVEV EKND KKKLIA ELESLSRQV KDQNKKVANL
801 KHKEQVEKKK SAQMLEEARR REDS LSDSSQ QLQDSLKED DRIEE LEEAL
851 RESVQITAER EMVLAQEEA RTMAEKQVEE LLMAME VKQ ELESMAKALS
901 STQQLAEKE THLTNRAER RKHLEEVLEM KQAL LAAS EKD ANIALLE
951 LSSSKKTQE EVA ALKREK RLWQLKQQT QNRMKLMADN YEDDHFSSR
1001 SNQTNHKPSP DQITQPLEL DQNRSKLKY IGHLTALCHD RDPILIRGLT
1051 PPASYNADGE QAAMENELQQ MTQEQLQNEL EKVEGDNAEL QEFANTILQQ
1101 IADHCPDILE QVVNALEESS

```

Figure 54. Identification of K10, K444 and K472 of ELKS as the acceptor sites for sumoylation. Protein sequence of ELKS with marked SUMO consensus sites found by mass spectroscopy.

Figure 54 shows that two of the SUMO modification sites (lysine 444 and lysine 472) are within the SUMO consensus sequence. One of the identified sites (K10) was not within a predicted consensus sequence

To determine whether SUMO conjugation sites identified *in vitro* by mass spectrometry are indeed the predominant sites of modification, the lysines at positions 10, 444 and 472, individually (K10R, K444R and K472R) or together (K444R/K472R), were mutated. The effects of these mutations on the sumoylation of ELKS wild type or mutant were examined in standard *in vitro* modification assays (Figure 55). This experiment revealed that the lysines at positions 444 and 472 are required for the SUMO modification of ELKS *in vitro*.

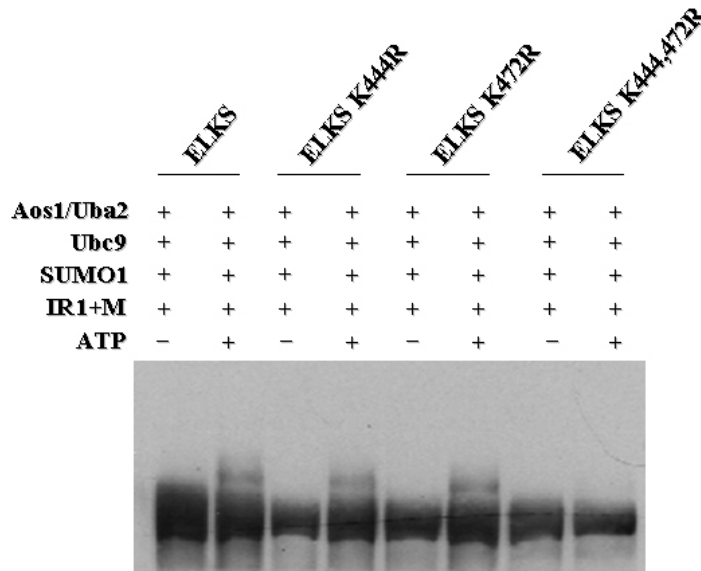


Figure 55. Identification of K444 and K472 of ELKS as the acceptor sites for sumoylation. 500 ng of His ELKS wt or ELKS mutants (K444R, K472R or K444,472R), 150 ng Aos1/Uba2, 150 ng Ubc9, 500 ng SUMO1, 30 ng IR1+M and ATP were applied in an *in vitro* shift assay. After incubation for 30 min at 30°C samples were analysed by immunoblotting with anti-ELKS.

4.2.19 ELKS sumoylation decreases its NF κ B stimulating activity

SUMO-modification has been found to antagonize the activation of several transcription factors (Müller et al., 2000; Sachdev et al., 2001; Ross et al., 2002; Chun et al., 2003). Recent studies have proposed that ELKS functions by recruiting I κ B α to the IKK complex and mediates an essential step in IKK activation (Ducut Sigala et al., 2004). To test whether sumoylation of ELKS plays any active role in the regulation of TNF- α stimulated NF κ B signaling, wild type ELKS and different ELKS-SUMO-mutated constructs were tested in reporter assays.

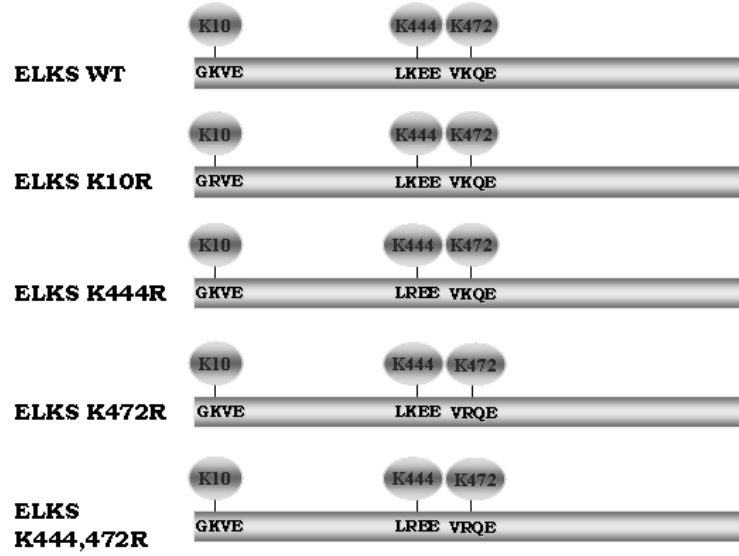
The Luciferase Reporter Vector fused to NF- κ B binding site contain the cDNA encoding luciferase (*luc+*) cloned from the North American firefly (*Photinus pyralis*) and a vector backbone that has been designed to provide enhanced reporter gene expression. When the reporter vector is expressed in transfected cells, upon activation (NF κ B), light is

produced by converting the chemical energy of luciferin oxidation through an electron transition, forming the product molecule oxyluciferin. Firefly luciferase, a monomeric 61kDa protein, catalyzes luciferin oxidation using ATP and Mg^{2+} as a cosubstrate. The enzymatic turnover results in increased light intensity that is nearly constant for at least 1 minute, and this light is measured using a luminometer.

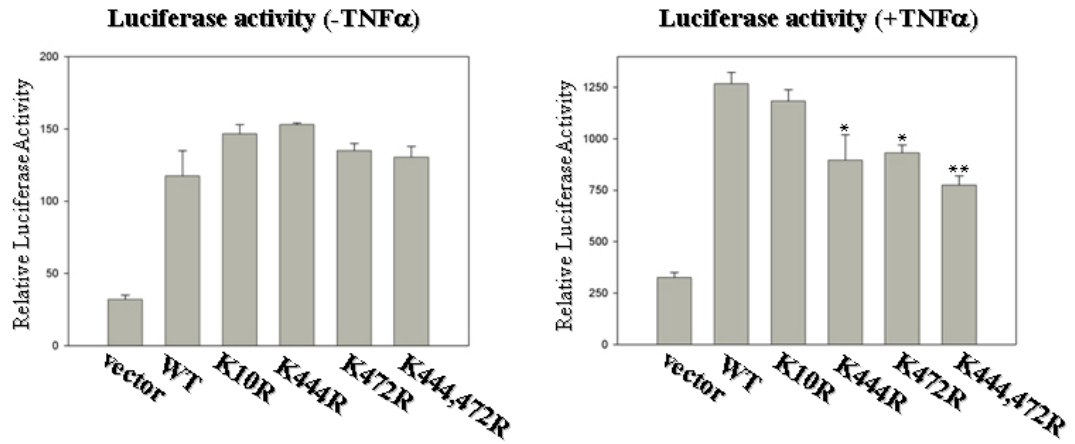
HeLa cell transfection assays were carried out in twelve-well plates at 80% confluence with Polyfectamine according to the manufacturer's instructions. Cells were transfected with both 3X κ B luciferase reporter construct, and either with HA tagged wild type ELKS or mutants of the SUMO sites. Additionally, since $TNF\alpha$ is a well known activator of the $NF\kappa B$ pathway and it was shown recently that ELKS mediates an essential step in its activation, HeLa cells were treated after 48 hours transfection with $TNF\alpha$ (20 ng/ml) for 4 hours prior to lysis. To assess the transfection efficiency, transfections were always done with a constant amount of a Renilla expression plasmid (kindly provided by Dr. Markus Moser, MPI Martinsried, Germany). Luciferase and Renilla activities were measured using a luminometer 48 hours post transfection (Figure 56b). To verify that the expression level of each mutants was the same, each sample was subjected to western blot with HA antibodies after cell lysis (Figure 56c).

As shown in figure 56b expression of ELKS wild type or mutant in the absence of $TNF\alpha$ led to no differences in the $NF\kappa B$ dependent luciferase activity. In contrast, after $TNF\alpha$ stimulation of transfected HeLa cells, mutation of two single sumoylation sites in ELKS (K444R and K472R) reduces $NF\kappa B$ activity. Interestingly, ELKS (K444/472R) showed more prominently decreased $NF\kappa B$ -dependent luciferase reporter gene activation compared to wild type. Wild-type ELKS increased reporter gene activation by a factor of up to 1250, whereas mutant ELKS (K444/472R) increased the level of reporter gene expression only by a factor of approximately 850, indicating a almost half-fold increase of luciferase activity compared to WT (Figure 55b). Mutation of the sumoylation site at position 10, 444 or 472 alone had no effect on ELKS stimulating activity of $NF\kappa B$ dependent transcription.

a)



b)



c)

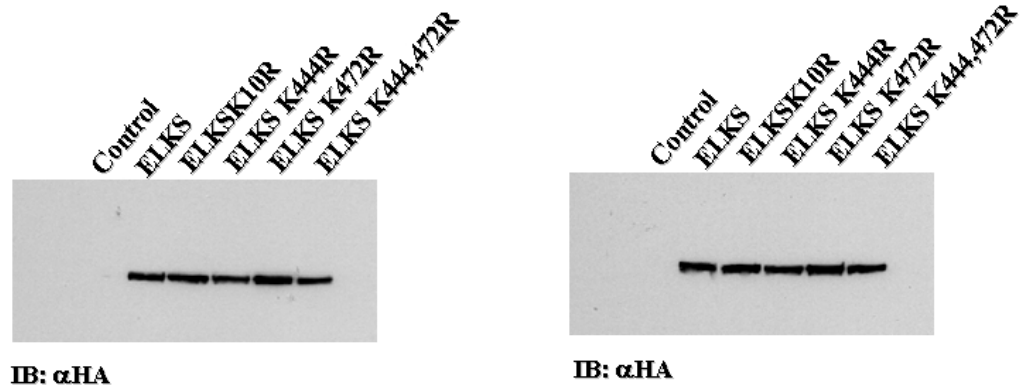


Figure 57. NF κ B-dependent 3X κ B luciferase reporter activity. a) Schematic representation of wild-type ELKS and mutant ELKS proteins containing mutations in the sumoylation sites, individually (K10R, K444R, K472R) or in combination (K444R/K472R). b) Activation of 3X κ B luciferase reporter construct. HeLA cells were transiently transfected with expression plasmids encoding wild type ELKS and mutated ELKS proteins, Renilla plasmid and 3X κ B luciferase reporter construct in the absence or presence of TNF- α (20 ng/ml; 4 hours) Relative activity (RLU) was calculated by dividing the luciferase activity from the Renilla activity. Bars represent the mean \pm SEM of three independent experiments carried in triplicate. All statistical significances were analysed by Student's *t* test, **P < 0.01 and *P < 0.05 c) HA western blot showed the same expression level of the ELKS constructs.

5 APPENDIX

Uba2 full length

band1) FilaminA, Splice isoform 6 of 075369 FilaminB, Splice isoform DPII of P15924 Desmoplacin, Spectrin alpha chain, brain hypothetical protein KIAA0023

band3) Splice isoform 2 of P06753 Tropomyosin alpha 3 chain, Splice isoform 1 of P07226 Tropomyosin alpha 4 chain, 14-3-3 protein, Cell division control protein 2, Guanine nucleotide-binding protein beta subunit-like protein 12.3, Actin, Cell division protein, Splice isoform Long of P25786 Proteasome subunit alpha type 1, F-actin capping protein beta, Splice isoform 1 of Q12920 Proteasome activator complex subunit 3, Glucosamine-6-phosphate isomerase, CCR4-NOT transcription complex subunit 7 isoform, Down syndrome critical region, Complement component 1, Q subcomponent binding protein, Chloride intracellular channel, Purine nucleoside phosphorylase, Microtubule-associated protein RP/EB family member 1

band5) Phosphoglycerate kinase 1, Actin cytoplasmic 2, Argininosuccinate synthase, Actin-like protein 2, Septin 2, SET protein, Creatine kinase B chain, Aspartate aminotransferase 1, MNUDC protein (Nuclear distribution gene C), Adenosylhomocysteinase, Squamous cell carcinoma antigen 1, Ribonucleoside-diphosphate reductase M2 chain, Citrate synthase precursor isoform α , Multifunctional protein ADE2 includes: phosphoribosylaminoimidazole-succinocarboxamide, Casein kinase I, epsilon isoform

band7) RuvB-like 1, Splice isoform I of Q14141 Septin 6, Tubulin alpha-1 chain, Histone acetyltransferase type B subunit 2, Glutathione reductase, mitochondrial precursor, Serine/threonine protein kinase MASK, Actin, cytoplasmic 2, Actin, gamma-enteric smooth muscle, S-adenosylmethionine synthetase gamma, Probable ATP-dependent RNA helicase, UDP-glucose pyrophosphorylase 2, Splice isoform Rpn10A of P55036 26S proteasome non-ATPase regulatory subunit 4, Serine/threonine protein phosphatase 2A, 55 KDA regulatory subunit B, alpha isoform, subunit B, alpha, Splice isoform 2 of P30566 Adenylosuccinate lyase, Histidyl-tRNA synthetase, Dynein light intermediate chain 2, cytosolic

band9) T-complex protein 1, theta subunit, Pyruvate kinase, M2 isozyme, Tyrosyl-tRNA synthetase, T-complex protein 1, zeta subunit, T-complex protein 1, epsilon subunit, Tubulin beta-5 chain, Actin, cytoplasmic 1, asparagine synthetase, Actin alpha 1 skeletal muscle protein, Similar to tubulin alpha 2, similar to UV excision repair protein RAD23 homolog B (HHR23B), T-complex protein 1, alpha subunit, (XP-C repair complementing complex 58 kDa protein) (P58)

Uba2 splice variant

band2) FilaminA, Splice isoform 1 of 075369 FilaminB, Spectrin alpha chain, Splice isoform DPII of P15924 Desmoplacin, Beta-spectrin 2 isoform, Dynein heavy chain

band 4) Splice isoform 2 of P06753 Tropomyosin alpha 3 chain, Splice isoform 1 of P07226 Tropomyosin alpha 4 chain, 14-3-3 protein, F-actin capping protein beta subunit, Cell division control protein 2 homolog, Glucosamine-6-phosphate isomerase, Actin, cytoplasmic 2, CCR4-NOT transcription complex, subunit 7, Splice isoform Short of P25786 Proteasome subunit alpha type 1, Ta2,4-dienoyl-CoA reductase, mitochondrial precursor, Guanine nucleotide-binding protein beta subunit-like protein 12.3

band6) Actin, cytoplasmic 2, Phosphoglycerate kinase 1, Septin 2, Argininosuccinate synthase, aspartate aminotransferase, Tactin-like protein 2, TaxTemplate acyivating factor-I alpha, Ubiquitous tropomodulin, Citrate synthase, mitochondrial precursor, Multifunctional protein ADE2 [includes: Phosphoribosylaminoimidazole succino-carboxamide synthase (EC 6.3.2.6) (SAICAR synthetase); Phosphoribosylaminoimidazole carboxylase (EC 4.1.1.21) (AIR carboxylase) (AIRC)], Adhesion regulating molecule 1 precursor

band8) RuvB-like 1, Tubulin beta-2 chain, Tubulin alpha-6 chain, Splice isoform I of Q14141 Septin 6, Chromatin assembly factor 1 subunit C, Serine hydroxymethyltransferase, mitochondrial precursor, Coronin 1C, Uridine 5'-monophosphate synthase (UMP synthase), Splice isoform 1 of P30566 Adenylosuccinate lyase, Serine/threonine protein phosphatase 2A, 55 KDA regulatory, subunit B, alpha isoform, Histidyl-tRNA synthetase, Actin, cytoplasmic 2, P68 TRK-T3 oncoprotein, Actin, gamma-enteric smooth muscle, Phosphoglycerate kinase 1

band10) T-complex protein 1, theta subunit, Pyruvate kinase, M2 isozyme, Tyrosyl-tRNA synthetase, T-complex protein 1, alpha subunit, T-complex protein 1, epsilon subunit, asparagine synthetase, T-complex protein 1, zeta subunit, T-complex protein 1delta subunit, T-complex protein 1eta subunit, DnaJ homolog subfamily C member 7, L plastin, Protein disulfide isomerase precursor, Ubiquitin carboxyl-terminal hydrolase 14, Elongation factor 2, Dynein light chain-A, UV excision repair protein RAD23 homolog B, Stress-induced-phosphoprotein 1, Tubulin alpha-8 chain

6 DISCUSSION

The long-term goal of my research presented in this thesis was to understand the role of SUMO E1 enzyme Aos1/Uba2. This work resulted in the characterisation of an Uba2 splice variant, and the identification and characterisation of ELKS as a novel SUMO target.

6.1 Characterisation of variant Uba2

In contrast to ubiquitin E1, the SUMO E1 enzyme consists of two subunits, Aos1 and Uba2 (Dohmen et al., 1995). In my work, I characterised a new splice variant of Uba2 which lacks one exon encoding 50 amino acids. To address the question whether the splice variant of Uba2 was expressed at all, since one exon was missing, RT-PCR of total RNA was performed. As it is demonstrated in Figure 15, RT-PCR of total RNA showed presence of the Uba2 splice variant in all selected mouse organs without any tissue specificity in comparison to Uba2 wild type. I could demonstrate that this splice variant is predominantly enriched in the nucleus consistent with the localisation of the full length Uba2 (Azuma et al., 2001). Next, I asked whether variant Uba2 is still able to stably interact with Aos1 and form an active SUMO E1 enzyme. In gel filtration experiments the recombinant Uba2 splice variant comigrates with recombinant Aos1, indicating stable interaction between both proteins (Figure 16). Thioester bond formation as well as modification assays revealed that the E1 enzyme formed between variant Uba2 and Aos1 was as active as its full length counter part. This result was surprising, since recently published structure of SUMO E1 enzyme (Lois and Lima, 2005, and Figure 58), suggested that missing residues in Uba2 splice variant could alter ¹⁾ the SUMO binding region significantly and ²⁾ disturb the Ubl domain. It will be very interesting to gain structural information on variant Uba2, as novel insights on the catalytic mechanism could be gained from this.

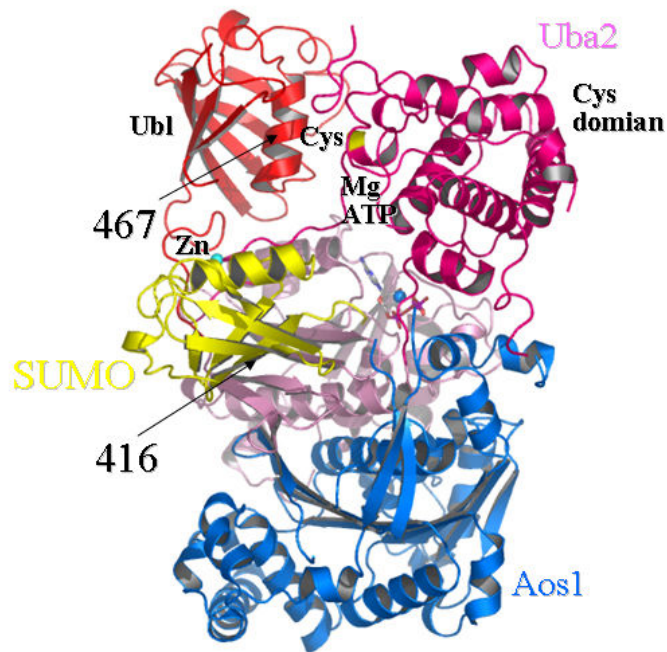


Figure 58. Ribbon diagram of the Aosl/Uba2-SUMO-1 complex. SUMO is colored yellow. Catalytic domain and Ubl domains are labeled. The active site cysteine is labeled and colored yellow. E1 with deletion in Uba2 is indicated on left with the black arrows from 416-467 (From Lois and Lima, 2005).

6.2 Identification of a novel SUMO target

6.2.1 Identification of a new Aosl binding partner

Originally, the SUMO E1 was described as a nuclear protein (Dohmen et al., 1995; Johnson et al., 1997; Azuma et al., 2001). Our lab extended these findings by demonstrating that both the SUMO E1 and the SUMO E2 enzyme are enriched in the nucleus but also faintly distributed in the cytoplasm (Pichler et al., 2002). Using immunofluorescence (Figure 25) and subcellular fractionation (Figure 23), I could show that a small fraction of the E1 subunit, Aosl is enriched at the Golgi apparatus. This led to the idea that there are several interaction partners possible for Aosl and Uba2. In this work, immunoprecipitation experiments with anti Aosl and anti Uba2 antibodies,

followed by subsequent mass spectrometry analysis, identified ELKS (epsilon) as a specific and strong binding partner to Aosl. In my further study I focused on the functional meaning for this interaction.

6.2.2 ELKS is a protein implicated in NFκB signaling and vesicle transport

The first ELKS family member was originally discovered by Nakata et al., 1999 as a protein fused to the RET (receptor tyrosine kinase) protein. The deduced polypeptide sequence is rich in glutamic acid (*E*; 13.5% of total residues), leucine (*L*; 11.7%), lysine (*K*; 10.7%), and serine (*S*; 9.3%). As these four amino acids occupy 45.1% of the total residues, the novel gene was named ELKS. The ELKS gene spans more than 500 kb of genomic DNA (Yokota et al., 2000) and is ubiquitously expressed. The secondary structure of the ELKS protein sequence is predicted to contain alpha-helical domains with short beta-turns or beta-sheets in the central region. The presence of heptad repeats in the helical domain regions suggests that the ELKS protein has a coiled-coil structure, because coiled-coil regions are generally alpha-helical with heptad periodicity. Furthermore, analysis of the ELKS protein sequence indicated dimer formation (Nakata et al., 1999).

So far, four ELKS splice variants are described in the literature, ELKS-β, -γ, -δ and -ε, with the prototype isoform being renamed to ELKS-α (Figure 59) (Nakata et al., 2002). ELKS-β, -γ, -δ, and -ε consist of 992-, 720-, 1088-, and 1116-aa residues, respectively (Figs. 59 and 60).

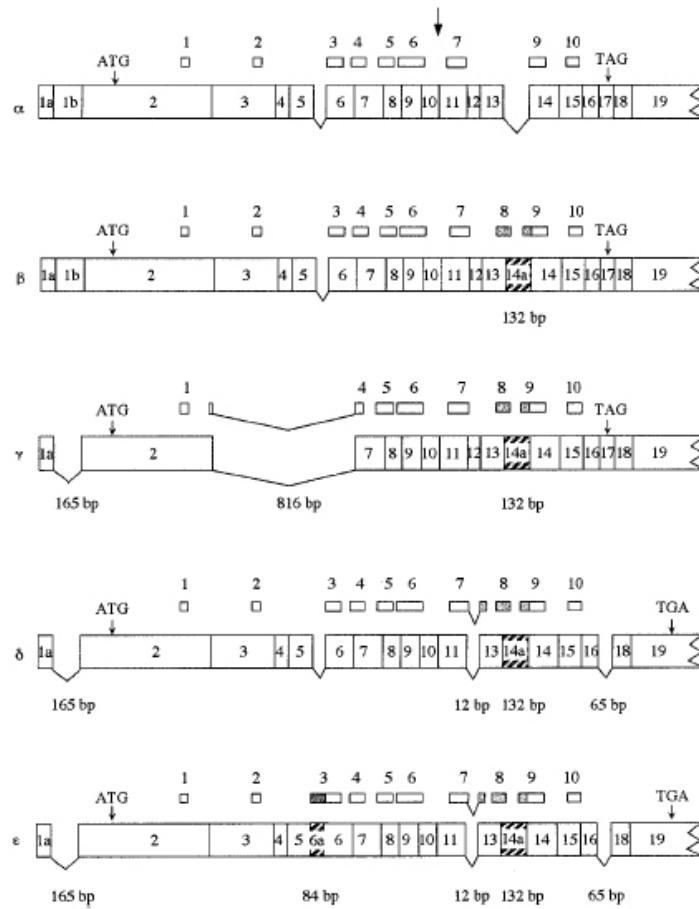


Figure 59. Schematic illustration of *ELKS* cDNA structures. Hatching denotes novel exons. A translation initiation codon (ATG) is present in exon 2, and translation stop codons (TAG or TGA) are found in exon 17 or exon 19. An arrow indicates the breakpoint for fusion of *ELKS* to *RET* in a papillary thyroid carcinoma. Numbers under boxes indicate the number of nucleotides inserted or deleted. Small boxes above each diagram denote coiled-coil domains; shading indicates differences from those of *ELKS* α . (From Nakata et al., 2002).

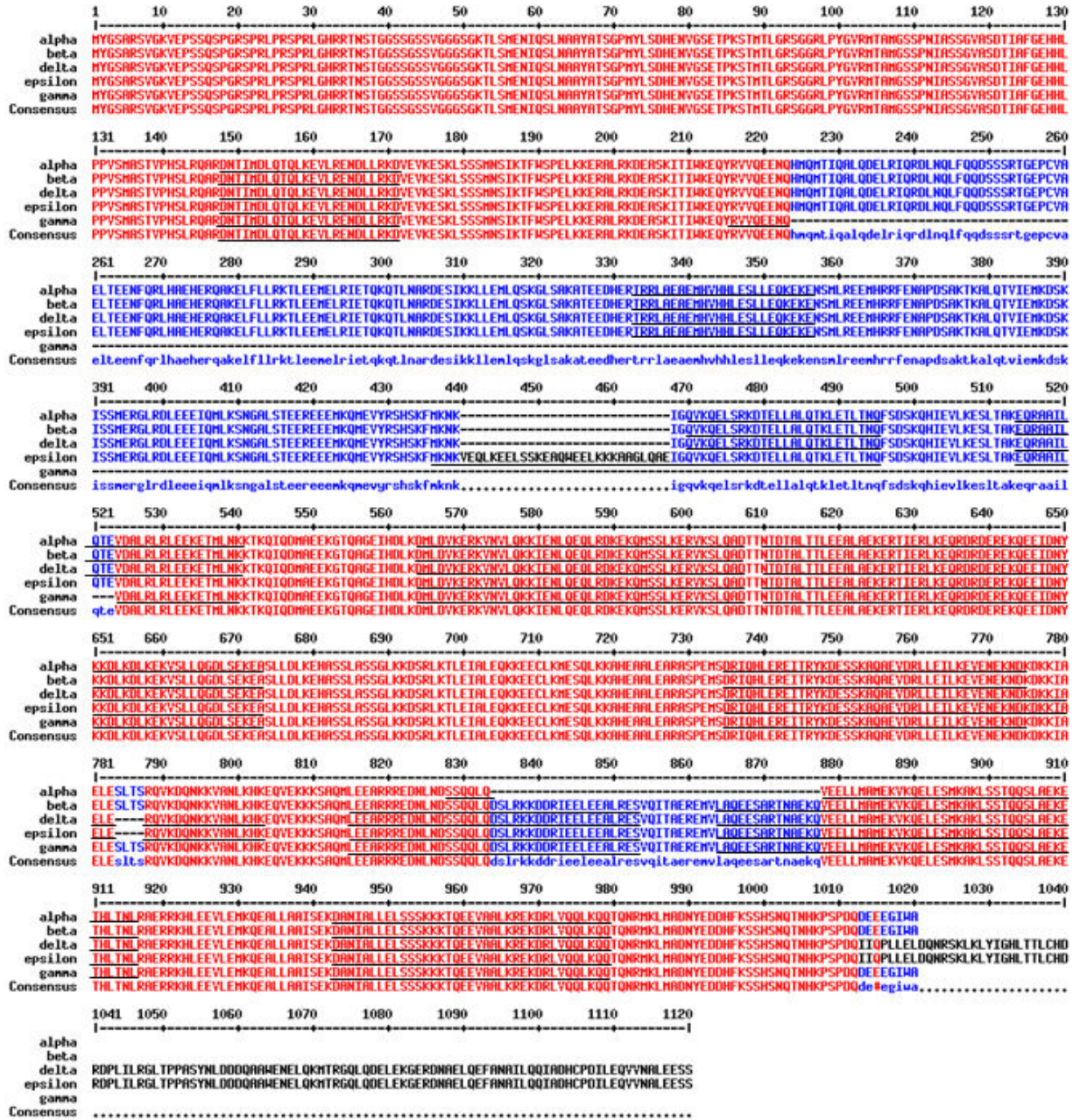


Figure 60. Amino-acid sequences of the five ELKS isoforms deduced from cDNAs. Predicted coiled-coil structures (only those that showed probabilities greater than 0.5 as predicted by MultiCoil) are indicated by lines under the respective amino acid sequences (Modified from Nakata et al., 2002).

A number of proteins highly homologous to the ELKS proteins were identified in rat, named CAZ-associated structural protein, CAST (CAST1, CAST2 α and CAST2 β ; Deguchi-Twarada et al., 2004; Ohtsuka et al., 2002) and ERC (ERC1a, ERC1b and ERC2; Wang et al., 2002). Another research group discovered two related mouse proteins that interact specifically with a small GTPase protein, Rab6, and therefore the proteins were named Rab6IP2A and Rab6IP2B (Monier et al., 2002). Sequence alignment has revealed that ELKS, CAST, ERC and Rab6IP2 are orthologous members of the same protein family in human, rat and mouse. Their expression profiles in different organs differ with different isoforms, ELKS- α , CAST2 α , Rab6IP2A, ERC1b and ERC2 are expressed only in the brain, while ELKS- ε , Rab6IP2B and ERC1a are expressed ubiquitously outside of the brain (Nakata et al., 2002; Deguchi-Twarada et al., 2004).

ELKS belongs to the class of cytosolic Rab partners and effectors that can be recruited on membranes in a GTP-dependent manner, and it was suggested that ELKS plays an essential role in membrane traffic in a Rab6-dependent manner (Monier et al., 2002; Wang et al., 2002). Additionally, ELKS was recently identified to function in insulin exocytosis, where the authors explored the localisation and function of ELKS in pancreatic β cells (Imaizumi et al 2005). This study proposed that ELKS may have a potential role in the translocation of insulin granules to a specialized exocytotic site, thus ELKS is a possible candidate for definition of the fusion site of insulin exocytosis. For further investigation it would be interesting to know if the exocytosis function of ELKS is restricted to pancreas only or whether this is a general function for ELKS.

6.3 Identification of additional ELKS and Aosl binding partners suggest possible functions in vesicle transport and NF κ B signaling

Albeit ELKS and Aosl clearly interact *in vivo*, bacterially expressed recombinant proteins do not interact directly. This could be due to the absence of eukaryotic modifications, or missing binding partners that were present in the immunoprecipitation. Therefore, I went on to search for new binding partners for Aosl and ELKS. Immunoprecipitation experiments and subsequent mass spectrometry analysis showed

several interaction candidates of Aosl and ELKS (Figure 41). Among them were RanBP2 (a SUMO E3 ligase), a putative NF κ B activating protein and protein transport Sec24A/Sec23B. Additionally, in the same immunoprecipitation experiment (Figure 42) small amount of Ubc9 was found. As it was described above, ELKS has been implicated in different events such as vesicle transport or NF κ B signaling. Therefore, finding these interactors is consistent with a role of ELKS in both processes. In particular, the finding of the Sec proteins (Sec24A/Sec23B) are very interesting for this study, since these proteins are involved in the transport from the ER to Golgi by promoting interaction of cargo with the coat complex II (COPII) budding machinery. Vesicles coated by the COPII coat mediate the export of newly synthesized proteins from the ER, whereas COPI-coated vesicles are involved at later stages of intracellular transport (Schekman et al., 1996). In mammalian cells, a relay between the two coats takes place at the level of ER–Golgi intermediate compartment, a dynamic compartment at the crossroads between the ER and the Golgi (Lippincott-Schwartz et al., 2000). Protein passengers like Sec23/24 deposited in the ER may remain there or be shuttled to the Golgi apparatus to be presented with further transportation options. Recent work has further addressed that ELKS which is a membrane protein, can be recruited on Golgi membranes (Monier et al., 2003). Based on this, one could imagine that ELKS could form a complex with Sec23/24 heterodimer and SUMO E1 enzyme, which then can regulate ELKS function in transport of cargo through the secretory pathway. This hypothesis will need to be tested, first by showing that ELKS, SUMO E1 and Sec24A/Sec23B indeed can indeed form a trimeric complex.

6.4 ELKS is a new SUMO substrate

The presence of Ubc9 and the RanBP2 E3 ligase in ELKS immunoprecipitation suggested the possibility that ELKS is a SUMO target. To prove this hypothesis I first investigated ELKS sumoylation *in vivo* (Figure 48) and *in vitro* (Figure 51) and could indeed describe ELKS as a new SUMO substrate. Using mass spectrometry analysis three consensus sumoylation sites in ELKS at lysines K10, K444, K472 were identified. I

investigated single and double mutants in our *in vitro* sumoylation assay, which demonstrated that the single mutants K10R, K444R and K472R could still be modified. Importantly, the double mutant (K444/472) is completely deficient for sumoylation. These data indicate that ELKS can be sumoylated predominantly at two sites, lysine 444 and lysine 472. Interestingly, the SUMO conjugating site in the middle of coiled coil region (LK⁴⁴⁴EE) is missing in other ELKS family members (ELKS- α , - β , - γ , and - δ). Therefore it will be important to investigate, if these members are also sumoylated and what are the respective consequences on their biological function.

6.5 SUMO does not change ELKS localisation and Rab6 interaction

Even though sumoylation is now an established posttranslational modification for a large number of proteins, the functional consequences of SUMO conjugation in most cases remain unclear. It was therefore important to characterise the effect of SUMO modification on the function of ELKS. It was reported that ELKS is involved in vesicle transport (Monier et al., 2002). ELKS can be recruited to Golgi membranes by the GTPase Rab6. In this work two experiments were performed to gain insight on the consequences of ELKS sumoylation.

In a number of cases, SUMO conjugation leads to changes in subcellular localisation of the modified protein. To test this possibility, I compared the localisation of ELKS wild type versus the sumoylation deficient double mutant ELKS K444/472R by expression of both proteins in HeLa cells and subsequent immunofluorescence (data not shown). Additionally, to test if sumoylation of ELKS interferes with its binding to Rab6 a pull down experiment using recombinant Rab6 and full length ELKS versus sumoylated ELKS was performed. This study shows that SUMO modification does not correlate with changes in the localisation of ELKS or interaction with Rab6 GTPase.

6.6 ELKS negatively regulates the NF κ B signaling pathway

NF κ B is a transcription factor involved in important biological processes including inflammation and apoptosis (Karin et al., 2002; Yamamoto et al., 2001). Many extracellular stimuli induce NF κ B activation. The physiological roles of NF κ B are both cell type and stimulus dependent (Karin et al., 2002; Yamamoto Y et al., 2001). Previous investigations have shown that activation of NF κ B by extracellular stimuli such as TNF α is predominantly mediated by a distinctive signaling pathway, where I κ B kinase (IKK) phosphorylates I κ B α and thereby induces its degradation. Activated NF κ B is translocated into the nucleus and binds to the promoter regions of its target genes (Karin et al., 2002). The large 700- to 900-kDa IKK complex is the centerpiece of NF κ B pathway. This complex consists of the kinase subunits IKK1 and IKK2, which are found in association with the regulatory subunit IKK γ /NEMO (Karin et al., 2002). The function of IKK2 as an essential subunit of IKK complex (Schmidt-Supprian et al., 2000; Makris et al., 2000) for classical NF κ B activation is well established. In contrast, IKK1 mediates transcription of the p52/relB target genes with an “alternative pathway” by regulating processing of p100 into p52 in response to stimuli such as lymphotoxin, CD40, and BAFF (Dejardin et al., 2002; Senftleben et al., 2001). In addition, IKK1 regulates the expression of some NF κ B target genes by phosphorylating histone H3 on Ser-10 (Yamamoto et al., 2003; Anest et al., 2003). Furthermore, IKK1 plays a critical role in the differentiation of epidermis independent of its kinase activity and NF κ B signaling pathway (Li et al., 1999; Hu et al., 2001).

ELKS was identified recently by gel filtration analysis and tandem mass spectrometry as a protein that copurified with an IKK complex that was immunoprecipitated with IKK2 antibodies from HeLa cells treated with TNF α (Ducut Sigala et al., 2004). ELKS seems to be essential for IKK activity and NF κ B activation as ELKS silencing causes a loss and delay of I κ B α phosphorylation and degradation in response to TNF α and IL-1 (Ducut Sigala et al., 2004). Therefore, I was interested to investigate if ELKS sumoylation plays a role in this process.

Interestingly, I found that abolishing either one of two specific sumoylation sites in ELKS (K444R and K472R) reduces NF κ B activity in TNF- α treated HeLa cells, while deletion of both sumoylation sites in ELKS (K444/472R) reduces this effect even more prominently. The third point mutation, which is not required for sumoylation (K10R) behaved like wild type. NF- κ B activity was not completely abolished in the presence of the K444/472R mutant; however residual activity was likely due to wild type ELKS that was present in the cells (Figure 61). In summary, my results strongly suggest that sumoylation of ELKS plays an essential role for NF κ B activity. While the molecular events that are regulated by sumoylation remain to be revealed, at least two possibilities can be envisioned: either sumoylation of ELKS is required for recruitment of I κ B α to the IKK complex, or sumoylation of ELKS is essential for direct binding to IKK2. Since NF κ B activation targets and induces gene expression it will be interesting to find out under which physiological circumstances the sumoylation of ELKS occurs and finally which genes specifically are targeted.

It would also be interesting to see if the localisation of ELKS, Aos1 or Uba2 is changed after stimuli with TNF α and if the change in localization has any influence for NF κ B signaling pathway.

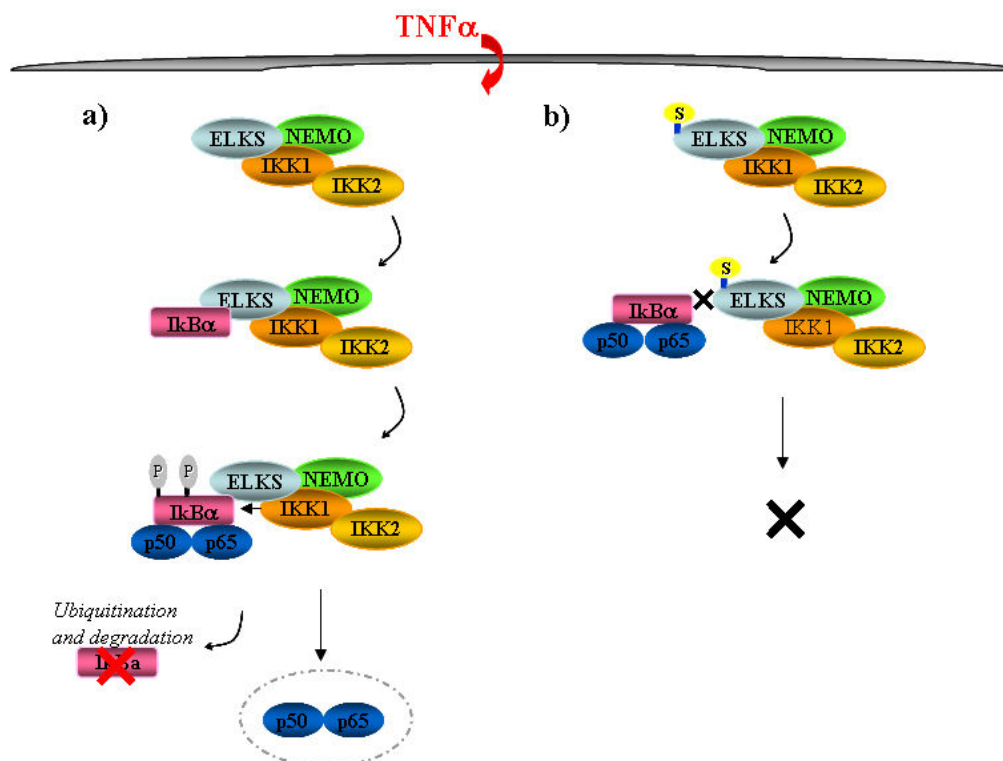


Figure 61. A potential role for ELKS upon NF κ B activation, (a) ELKS associates with IKK complex upon TNF α stimuli and recruit I κ B α to the IKK complex leading to phosphorylation and degradation of I κ B α and release of p50 and p65 for accumulation in the nucleus, (b) Sumoylation of ELKS at lysine 444 and 472 prevents association of ELKS to I κ B α and further phosphorylation and degradation of I κ B α .

6.7 RanBP2-an E3 ligase for ELKS?

E3 ligases are considered to be responsible for the substrate specificity. Three different types of SUMO E3 ligases have been discovered recently, members of the PIAS family, RanBP2/Nup358 and Pc2 (see Introduction). For my study it was interesting to define an E3 ligase for ELKS sumoylation.

Based on immunoprecipitation and *in vitro* activity, RanBP2 seems to serve as an E3 ligase for ELKS. This does however not exclude that other ligases such as PIAS may have a role in enhancing ELKS sumoylation. At least *in vitro*, PIAS α also can enhance ELKS sumoylation (Figure 52a).

Considering the fact that RanBP2 is a core component of the cytoplasmic filaments of nuclear pore complexes (Wu et al., 1995), this raised the question, whether ELKS could be translocated through the nuclear pore complex. However, according to immunofluorescence experiments (Figure 36) and data in the literature, ELKS is localised exclusively in the cytoplasm. To determine if ELKS could shuttle between cytoplasm and nucleus, immunofluorescence experiments were carried out by overexpressing ELKS in HeLa cells and treatment with leptomycin B (data not shown). Leptomycin B specifically inhibits the CRM1/exportin1 nuclear export pathway. Leptomycin B treatment did not lead to accumulation of ELKS in the nucleus indicating that ELKS is indeed restricted to the cytoplasm. RanBP2 is a very elongated protein, reaching up to 100 nm into the cytoplasm from nuclear pore complex (Delphin et al., 1997). Its E3 ligase domain, which resides at the C-terminal part of the protein, is at the NPC-distal site (Bernad et al., 2004). Consequently, cytoplasmic proteins could well have easy access to RanBP2's E3 ligase domain.

An attractive hypothesis would also be that ELKS is sumoylated predominantly in mitosis, when nuclear pore complex disassemble and RanBP2 is diffusely distributed

throughout the cell. This could be addressed by an analysis of ELKS sumoylation in cell cycle synchronized HeLa cells.

REFERENCES

- al-Khodairy F, Enoch T, Hagan IM, Carr AM. The *Schizosaccharomyces pombe* hus5 gene encodes a ubiquitin conjugating enzyme required for normal mitosis. *J. Cell Sci.* (1995) 108 (Pt. 2): 475–86
- Amerik, A. Y. & Hochstrasser, M. Mechanism and function of deubiquitinating enzymes. *Biochim. Biophys. Acta* (2004) 1695: 189–207.
- Aravind L. and Koonin E. V. SAP—a putative DNA binding motif involved in chromosomal organization. *Trends Biochem. Sci.* (2000) 25: 112–114
- Anest V., Hanson J.L., Cogswell P.C., Steinbrecher K.A., Strahl B.D., Baldwin A.S. A nucleosomal function for I κ B kinase- α in NF- κ B-dependent gene expression. *Nature* (2003);423 (6940): 596–7.
- Arora T., B. Liu, H. He, J. Kim, T.L. Murphy, K.M. Murphy, R.L. Modlin, K. Shuai, PIASx is a transcriptional co-repressor of signal transducer and activator of transcription 4, *J. Biol. Chem.* (2003) 278 21327–21330.
- Azuma, Y., Tan, S.H., Cavenagh, M.M., Ainsztein, A.M., Saitoh, H., and Dasso, M. Expression and regulation of the mammalian SUMO-1 E1 enzyme. *FASEB J.* (2001) 15: 1825–1827.
- Azuma Y., A. Arnaoutov, M. Dasso, SUMO-2/3 regulates topoisomerase II in mitosis, *J. Cell Biol.* (2003) 163: 477–487.
- Baba D, Maita N, Jee JG, Uchimura Y, Saitoh H, Sugasawa K, Hanaoka F, Tochio H, Hiroaki H, Shirakawa M. Crystal structure of thymine DNA glycosylase conjugated to SUMO-1. *Nature* (2005) 435 (7044): 979–82.
- Barlowe C, Orci L, Yeung T, Hosobuchi M, Hamamoto S, Salama N, Rexach MF, Ravazzola M, Amherdt M, Schekman R: COPII: a membrane coat formed by Sec proteins that drive vesicle budding from the endoplasmic reticulum. *Cell* (1994) 77: 895–907.
- Bayer, P., A. Arndt, S. Metzger, R. Mahajan, F. Melchior, R. Jaenicke, and J. Becker. Structure determination of the small ubiquitin-related modifier SUMO-1. *J Mol Biol* (1998) 280: 275–86.
- Bencsath KP, Podgorski MS, Pagala VR, Slaughter CA, Schulman BA. Identification of a multifunctional binding site on Ubc9p required for Smt3p conjugation *J. Biol. Chem.* (2002) 277: 47938–47945

- Bernad, R. van der Velde, H, Fomerod, M. Pickersgill, H. Nup358/RanBP2 attaches to the nuclear pore complex via association with Nup88 and214/CAN and plays a supporting role in CRM1-mediated nuclear protein export. *Mol. Cell Biol.* (2004) 24: 2373-84.
- Bernier-Villamor V, Sampson DA, Matunis MJ, Lima CD. Structural basis for E2-mediated SUMO conjugation revealed by a complex between ubiquitin-conjugating enzyme and RanGAP1. *Cell* (2002) 108: 345–56
- Bohren K.M., V. Nadkarni, J.H. Song, K.H. Gabbay, D. Owerbach, A M55V polymorphism in a novel SUMO gene (SUMO-4) differentially activates heat shock transcription factors and is associated with susceptibility to type I diabetes mellitus, *J. Biol. Chem.* (2004) 279: 27233-8.
- Borodovsky, A., Kessler, M.B., Casagrande, R., Overkleeft, H.S., Wilkinson, D.K., Ploegh, L.H. A novel active site-directed probe specific for deubiquitylating enzymes reveals proteasome association of USP14. *EMBO J.* (2001) 20: 5187-5196.
- Boyd J.M., Subramanian T., Schaeper U., La Regina M., Bayley S., Chinnadurai G. A region in the C-terminus of adenovirus 2/5 E1a protein is required for association with a cellular phosphoprotein and important for the negative modulation of T24-ras mediated transformation, tumorigenesis and metastasis. *EMBO J.* 1993 Feb;12(2): 469-78.
- Chakrabarti, S.R., R. Sood, S. Nandi, and G. Nucifora. Posttranslational modification of TEL and TEL/AML1 by SUMO-1 and cell-cycle-dependent assembly into nuclear bodies. *Proc Natl Acad Sci U S A* (2000) 97: 13281-5.
- Chung C.D., J. Liao, B. Liu, X. Rao, P. Jay, P. Berta, K. Shuai, Specific inhibition of Stat3 signal transduction by PIAS3, *Science* (1997) 278: 1803– 1805.
- Comerford K.M., M.O. Leonard, J. Karhausen, R. Carey, S.P. Colgan, C.T. Taylor, Small ubiquitin-related modifier-1 modification mediates resolution of CREB-dependent responses to hypoxia, *Proc. Natl. Acad. Sci. U. S. A.* (2003) 100: 986–991.
- Coux, O., K. Tanaka, and A.L. Goldberg. Structure and functions of the 20S and 26S proteasomes. *Annu Rev Biochem* (1996) 65: 801-47.
- Dealtry, G.B. and D. Rickwood, eds. (1992). *Cell biology lab fax*. BIOS Scientific Publishers, Oxford, United Kingdom.
- Dejardin, E., Droin, N.M., Delhase, M., Haas, E., Cao, Y., Makris, C., Li, Z.W., Karin, M., Ware, C.F., Green, D.R. The lymphotoxin-beta receptor induces different patterns of gene expression via two NF-kappaB pathways. *Immunity* (2002) 17: 525-35.

- Delphin, C., Guan, T., Melchior, F., and Gerace, L. RanGTP targets p97 to RanBP2, a filamentous protein localized at the cytoplasmic periphery of the nuclear pore complex. *Mol. Biol. Cell* (1997) 8: 2379-2390.
- del Olmo M, Mizrahi N, Gross S, Moore CL. The Uba2 and Ufd1 proteins of *Saccharomyces cerevisiae* interact with poly(A) polymerase and affect the polyadenylation activity of cell extracts. *Mol. Gen. Genet.* (1997) 255:209–18
- Deguchi-Tawarada, M., Inoue, E., Takao-Rikitsu, E., Inoue, M., Ohtsuka, T., and Takai, Y. CAST2: identification and characterization of a protein structurally related to the presynaptic cytomatrix protein CAST. *Genes Cells* (2004) 9: 15-23.
- Deng, L., C. Wang, E. Spencer, L. Yang, A. Braun, J. You, C. Slaughter, C. Pickart, and Z.J. Chen. Activation of the IkappaB kinase complex by TRAF6 requires a dimeric ubiquitin-conjugating enzyme complex and a unique polyubiquitin chain. *Cell* (2000) 103: 351-61.
- Desterro J.M., J. Thomson, R.T. Hay, Ubch9 conjugates SUMO but not ubiquitin, *FEBS Lett.* 417 (1997) 297–300.
- Desterro J.M., M.S. Rodriguez, R.T. Hay, SUMO-1 modification of IkappaBalpha inhibits NF-kappaB activation, *Mol. Cell* (1998) 2:233– 239.
- Desterro JM, Rodriguez MS, Kemp GD, Hay RT. Identification of the Enzyme Required for Activation of the Small Ubiquitin-like Protein SUMO-1* *J. Biol. Chem.* (1999) 274: 10618–24
- Dohmen R.J., R. Stappen, J.P. McGrath, H. Forrova, J. Kolarov, A.Goffeau, A. Varshavsky, An essential yeast gene encoding a homolog of ubiquitin-activating enzyme, *J. Biol. Chem.* (1995) 270:18099–18109.
- Dohmen R.J. SUMO protein modification *Biochimica et Biophysica Acta* (2004) 1695: 113–131
- Donaghue C., H. Bates, S. Cotterill, Identification and characterization of the *Drosophila* homologue of the yeast Uba2 gene, *Biochim. Biophys. Acta* 1518 (2001) 210– 214.
- Ducut Sigala, J.L., Bottero, V., Young, D.B., Shevchenko, A., Mercurio, F., and Verma, I.M.. Activation of transcription factor NF-kappaB requires ELKS, an IkappaB kinase regulatory subunit. *Science* (2004) 304: 1963-7.
- Eaton E.M., L. Sealy, Modification of CCAAT/enhancer-binding protein-beta by the small ubiquitin-like modifier (SUMO) family members, SUMO-2 and SUMO-3, *J. Biol. Chem.* 278 (2003) 33416–33421.

- Echard A, de Opdam FJM, Leeuw HJPC, Jollivet F, Savelkoul P, Hendriks W, Voorberg J, Goud B, Fransen JAM. Alternative splicing of the human Rab6A gene generates two close but functionally different isoforms. *Mol Biol Cell* (2000) 11:3819±3833.
- Epps JL, Tanda S. 1998. The *Drosophila* semushi mutation blocks nuclear import of bicoid during embryogenesis. *Curr. Biol.* (1998) 8: 1277–80
- Gan-Erdene, T., Kolli, N., Yin, L., Wu, K., Pan, Z. Q., and Wilkinson, K. D. Identification and characterization of DEN1, a deneddylase of the ULP family. *J. Biol. Chem.* (2003) 278: 28892-28900.
- Ghosh, S., and Karin, M. Missing pieces in the NF-kappaB puzzle. *Cell* (2002) 109: 81-96.
- Gill G. SUMO and ubiquitin in the nucleus: different functions, similar mechanisms? *Genes Dev.* (2004) 18: 2046-2059
- Girod A, Storrie B, Simpson JC, Johannes L, Goud B, Roberts LM, Lord JM, Nilsson T, Pepperkok R. Evidence for a COP-I-independent transport route from the Golgi complex to the endoplasmic reticulum. *Nat Cell Biol.* (1999) 1:423±430.
- Gobom, J., E. Nordhoff, E. Mirgorodskaya, R. Ekman, and P. Roepstorff. Sample purification and preparation technique based on nano scale reversed-phase columns for the sensitive analysis of complex peptide mixtures by matrix-assisted laser desorption/ionization mass spectrometry. *J. Mass Spectrom.* (1999) 34:105–116.
- Gong, L., Millas, S., Maul, G. G., and Yeh, E. T. Differential regulation of sentrinized proteins by a novel sentrin-specific protease. *J. Biol. Chem.* (2000) 275, 3355-3359.
- Gottlicher M, Heck S, Doucas V, Wade E, Kullmann M, Cato AC, Evans RM, Herrlich P. Interaction of the Ubc9 human homologue with c-Jun and with the glucocorticoid receptor. *Steroids.* 1996 Apr; 61(4): 257-62.
- Goud B, Zahraoui A, Tavitian A, Saraste J. Small GTP-binding protein associated with Golgi cisternae. *Nature* (1990) 345: 553±556.
- Gross, M., Liu, B., Tan, J., French, F. S., Carey, M., and Shuai, K. Distinct effects of PIAS proteins on androgen-mediated gene activation in prostate cancer cells. *Oncogene* (2001) 20: 3880-3887.
- Hang J, Dasso M. Association of the Human SUMO-1 Protease SENP2 with the Nuclear Pore* *J. Biol. Chem.* (2002) 277: 19961–66
- Hardeland U, Steinacher R, Jiricny J, Schär P. Modification of the human thymine-DNA glycosylase by ubiquitin-like proteins facilitates enzymatic turnover. *EMBO J.* (2002) 21: 1456–64

- Hatfield, P.M. and Vierstra, R.D. Multiple forms of ubiquitin activating enzyme E1 from wheat. Identification of an essential cysteine by *in vitro* mutagenesis. *J. Biol. Chem.* (1992) 267: 14799–14803.
- Hayashi T, Seki M, Maeda D, Wang W, Kawabe Y, et al. Ubc9 Is Essential for Viability of Higher Eukaryotic Cells *Exp. Cell Res.* (2002) 280: 212–21
- Hershko, A., Ciechanover, A. *Annu. Rev. Biochem.* (1998) 67: 425–79
- Hicke, L. Protein regulation by monoubiquitin. *Nat Rev Mol Cell Biol* (2001)2: 195-201.
- Hicke, L., Schubert, H.L., Hill, C.P. Ubiquitin-binding domains. *Nat Rev Mol Cell Biol.* (2005) 8: 610-21.
- Ho, J.C., N.J. Warr, H. Shimizu, F.Z. Watts, SUMO modification of Rad22, the *Schizosaccharomyces pombe* homologue of the recombination protein Rad52, *Nucleic Acids Res.* (2001) 29: 4179–4186.
- Hoegge, C., B. Pfander, G.L. Moldovan, G. Pyrowolakis, and S. Jentsch. RAD6-dependent DNA repair is linked to modification of PCNA by ubiquitin and SUMO. *Nature* (2002) 419: 135-41.
- Hochstrasser M There's the rub: a novel ubiquitin-like modification linked to cell cycle regulation. *Genes Dev* (1998) 12: 901–907
- Hochstrasser, M. Biochemistry. All in the ubiquitin family. *Science* (2000) 289: 563-4.
- Hochstrasser M. SP-RING for SUMO: new functions bloom for a ubiquitin-like protein. *Cell* (2001) 107: 5–8
- Hu Y., Baud V., Oga T., Kim K.I., Yoshida K., Karin M. IKK α controls formation of the epidermis independently of NF- κ B. *Nature*. 2001 Apr 5; 410(6829): 710-4.
- Imaizumi O., Ohtsuka, T., Matsushima, S., Akimoto, Y., Nishiwaki, Y., Kikuta, T., Nagai, S., Kawakami, H., Watanabe, T., Nagamatsu, S., ELKS, a protein structurally related to the active zone-associated protein CAST, is expressed in pancreatic beta cells and functions in insulin exocytosis: interaction of ELKS with exocytotic machinery analyzed by total internal reflection fluorescence microscopy. *Mol. Biol. Cell.* (2005) 16: 3289-300.
- Imoto S., K. Sugiyama, R. Muromoto, N. Sato, T. Yamamoto, T. Matsuda, Regulation of transforming growth factor- β signaling by protein inhibitor of activated STAT, PIASy through Smad3, *J. Biol. Chem.* (2003) 278: 34253– 34258.

- Iñiguez-Lluhi JA, Pearce D. A common motif within the negative regulatory regions of multiple factors inhibits their transcriptional synergy. *Mol. Cell. Biol.* (2000) 20: 6040–50
- Jackson, P. K. A new RING for SUMO: wrestling transcriptional responses into nuclear bodies with PIAS family E3 SUMO ligases. *Genes Dev.* (2001) 15: 3053–3058
- Jentsch, S. and G. Pyrowolakis. Ubiquitin and its kin: how close are the family ties? *Trends Cell Biol.* (2000) 10: 335-42.
- Jimenez-Lara, A. M., Heine, M. J., and Gronemeyer, H. PIAS3 (protein inhibitor of activated STAT-3) modulates the transcriptional activation mediated by the nuclear receptor coactivator TIF2. *FEBS Lett.* (2002) 526: 142-146.
- Joazeiro C. A. and Weissman A. M. RING finger proteins: mediators of ubiquitin ligase activity. *Cell* (2000) 102: 549–552.
- Johnson E.S., G. Blobel. Ubc9p is the conjugating enzyme for the ubiquitin-like protein Smt3p, *J. Biol. Chem.* (1997) 272: 26799–26802.
- Johnson E.S., I. Schwienhorst, R.J. Dohmen, G. Blobel. The ubiquitin-like protein Smt3p is activated for conjugation to other proteins by an Aos1p/Uba2p heterodimer, *EMBO J.* (1997) 16: 5509– 5519.
- Johnson E.S. Protein modification by SUMO *Annu. Rev. Biochem.* (2004) 73: 355–82
- Joseph, J., Tan, S. H., Karpova, T. S., McNally, J. G., and Dasso, M. SUMO-1 targets RanGAP1 to kinetochores and mitotic spindles. *J. Cell Biol.* (2002) 156: 595-602.
- Kadare, G., Toutant, M., Formstecher, E., Corvol, J. C., Carnaud, M., Bouterin, M. C., and Girault, J. A. PIAS1-mediated sumoylation of focal adhesion kinase activates its autophosphorylation. *J. Biol. Chem.* (2003) 278: 47434-47440.
- Kagey MH, Melhuish TA, Wotton D. The polycomb protein Pc2 is a SUMO E3. (2003) *Cell* 113: 127–37
- Kahyo, T., Nishida, T., and Yasuda, H. Involvement of PIAS1 in the sumoylation of tumor suppressor p53. *Mol. Cell* (2001) 8: 713-718.
- Kim, K. I., Baek, S. H., Jeon, Y. J., Nishimori, S., Suzuki, T., Uchida, S., Shimbara, N., Saitoh, H., Tanaka, K., and Chung, C. H. A new SUMO-1-specific protease, SUSP1, that is highly expressed in reproductive organs. *J. Biol. Chem.* (2000) 275, 14102-14106.
- Kirsh O., J.S. Seeler, A. Pichler, A. Gast, S. Mqller, E. Miska, M. Mathieu, A. Harel-Bellan, T. Kouzarides, F. Melchior, A. Dejean, The SUMO E3 ligase RanBP2

- promotes modification of the HDAC4 deacetylase, *EMBO J.* (2002) 21: 2682–2691.
- Kotaja N., Karvonen U., Janne O. A. and Palvimo J. J. PIAS proteins modulate transcription factors by functioning as SUMO-1 ligases. *Mol. Cell Biol.* (2002) 22: 5222–5234
- Koushika, S. P., Richmond, J. E., Hadwiger, G., Weimer, R. M., Jorgensen, E. M. & Nonet, M. L. *Nat. Neurosci.* (2001) 4: 997–1005.
- Kurtzman A.L., N. Schechter, Ubc9 interacts with a nuclear localization signal and mediates nuclear localization of the pairedlike homeobox protein Vsx-1 independent of SUMO-1 modification, *Proc. Natl. Acad. Sci. U. S. A.* (2001) 98: 5602–5607.
- Kuryshv, Y. A., Gudz, T. I., Brown, A. M., and Wible, B. A. KChAP as a chaperone for specific K(+) channels. *Am. J. Physiol. Cell. Physiol.* (2000) 278, C931-941.
- Laemmli U.K. Cleavage of structural proteins during the assembly of the head of bacteriophage T4. *Nature* (1970) 227: 680-5.
- Lee, P. S., Chang, C., Liu, D., and Derynck, R. Sumoylation of Smad4, the common Smad mediator of transforming growth factor-beta family signaling. *J. Biol. Chem.* (2003) 278: 27853-27863.
- Lehming, N., S. A. Le, J. Schüller, and M. Ptashne. Chromatin components as part of a putative transcriptional repressing complex. *Proc. Natl. Acad. Sci. USA* (1998) 95: 7322–7326.
- Li S.J, Hochstrasser M. A new protease required for cell-cycle progression in yeast *Nature* (1999) 398:246–51.
- Li, S.J. and Hochstrasser, M.. The yeast ULP2 (SMT4) gene encodes a novel protease specific for the ubiquitin-like Smt3 protein. *Mol Cell Biol* (2000) 20: 2367-77.
- Li Q., Lu Q., Hwang J.Y., Buscher D., Lee K.F., Izpisua-Belmonte J.C, Verma IM. IKK1-deficient mice exhibit abnormal development of skin and skeleton. *Genes Dev.* (1999) 15; 13(10): 1322-8.
- Liao, J., Fu, Y., and Shuai, K. Distinct roles of the NH2- and COOH-terminal domains of the protein inhibitor of activated signal transducer and activator of transcription (STAT) 1 (PIAS1) in cytokine-induced PIAS1-Stat1 interaction. *Proc. Natl. Acad. Sci. USA* (2000) 97: 5267-5272.

- Lin X., B. Sun, M. Liang, Y.Y. Liang, A. Gast, J. Hildebrand, F.C. Brunicardi, F. Melchior, X.H. Feng, Opposed regulation of corepressor CtBP by SUMOylation and PDZ binding, *Mol. Cell* (2003) 11:1389–1396.
- Lippincott-Schwartz J, Roberts TH, Hirschberg K: Secretory protein trafficking and organelle dynamics in living cells. *Annu Rev Cell Dev Biol* (2000) 16:557-589.
- Liu B., J. Liao, X. Rao, S.A. Kushner, C.D. Chung, D.D. Chang, K. Shuai, Inhibition of Stat1-mediated gene activation by PIAS1. *Proc. Natl. Acad. Sci. U. S. A.* 95 (1998) 10626–10631.
- Lois L.M., Lima D. Ch. Structures of the SUMO E1 provide mechanistic insights into SUMO activation and E2 recruitment to E1. *The EMBO Journal* (2005) 24: 439–451
- Mahajan R, Delphin C, Guan T, Gerace L, Melchior F. Cell A small ubiquitin-related polypeptide involved in targeting Ran-GAP1 to nuclear pore complex protein RanBP2 (1997) 88:97–107.
- Mahajan R., L. Gerace, F. Melchior, Molecular characterization of the SUMO-1 modification of RanGAP1 and its role in nuclear envelope association. *J. Cell Biol.* 140 (1998) 259–270.
- Mao Y, Desai S.D, Liu LF. SUMO-1 Conjugation to Human DNA Topoisomerase II Isozymes. *J. Biol. Chem.* (2000) 275: 26066–73.
- Makris, C., Godfrey, VL., Krahn-Senftleben, G., Takahashi, T., Roberts, JL., Schwarz, T., Feng, L., Johnson, RS., Karin, M. Female mice heterozygous for IKK gamma/NEMO deficiencies develop a dermatopathy similar to the human X-linked disorder incontinentia pigmenti. *Mol Cell* (2000) 5: 969-79.
- Martinez O, Antony C, Pehau-Arnaudet G, Berger EG, Salamero J, Goud B. GTP-bound forms of rab6 induce the redistribution of Golgi proteins into the endoplasmic reticulum. *Proc Natl Acad Sci USA* (1997) 94: 1828±1833.
- Matunis J. M., Coutavas E, and Blobel G. A Novel Ubiquitin-like Modification Modulates the Partitioning of the Ran-GTPase-activating Protein RanGAP1 between the Cytosol and the Nuclear Pore Complex. *J. Cell Biol.* (1996) 136: 1451–1470.
- Matunis MJ, Wu J, Blobel G. SUMO-1 modification and its role in targeting the Ran GTPase-activating protein, RanGAP1, to the nuclear pore complex, *J. Cell Biol.* (1998) 140:499–509.
- Mayer, R.J., M. Landon, and Layfield R. Ubiquitin superfolds: intrinsic and attachable regulators of cellular activities? *Fold Des* (1998) 3: R97-9.

- Melchior F. SUMO-nonclassical ubiquitin, *Annu. Rev. Cell Dev. Biol.* (2000) 16: 591–626.
- Melchior F., Schergaut M., Pichler A. SUMO: ligases, isopeptidases and nuclear pores *Trends Biochem Sci.* (2003) 28: 612-618.
- Mendoza, H. M., Shen, L. N., Botting, C., Lewis, A., Chen, J., Ink, B., and Hay, R. T. NEDP1, a highly conserved cysteine protease that deNEDDylates cullins. *J. Biol. Chem.* (2003) 278: 25637-25643.
- Miller, E., B. Antonny, S. Hamamoto, and R. Schekman. Cargo selection into COPII vesicles is driven by the Sec24p subunit. *EMBO J.* (2002) 21:6105–6113.
- Minty A., Dumont X., Kaghad M. and Caput D. Covalent modification of p73alpha by SUMO-1. Two-hybrid screening with p73 identifies novel SUMO-1-interacting proteins and a SUMO-1 interaction motif. *J. Biol. Chem.* (2000) 275: 36316–36323.
- Miyauchi, Y., Yogosawa, S., Honda, R., Nishida, T., and Yasuda, H. Sumoylation of Mdm2 by protein inhibitor of activated STAT (PIAS) and RanBP2 enzymes. *J. Biol. Chem.* (2002) 277: 50131-50136.
- Mizushima N, Noda T, Yoshimori T, Tanaka Y, Ishii T, George MD, Klionsky DJ, Ohsumi M, Ohsumi Y A protein conjugation system essential for autophagy. *Nature* (1998) 395: 395–398.
- Moilanen A.M., U. Karvonen, H. Poukka, W. Yan, J. Toppari, O.A. Janne, J.J. Palvimo, A testis-specific androgen receptor coregulator that belongs to a novel family of nuclear proteins, *J. Biol. Chem.* (1999) 274:3700–3704.
- Monier, S., Jollivet, F., Janoueix-Lerosey, I., Johannes, L., and Goud, B. Characterization of novel Rab6-interacting proteins involved in endosome-to-TGN transport. *Traffic* (2002) 3:289-97.
- Mossessova E, Lima CD. Ulp1-SUMO Crystal Structure and Genetic Analysis Reveal Conserved Interactions and a Regulatory Element Essential for Cell Growth in Yeast *Mol. Cell* (2000) 5: 865–76.
- Müller, S., M. Berger, F. Lehembre, J.S. Seeler, Y. Haupt, and A. Dejean. c-Jun and p53 activity is modulated by SUMO-1 modification. *J Biol Chem* (2000) 275: 13321-9.
- Nakagawa, K., and Yokosawa, H. PIAS3 induces SUMO-1 modification and transcriptional repression of IRF-1. *FEBS Lett.* (2002) 530: 204-208.
- Nakata, T., Kitamura, Y., Shimizu, K., Tanaka, S., Fujimori, M., Yokoyama, S., Ito, K., and Emi, M. Fusion of a novel gene, *ELKS*, to *RET* due to translocation t

- (10;12)(q11;p13) in a papillary thyroid carcinoma. *Genes Chromosomes Cancer* (1999) 25: 97-103.
- Nakata, T., Yokota, T., Emi, M., and Minami, S. Differential expression of multiple isoforms of the *ELKS* mRNAs involved in a papillary thyroid carcinoma. *Genes Chromosomes Cancer* (2002) 355: 30-7.
- Nishida, T., and Yasuda, H. PIAS1 and PIASx α function as SUMO E3 ligases toward androgen receptor and repress androgen receptor-dependent transcription. *J. Biol. Chem.* (2002) 277: 41311-41317.
- Ohtsuka, T., Takao-Rikitsu, E., Inoue, E., Inoue, M., Takeuchi, M., Matsubara, K., Deguchi-Tawarada, M., Satoh, K., Morimoto, K., Nakanishi, H., and Takai, Y. Cast: a novel protein of the cytomatrix at the active zone of synapses that forms a ternary complex with RIM1 and Munc13-1. *J. Cell Biol.* (2002) 158: 577-590.
- Opdam FJM, Echard A, Croes HJE, van den Hurk JAJM, van de Vorstenbosch RA, Ginsel LA, Goud B, Fransen JAM. The small GTPase Rab6B, a novel Rab6 subfamily member, is cell-type specifically expressed and localised to the Golgi apparatus. *J Cell Sci* (2000) 113: 2725-2735.
- Osaka F, Kawasaki H, Aida N, Saeki M, Chiba T, Kawashima S, Tanaka K, Kato S A new NEDD8-ligating system for cullin-4A. *Genes Dev* (1998) 12: 2263-2268.
- Panse VG, Ku"ster B, Gerstberger T, Hurt E. Unconventional tethering of Ulp1 to the transport channel of the nuclear pore complex by karyopherins. *Nat. Cell Biol.* (2003) 5:21-27.
- Pichler, A., A. Gast, J.S. Seeler, A. Dejean, and F. Melchior. The nucleoporin RanBP2 has SUMO E3 ligase activity. *Cell* (2002) 108:109-120.
- Pichler, A., Knipscheer, P., Saitoh, H., Sixma, TK., and Melchior, F. The RanBP2 SUMO E3 ligase is neither HECT- nor RING-type. *Nat. Struct. Mol. Biol.* (2004) 11: 984-991.
- Pichler, A., Melchior, F. SUMO E3 ligases. Chapter in book edited by Wilson V., G. (2004), 131-175.
- Pickart, CM. Mechanism underlying ubiquitination. *Annu. Rev. Biochem.* (2001) 70: 503-33.
- Pickart, C.M., Eddins, M.J. Ubiquitin: structures, functions, mechanisms. *Biochimica et Biophysica Acta* (2004) 1695:55-72.

- Pitterle, D.M. and Rajagopalan, K.V. Two proteins encoded at the *chlA* locus constitute the converting factor of *Escherichia coli* *chlA1*. *J. Bacteriol.* (1989) 171: 3373–3378.
- Pollok, B.A., Heim, R. Using GFP in FRET based applications. *Trends Cell Biol.* (1999) 2: 57–60.
- Pryer, N.K., N.R. Salama, R. Schekman, and C.A. Kaiser. Cytosolic Sec13p complex is required for vesicle formation from the endoplasmic reticulum in vitro. *J. Cell Biol.* (1993) 120: 865–875.
- Reverter, D., Lima C.D. Insights into E3 ligase activity revealed by a SUMO-RanGAP1-Ubc9-Nup358 complex. *Nature* (2005) 435(7042): 687–92.
- Rodel, B., Tavassoli, K., Karsunky, H., Schmidt, T., Bachmann, M., Schaper, F., Heinrich, P., Shuai, K., Elsasser, H. P., and Moroy, T. The zinc finger protein Gfi-1 can enhance STAT3 signaling by interacting with the STAT3 inhibitor PIAS3. *EMBO J.* (2000) 19: 5845–5855.
- Rodriguez, M.S., J.M. Desterro, S. Lain, C.A. Midgley, D.P. Lane, and R.T. Hay. SUMO-1 modification activates the transcriptional response of p53. *Embo J* (1999) 18: 6455–61.
- Rogers R.S., C.M. Horvath, M.J. Matunis, SUMO modification of STAT1 and its role in PIAS-mediated inhibition of gene activation, *J. Biol. Chem.* (2003) 278:30091–30097.
- Ross, S., J.L. Best, L.I. Zon, and G. Gill. SUMO-1 modification represses Sp3 transcriptional activation and modulates its subnuclear localization. *Mol Cell* (2002) 10: 831–42.
- Rui, H. L., Fan, E., Zhou, H. M., Xu, Z., Zhang, Y., and Lin, S. C. SUMO-1 modification of the C-terminal KVEKVD of Axin is required for JNK activation but has no effect on Wnt signaling. *J. Biol. Chem.* (2002) 277: 42981–42986.
- Saitoh, H., D.B. Sparrow, T. Shiomi, R.T. Pu, T. Nishimoto, T.J. Mohun, M. Dasso, Ubc9p and the conjugation of SUMO-1 to RanGAP1 and RanBP2, *Curr. Biol.* (1998) 8: 121–124.
- Sachdev, S., Bruhn L., Sieber H., Pichler A., Melchior F. And Grosschedl R. PIASy, a nuclear matrix-associated SUMO E3 ligase, represses LEF1 activity by sequestration into nuclear bodies. *Genes Dev.* (2001) 15: 3088–3103.
- Saitoh, H., Pu R., Cavenagh M., Dasso M. SUMO-1: wrestling with a new ubiquitin-related modifier. *Proc. Natl. Acad. Sci. USA* (1997) 94: 3736–41.

- Saitoh, H., Sparrow, D. B., Shiomi, T., Pu, R. T., Nishimoto, T., Mohun, T. J., and Dasso, M. (1998) Ubc9p and the conjugation of SUMO-1 to RanGAP1 and RanBP2. *Curr. Biol.* (1998) 8: 121-124.
- Saitoh, H., Hinchev, J. Functional heterogeneity of small ubiquitinrelated protein modifiers SUMO-1 versus SUMO-2/3, *J. Biol. Chem.* 275 (2000) 6252– 6258.
- Sapetschnig, A., Rischitor G., Braun H., Doll A., Schergaut M., Melchior F., Suske, G. Transcription factor Sp3 is silenced through SUMO modification by PIAS1. *EMBO J.* (2002) 21: 5206–5215.
- Schaeper, U., Boyd J.M., Verma S., Uhlmann E., Subramanian T., Chinnadurai G. Molecular cloning and characterization of a cellular phosphoprotein that interacts with a conserved C-terminal domain of adenovirus E1A involved in negative modulation of oncogenic transformation. *Proc Natl Acad Sci U S A* (1998) 95(24):14584.
- Schekman, R., Orci L: Coat proteins and vesicle budding. *Science* (1996) 271:1526-1533.
- Shen, Z., Pardington-Purtymun P.E., Comeaux J.C., Moyzis R.K., Chen D.J. Associations of UBE2I with RAD52, UBL1, p53, and RAD51 proteins in a yeast two-hybrid system. *Genomics* (1996) 37(2): 183-6.
- Shevchenko, A., M. Wilm, O. Vorm, and M. Mann. Mass spectrometric sequencing of proteins from silver-stained polyacrylamide gels. *Anal. Chem.* (1996) 68: 850–858.
- Schmidt, D. and Müller S. Members of the PIAS family act as SUMO ligases for c-Jun and p53 and repress p53 activity. *Proc Natl Acad Sci USA* (2002) 99: 2872-7.
- Schmidt-Supprian, M., Bloch, W., Courtois, G., Addicks, K., Israel, A., Rajewsky, K., and Pasparakis, M. NEMO/IKK gamma-deficient mice model incontinentia pigmenti. *Mol. Cell* (2000) 5: 981-92.
- Shuai, K. Modulation of STAT signaling by STAT-interacting proteins. *Oncogene* (2000) 19: 2638–2644.
- Seeler, J.-S., A. Marchio, D. Sitterlin, C. Transy, and Dejean A. Interaction of SP100 with HP1 proteins: a link between the promyelocytic leukemia-associated nuclear bodies and the chromatin compartment. *Proc. Natl. Acad. Sci. USA* (1998) 95:7316–7321.
- Seeler, J.S., Dejean A., Nuclear and unclear functions of SUMO, *Nat. Rev., Mol. Cell Biol.* (2003) 4:690–699.

- Senftleben, U., Cao, Y., Xiao, G., Greten, F.R., Krahn, G., Bonizzi, G., Chen, Y., Hu, Y., Fong, A., Sun, S.C., Karin, M. Activation by IKK α of a second, evolutionary conserved, NF- κ B signaling pathway. *Science* (2001) 293: 1495-9.
- Seufert, W., Futcher, B., Jentsch S. Nature Role of a ubiquitin-conjugating enzyme in degradation of S- and M-phase cyclins. (1995) 373: 78–81.
- Schwienhorst, I., Johnson, E.S, Dohmen R.J. SUMO conjugation and deconjugation *Mol. Gen. Genet.* (2000) 263: 771–86.
- Sobko, A., Ma H., Firtel, R.A. Regulated SUMOylation and Ubiquitination of DdMEK1 Is Required for Proper Chemotaxis *Dev. Cell* (2002) 2: 745–56.
- Stelter, P., Ulrich, H.D. Control of spontaneous and damage-induced mutagenesis by SUMO and ubiquitin conjugation. *Nature* (2003) 425: 188– 191.
- Takahashi, K., Taira, T., Niki, T., Seino, C., Iguchi-Ariga, S. M., and Ariga, H. DJ-1 positively regulates the androgen receptor by impairing the binding of PIAS α to the receptor. *J. Biol. Chem.* (2001) 276, 37556-37563.
- Tan, J., Hall, S. H., Hamil, K. G., Grossman, G., Petrusz, P., Liao, J., Shuai, K., and French, F. S. Protein inhibitor of activated STAT-1 (signal transducer and activator of transcription-1) is a nuclear receptor coregulator expressed in human testis. *Mol. Endocrinol.* (2000) 14: 14-26.
- Tanaka K, Nishide J, Okazaki K, Kato H, Niwa O, et al. *Mol. Cell. Biol.* (1999) 19:8660–72
- Tatham, M.H., E. Jaffray, O.A. Vaughan, J.M. Desterro, C.H. Botting, J.H. Naismith, Hay, R.T. Polymeric chains of SUMO-2 and SUMO-3 are conjugated to protein substrates by SAE1/SAE2 and Ubc9, *J. Biol. Chem.* 276 (2001) 35368–35374.
- Tatham, MH, Chen, Y, Hay, RT. Role of two residues proximal to the active site of Ubc9 in substrate recognition by the Ubc9.SUMO-1 thiolester complex. *Biochemistry* (2003) 42: 3168–79.
- Tatham, M.H., S. Kim, B. Yu, E. Jaffray, J. Song, J. Zheng, M.S. Rodriguez, R.T. Hay, Chen Y. Role of an N-terminal site of Ubc9 in SUMO-1, -2, and -3 binding and conjugation, *Biochemistry* (2003) 42: 9959–9969.
- Tatham, M.H., Kim S., Jaffray E., Song, J., Chen, Y., and Hay, RT. Unique binding interactions among Ubc9, SUMO and RanBP2 reveal a mechanism for SUMO paralog selection. *Nat. Struct. Mol. Biol.* (2005) 12: 67-74.

- Taylor, D. L., Ho, J. C., Oliver, A., and Watts, F. Z. Cell-cycle-dependent localisation of Ulp1, a *Schizosaccharomyces pombe* Pmt3 (SUMO)-specific protease. *J. Cell. Sci.* (2002) 115: 1113-1122.
- Tian, S., Poukka, H., Palvimo, J.J., Jänne O.A. Small ubiquitin-related modifier-1 (SUMO-1) modification of the glucocorticoid receptor. *Biochem. J.* (2002) 367: 907–11.
- Tsien, R.Y. The green fluorescent protein. *Ann Rev Biochem.* (1998) 67: 509-44.
- Ungureanu D., S. Vanhatupa, N. Kotaja, J. Yang, S. Aittomaki, O.A. Janne, J.J. Palvimo, O. Silvennoinen, PIAS proteins promote SUMO-1 conjugation to STAT1, *Blood* (2003) 102: 3311– 3313.
- Walsh, Ch. *Posttranslational Modification of Proteins.* (2005).
- Vander, Horn, P.B., Backstrom, A.D., Stewart, V. and Begley, T.P. Structural genes for thiamine biosynthetic enzymes (thiCEFGH) in *Escherichia coli* K-12. *J. Bacteriol.*, (1993) 175: 982–992.
- Wang, Y., Sugita, S. & Südhof, T. C. The RIM/NIM family of neuronal C2 domain proteins. Interactions with Rab3 and a new class of Src homology 3 domain proteins. *J. Biol. Chem.* (2000) 275: 20033–20044.
- Wang, Y., Liu, X., Biederer, T., and Südhof, T.C. A family of RIM-binding proteins regulated by alternative splicing: implications for the genesis of synaptic active zones. *Proc. Natl. Acad. Sci. USA.* (2002) 99: 14464–14469.
- Wible, B. A., Wang, L., Kuryshev, Y. A., Basu, A., Haldar, S., and Brown, A. M. Increased K⁺ efflux and apoptosis induced by the potassium channel modulatory protein KChAP/PIAS3beta in prostate cancer cells. *J. Biol. Chem.* (2002) 277, 17852-17862.
- Wu, J., Matunis, M. J., Kraemer, D., Blobel, G., and Coutavas, E. Nup358, a cytoplasmically exposed nucleoporin with peptide repeats, Ran-GTP binding sites, zinc fingers, a cyclophilin A homologous domain, and a leucine-rich region. *J. Biol. Chem.* (1995) 270; 14209-14213.
- Yamamoto, Y., and Gaynor, R.B. Role of the NF-kappaB pathway in the pathogenesis of human disease states. *Curr Mol Med.* (2001) 3: 287-96.
- Yamamoto, Y., Verma, UN., Prajapati, S., Kwak, YT., Gaynor, RB. Histone H3 phosphorylation by IKK-alpha is critical for cytokine-induced gene expression. *Nature.* (2003) 423: 655-9.

- Yang, S.H., Sharrocks A.D., SUMO promotes HDAC-mediated transcriptional repression, *Mol. Cell* 13 (2004) 611 – 617.
- Yaseen, N. R., and Blobel, G. Two distinct classes of Ran-binding sites on the nucleoporin Nup-358. *Proc. Natl. Acad. Sci. USA* (1999) 96: 5516-5521.
- Yeh, E. T., Gong, L., and Kamitani, T. Ubiquitin-like proteins: new wines in new bottles. *Gene* (2000) 248, 1-14.
- Yokota, T., Nakata, T., Minami, S., Inazawa, J., and Emi, M. Genomic organization and chromosomal mapping of ELKS, a gene rearranged in a papillary thyroid carcinoma. *J. Hum. Genet.* (2000) 45: 6-11.
- Yokoyama, N., Hayashi, N., Seki, T., Pante, N., Ohba, T., Nishii, K., Kuma, K., Hayashida, T., Miyata, T., Aebi, U., and *et al.* A giant nucleopore protein that binds Ran/TC4. *Nature* (1995) 376; 184-188.
- Zentner, M. D., Lin, H. H., Deng, H. T., Kim, K. J., Shih, H. M., and Ann, D. K. Requirement for high mobility group protein HMGI-C interaction with STAT3 inhibitor PIAS3 in repression of alpha-subunit of epithelial Na⁺ channel (alpha-ENaC) transcription by Ras activation in salivary epithelial cells. *J. Biol. Chem.* (2001) 276, 29805-29814.
- Zhang, H., H. Saitoh, Matunis, M.J., Enzymes of the SUMO modification pathway localize to filaments of the nuclear pore complex, *Mol. Cell. Biol.* 22 (2002) 6498–6508.

8 ACKNOWLEDGEMENTS

I wish to express my sincere gratitude to the following people:

Prof. Dr. Frauke Melchior who welcomed me at Max Planck Institute. I am deeply indebted to you for your kindness, scientific guidance, patience and never-ending enthusiasm throughout my years of research studies.

All present and past colleagues in our laboratory for their efforts to keep the lab work in a friendly and cooperative environment. In particular Guillaume, for giving help and showing such patience with my endless enquires; Frank for lending a helping hand whenever I need it; Florian and Annette for their friendship and good time in the lab.

I am especially grateful to Andrea and Sowmya from whom I learned a lot during our scientific and non scientific discussion and for all the laughs. I extend my thanks to Andrea, especially for wine tasting, for her chocolates and for being a friend.

I am warmly thank all “Hengst” members, for their support, especially Michael Kullmann for friendship and good time in the lab.

I wish to acknowledge Prof. Reinhard Fässler for help and support during my stay in his laboratory and his energetic attitude towards research.

Carol and Basile, who have always been a lovely company and have helped me to feel not so lonely living in a foreign country.

To Agnieszka, my best friend in Poland for all her sincere friendship throughout the years.

My heartfelt thanks to my family; my parents: Ania and Stanislaw, my brother Krzysztof with Paulina and Bartus, and “little judge-sister” Agata, for their love and unconditional support.

My special gratitude goes to my second family in Sweden: Sara, Göran and Ramtin for unique positive attitude and for the nice time we shared/will share together.

I would like to express my deepest gratitude to the special person in my life Ramin, for his love, patience, constant support and for always bringing me smile.

9 PUBLICATIONS

Palacios, S., Perez, L.H., Welsch, S., Schleich, S., **Chmielarska, K.**, Melchior, F., and Krijnse Locke, J. (2005) Quantitative SUMO-1 modification of a vaccinia virus protein is required for its specific localization and prevents its self-association. *Mol Biol Cell* 16(6):2822-35

Bossis, G., **Chmielarska, K.**, Gärtner, U., Pichler, A., Stieger, E., and Melchior, F. (2005) A FRET-based assay to study SUMO modification in solution. *Methods in Enzymology*. 398 (A): 20-32

Massoumi, R., **Chmielarska, K.**, Hennecke, K., Pfeifer, A., and Fässler R. (2005) Cyld inhibits tumor cell proliferation by blocking Bcl-3-dependent NF- κ B signaling. Manuscript submitted

Chmielarska, K., Massoumi, R., Nousiainen M., Körner, R., Monier, S., Goud, B. and Melchior, F. (2005) Sumoylation of the IKK and Aos1 binding partner ELKS contributes to the NF- κ B signaling. Manuscript in preparation.

10 CURRICULUM VITAE

Personal details:

Name Katarzyna Chmielarska
Date of birth: 21 May 1977
Place of birth: Kielce, Poland
Nationality: Polish
Marital status: Single
Address: Georg-August-University Göttingen
Biochemie I
Humboldtallee 23
37073 Göttingen

Education:

1992-1996 Secondary School No.1, Kielce, Poland

1996-2001 Studies of Molecular Biology at the *Jagiellonian University of Kraków, Poland*

February 1999-August 1999 Research training in the frame of TEMPUS programme, *Centre de Biophysique Moleculaire at the Universite d'Orleans, France*. Projects: 1)"Study of Cell Adhesion in High Endothelial Cell Lines
2) Endogenous Lectin Expression on Endothelial Cells".

June 2001 Master of Science, *Jagiellonian University of Kraków*
"Influence of actin cytoskeleton destabilising factors, on morphology, amount of F- actin and fluid-phase endocytosis of human skin fibroblast".

November 2001-2005 Ph.D. Research
Max-Planck Institute of Biochemistry, Munich, since January 2005 *Georg-August-University Göttingen*
Prof. Dr. Frauke Melchior
Characterization of SUMO E1 activating enzyme Aos1/Uba2